# UNDERSTANDING THE CEREBROPROTECTIVE ACTIONS OF THE ACE2/ANG-(1-7)/MAS AXIS DURING ISCHEMIC AND HEMORRHAGIC STROKE

By

ROBERT W. REGENHARDT

A DISSERTATION PRESENTED TO THE GRADUATE SCHOOL
OF THE UNIVERSITY OF FLORIDA IN PARTIAL FULFILLMENT
OF THE REQUIREMENTS FOR THE DEGREE OF
DOCTOR OF PHILOSOPHY

UNIVERSITY OF FLORIDA

2012

© 2012 Robert W. Regenhardt

ACKNOWLEDGMENTS

First, I would like to thank my Ph.D. mentor, Colin Sumners. He has been a great personal and professional role model since I was admitted to medical school in 2006 through an early acceptance program he directs. Since starting my Ph.D. in his lab in 2009, I have grown as a scientist and a person under his mentorship. Dr. Sumners has guided me through graduate school and kept me directed, while teaching me how to be a great scientist. I have a learned a great deal about designing experiments, writing manuscripts and grants, leadership, administration, and mentoring. We have had some great times in and out of the lab over the past 3 years, and I am truly grateful for his friendship. I have enjoyed the opportunities to travel with him around the country and present our work at professional meetings.

I would also like to thank my committee members, Mohan Raizada, Mike Katovich, Judy Delp, J Mocco, and Mike Waters. Each has provided invaluable input toward my dissertation project over these last 3 years. Their guidance has helped me broaden my skillset as a scientist and shape the way I think. Dr. Raizada, the PI for the adjacent lab and long time collaborator with my PI, has given me much advice over the years. One that sticks with me is to “do the last experiment first.” I have learned this is a good way to approach a lot of problems. Dr. Katovich has also been instrumental in my scientific development and has provided great input in the design of our experiments. His expertise in the renin-angiotensin system was a great complement to that of Dr. Sumners and Dr. Raizada. Dr. Delp’s expertise in vascular biology has given us great insight into the pathophysiology of our stroke models. I was also fortunate to learn how to do vascular reactivity experiments in her lab, while none are presented in this dissertation. Drs. Mocco and Waters have been great for not only their expertise as

scientists, but also clinicians. They have encouraged me to always think about translation to the bedside and given me great clinical perspectives on stroke.

The many people I have worked with in the Sumners lab and other labs have been instrumental to my progress and have become good friends. Many thanks are owed to Adam Mecca, Fiona Desland, Jason Joseph, Vermali Rodriguez, Tim O'Conner, David Pioquinto, Neal Patel, Phillip Ritucci, Jacob Ludin, David Greenstein, Peng Shi, Hongwei Li, Nan Jiang, Ying Dong, Annette de Kloet, Cristina Banuelos, Cristina Kitchen, and Kat Marulanda. I would also like to thank Ron Mandel for his guidance with behavioral exams and Jennifer Bizon for her expertise in stereology. In addition, I would like to acknowledge Marda Jorgensen from the Histology Resource lab for her immunohistochemistry expertise and Mary Reinhard for her expertise as a licensed veterinary pathologist. Glen Walter and Huadong Zeng were also helpful in teaching us the technical aspects of MRI. Chris Baylis also deserves special recognition as director of the Hypertension Center and PI for the NIH T32 training grant I was awarded.

Finally and most importantly, I would like to thank my friends and family for their unwavering support throughout my life and during graduate school. I would especially like to thank Adam Mecca. He is one of the most outstanding friends I have ever known, and his mentorship in the lab and in life can not be overstated. I would also like to thank my hometown friends Kevin Vickers and Jeremiah Ross. They have always been there for me even when we have lived hours apart. Alex Dickert and Matt Bienkowski have been truly amazing friends since I met them just before Alex and I started medical school in 2007. Vermali Rodriguez has been one of the best people to have a few drinks with during my Ph.D studies. I cannot thank her enough for many rides home and

showing me around Puerto Rico. Jason Joseph and I have become great friends since meeting in lab, and I will never forget our amazing times driving some of the world's most exotic super cars and traveling throughout Asia and Europe. There are many other friends I wish I had room to acknowledge. My grandmother, father, mother, and sister also deserve a very special acknowledgement for putting up with me when I have been burdened with work and unable to spend time with them.

TABLE OF CONTENTS

page

ACKNOWLEDGMENTS ..... 3

LIST OF TABLES ..... 9

LIST OF FIGURES ..... 10

ABSTRACT ..... 12

CHAPTER

1 STROKE AND THE ROLE OF THE RENIN ANGIOTENSIN SYSTEM ..... 15

Stroke Epidemiology ..... 15
Pathophysiology of Ischemic Stroke ..... 16
Pathophysiology of Hemorrhagic Stroke ..... 21
Renin Angiotensin System Components ..... 26
Ang-(1-7)/Mas Opposes Ang II/AT1R Signaling ..... 28
Targeting the Renin Angiotensin System for Stroke Therapy ..... 30
Summary ..... 35

2 ANTI-INFLAMMATORY EFFECTS OF ANGIOTENSIN-(1-7) IN ENDOTHELIN-1 INDUCED MIDDLE CEREBRAL ARTERY OCCLUSION: POTENTIAL MECHANISM FOR CEREBROPROTECTION ..... 46

Introduction ..... 46
Methods ..... 47
Animals and Ethical Approval ..... 47
Implantation of Intracranial Cannulae and Osmotic Pumps ..... 48
ET-1 Induced Middle Cerebral Artery Occlusion (MCAO) ..... 48
Post Mortem Analyses ..... 49
PCR Array Hypoxia Signaling Pathway ..... 50
qRT-PCR ..... 50
Western Blotting ..... 51
Mas Immunohistochemistry ..... 52
Nitric oxide Production by Primary Glial Cultures ..... 53
HPLC Analysis of Ang-(1-7) ..... 54
Chemicals ..... 54
Data analysis ..... 54
Results ..... 55
Cerebroprotective Ang-(1-7) Reduces Infarct Size 24 h after ET-1-induced MCAO ..... 55
Increased Expression of Hypoxia-related Genes in the Ipsilateral Cerebral Cortex following ET-1-induced MCAO; Inhibitory Action of Ang-(1-7) ..... 55

Effects of Ang-(1-7) on the Expression of Nitric Oxide Synthase (NOS) Isozymes, PICs, and Inflammatory Cell Markers in the Ipsilateral Cerebral Cortex following ET-1-induced MCAO ..... 56
Cellular Localization of Mas within Rat Cerebral Cortex ..... 58
Ang-(1-7) Blunts LPS Induction of NO in Primary Mixed Glial Cultures ..... 59
Discussion ..... 60

3 ANGIOTENSIN-(1-7) HAS CEREBROPROTECTIVE POTENTIAL IN HEMORRHAGIC STROKE AND INCREASES SURVIVAL OF STROKE-PRONE SPONTANEOUSLY HYPERTENSIVE RATS ..... 77

Introduction ..... 77
Methods ..... 79
Ethical Approval and Animals ..... 79
Implantation of Intracranial ICV Cannulae and Osmotic Pumps ..... 79
Hemorrhage Number and Severity Assessment ..... 80
Hermorrhage Volume ..... 81
Brain Water Content ..... 81
Video Tracking and Locomotor Activity ..... 82
Sunflower Seed Task ..... 82
Morris Water Maze ..... 83
Mas Co-localization Immunohistochemistry ..... 83
Stereology and Immunostaining ..... 84
qRT-PCR ..... 86
Direct Blood Pressure ..... 87
Indirect Blood Pressure ..... 87
Body weight ..... 88
Corticosterone ..... 88
Creatinine and BUN ..... 88
Kidney and Heart Pathology ..... 88
Chemicals ..... 89
Data Analysis ..... 90
Results ..... 90
Ang-(1-7) Treatment Improves Survival of Stroke-prone Spontaneously Hypertensive Rats ..... 90
Ang-(1-7) Treatment Decreases the Number and Severity of Hemorrhages in the Subcortex/Striatum, but not in the Cortex at the Time of Death of spSHR ..... 90
Ang-(1-7) Treatment has no Effect on Brain Hemorrhage Volume (Hemoglobin Content) or Water Content ..... 91
Ang-(1-7) Treatment Improves the Neurological Status of spSHR, but has no Effect on Visuospatial Memory ..... 91
Cellular Localization of Immunoreactive Mas in spSHR Striatum ..... 92
Ang-(1-7) Decreases Microglia and Increases Neuron Survival in the Striatum ..... 93
Ang-(1-7) does not Alter the Expression of Genes Related to Inflammation in Whole Brain Homogenate ..... 93

Ang-(1-7) has no Effect on Mean Blood Pressure during Infusion in spSHR, but Rats Treated with Ang-(1-7) have Lower Mean Blood Pressure later in Life after Treatment Ends ..... 94
Ang-(1-7) has no Effect on Body Weight, Corticosterone, Creatinine, BUN, or Kidney/Heart Pathology ..... 94
Discussion ..... 95

4 SUMMARY AND CONCLUSIONS ..... 111

Summary ..... 111
Specific Aim 1: Investigate the Mechanism of the Cerebroprotective Actions of Ang-(1-7) in Ischemic Stroke ..... 111
Specific Aim 2: Determine whether Ang-(1-7) also Exerts Cerebroprotective Actions in Hemorrhagic Stroke ..... 112
Discussion ..... 114

LIST OF REFERENCES ..... 123

BIOGRAPHICAL SKETCH ..... 145

LIST OF TABLES

Table page

2-1 PCR array data showing fold changes in gene expression in ipsilateral (right) cerebrocortical tissue 6 h after endothelin-1 (ET-1)-induced middle cerebral artery occlusion (MCAO) stroke compared to sham controls (0.9% saline instead of ET-1). ..... 67

2-2 PCR array data showing fold changes in gene expression in ipsilateral (right) cerebrocortical tissue 24 h after ET-1-induced MCAO stroke compared to sham controls. ..... 67

2-3 Degradation of Ang-(1-7) in media of primary mixed glial cultures ..... 68

3-1 Parameters used for stereology..... 99

LIST OF FIGURES


Figure page

1-1 Prevalence of silent cerebral ischemia for age ranges ..... 38

1-2 Two types of stroke ..... 39

1-3 Time course of mediators in ischemic stroke damage ..... 40

1-4 The two sides of NO. ..... 41

1-5 RAS components..... 42

1-6 Ang-(1-7) opposes AT1R signaling..... 43

1-7 Renin Angiotensin System axes are involved in the pathophysiology of stroke . 44

1-8 Summary of our focus on the therapeutic potential of the RAS ..... 45

2-1 Intracerebral pretreatment with Ang-(1-7) reduces infarct size 24 h after ET-1-induced MCAO ..... 69

2-2 Gene expression in ipsilateral (right) cerebrocortical tissue 6 h after ET-1-induced MCAO ..... 70

2-3 Gene expression of NOS isozymes and pro-inflammatory cytokines in ipsilateral (right) cerebrocortical tissue 24 h after ET-1-induced MCAO ..... 71

2-4 Gene expression of cell markers and migratory factors in ipsilateral (right) cerebrocortical tissue 24 h after ET-1-induced MCAO ..... 72

2-5 Levels of iNOS protein in ipsilateral (right) cerebrocortical tissue 24 h after ET-1-induced MCAO stroke or sham procedure..... 73

2-6 Cellular localization of immunoreactive Mas in normal rat cerebral cortex and 24 h after ET-1-induced MCAO ..... 74

2-7 Ang-(1-7) blunts lipopolysaccharide (LPS)-induced increases in nitrite in the media of primary mixed glial cultures ..... 76

3-1 Ang-(1-7) treatment improves survival of stroke-prone Spontaneously Hypertensive Rats (spSHR)..... 100

3-2 Ang-(1-7) treatment decreases the number of hemorrhages in the subcortex/striatum, but not in the cortex at the time of death of spSHR ..... 101

3-3 Ang-(1-7) has no effect on brain hemorrhage volume or water content..... 102

3-4 Ang-(1-7) treatment improves neurological status of spSHR ..... 103

3-5 Ang-(1-7) does not improve performance visuospatial memory as assessed by the Morris Water Maze Task ..... 104

3-6 Cellular localization of immunoreactive Mas in spSHR striatum ..... 105

3-7 Ang-(1-7) decreases activated microglia and increases neuron survival in the striatum just before treatment ends ..... 106

3-8 Ang-(1-7) does not alter the expression of genes related to inflammation in whole brain homogenate after treatment ends ..... 107

3-9 Ang-(1-7) administered intracerebroventricularly (ICV) has no effect on mean blood pressure during infusion in spSHR, but rats treated with Ang-(1-7) have lower mean blood pressure later after treatment ends ..... 108

3-10 Ang-(1-7) has no effect on body weight, corticosterone, creatinine, or BUN. ... 109

3-11 Ang-(1-7) has no effect on kidney or heart pathology just before treatment ends..... 110

4-1 Schematic of proposed mechanism..... 122

Abstract of Dissertation Presented to the Graduate School
of the University of Florida in Partial Fulfillment of the
Requirements for the Degree of Doctor of Philosophy

UNDERSTANDING THE CEREBROPROTECTIVE ACTIONS OF THE
ACE2/ANG-(1-7)/MAS AXIS DURING ISCHEMIC AND HEMORRHAGIC STROKE

By

Robert W. Regenhardt

August 2012

Chair: Colin Sumners
Major: Mecial Sciences – Physiology and Pharmacology

A recently characterized axis of the renin angiotensin system (RAS) has been the focus of much research in cardiovascular therapeutics. This axis is composed of angiotensin converting enzyme 2 (ACE2), which generates angiotensin-(1-7) (Ang-(1-7)) from angiotensin II (Ang II). Ang-(1-7) then exerts its effects through its receptor, Mas. Activating this axis in any number of ways is proving to have therapeutic potential in several disease states, including stroke. We previously showed that exogenous central Ang-(1-7) is cerebroprotective in an endothelin-1 (ET-1) induced model of middle cerebral artery occlusion (MCAO), decreasing the size of the infarct and improving rats' performance on neurological exams. These effects were observed without any changes to cerebral blood flow, percent vessel constriction, or blood pressure. Because of this, we began thinking of alternative mechanisms for this cerebroprotection.

Specific Aim 1 was desgined to screen for changes in the expression of certain genes that may be involved in decreasing the damage due to ischemic stroke, using the ET-1 induced MCAO model. In this study a PCR array was used to identify several markers of inflammation that were increased in stroke and blunted by ICV Ang-(1-7) therapy. It has previously been shown that damage due to stroke may be amplified by

excessive inflammation. The findings from the array and changes in the expression of other genes, namely iNOS, IL1α, CXCR4, and CD11b, were verified by real time PCR. A western blot was used to show that the changes in iNOS mRNA also existed at the protein level. To uncover which cell types were involved, we performed a co-localization study with the Ang-(1-7) receptor Mas and different cell markers. Microglia, endothelial cells, and neurons express Mas. Furthermore, we showed that Ang-(1-7) has a Mas dependent in vitro anti-inflammatory effect to blunt nitric oxide production in a mixed glia culture system after LPS insult. These findings indicate for the first time an anti-inflammatory property of Ang-(1-7) treatment in the CNS and provide a potential mechanism of cerebroprotection.

As we demonstrated Ang-(1-7) had an *in vivo* anti-inflammatory effect during MCAO in rats and an *in vitro* anti-inflammatory effect in a mixed glia culture system in Specific Aim 1, Specific Aim 2 was designed to examine the therapeutic potential of this peptide in hemorrhagic stroke. There is much overlap in the pathophysiology of ischemic and hemorrhagic stroke, especially regarding the role of excessive inflammation. We fed stroke-prone Spontaneously Hypertensive Rats (spSHR) a high salt diet from the time of weaning and administered Ang-(1-7) centrally for 6 weeks starting at 49 days of age. Ang-(1-7) increased the survival of spSHR and decreased the number of hemorrhages in the striatum. spSHR treated with Ang-(1-7) also showed less lethargy and improved neurological status. We confirmed the presence of the Ang-(1-7) receptor Mas on neurons, microglia, and endothelial cells and showed that Ang-(1-7) decreases the number of microglia and increases the number of neurons in the striatum. There was no effect of Ang-(1-7) on markers of peripheral disease, such as

kidney pathology, heart pathology, body weight, corticosterone levels, or extent of hypertension. This supports that the actions of this peptide are indeed primarily central in our model. These findings indicate for the first time ICV Ang-(1-7) has cerebroprotective actions in hemorrhagic stroke and can increase the survival of spSHR.

# CHAPTER 1
# STROKE AND THE ROLE OF THE RENIN ANGIOTENSIN SYSTEM

## Stroke Epidemiology

In the United States, stroke is the fourth leading cause of death and a major cause of severe, long-term disability. A stroke occurs every 40 seconds and results in a death every 4 minutes. Each year 795,000 people experience a stroke, with primary strokes accounting for 610,000 and secondary strokes accounting for 185,000. Stroke prevalence in adults is 2.6% for men, 2.6% for women, 2.4% for Caucasians, 4.0% for blacks, 1.4% for Asians, 2.5% for Hispanics, and 5.8% for Native Americans [1]. The estimated cost attributed to treating stroke in 2009 was $68.9 billion. Risk factors for stroke include: atrial fibrillation, hypertension, diabetes, smoking, advancing age, low levels of physical activity, dyslipidemias, hormone replacement therapy, and pregnancy/postpartum period [2]. Patients who have a primary stroke or transient ischemic attack are also at an increase risk of having a recurrent stroke [3]. Interestingly, there are many subclinical infarcts that are discovered incidentally during imaging studies. The prevalence of these silent cerebral infarctions increases dramatically with age (Figure 1-1) [4]. A multitude of evidence supports the importance of studies for preventing and treating stroke.

Strokes can be classified into two types: ischemic and hemorrhagic (Figure 1-2). Ischemic stroke occurs when blood supply to the brain is decreased by a blocked vessel, depriving the brain of oxygen and nutrients. Hemorrhagic stroke, in contrast, occurs when a blood vessel within the brain ruptures and releases blood into the brain [2]. Of all reported strokes, 80-90% are ischemic strokes and 10-20% are an intracerebral hemorrhagic strokes and subarachnoid hemorrhages. The treatment of ischemic

strokes is focused on restoring cerebral blood flow to the affected vascular territory, currently most commonly through the use of systemic administration of recombinant tissue Plasminogen Activator (rtPA). Despite the existence of rtPA, only 4-8% of patients with stroke are candidates for thrombolytic therapy because of the high risk of hemorrhagic transformation and a limited window of time for treatment after stroke onset [4]. On the other hand, hemorrhagic strokes, while being less prevalent, can be even more difficult to treat with virtually no medical therapies. Furthermore, hemorrhagic stroke has a disproportionate affinity for Asians and African Americans [5]. Patients with hemorrhagic strokes have very poor prognoses, often much worse than ischemic strokes of similar size. In fact, up to 30% of patients with ischemic stroke undergo hemorrhagic transformation [6], and many patients with ischemic strokes develop hemorrhages and symptomatic hematomas following thrombolysis [7].

Regardless of type, the outcome of stroke is essentially the same. Neuronal death and consequent behavioral and motor symptoms result from the absence of oxygen and nutrients and/or sudden bleeding into the brain. It is of critical importance to advance our understanding of the mechanisms underlying stroke and to investigate new strategies for therapeutics as stroke has an extremely high prevalence and there are very few therapeutic options.

## Pathophysiology of Ischemic Stroke

The greatest risk factors for ischemic stroke are hypertension and other cardiovascular dysregulation/disease. The etiology of ischemic stroke can be classified into a few different categories that aid in understanding the pathophysiology and treatment [8]: cardioembolic stroke, large-artery atherosclerosis, small-artery occlusion, stroke of other determined causes, and stroke of undetermined causes [9]. A majority of

ischemic strokes are thromboembolic, with the middle cerebral artery being most commonly affected [10]. Most patients who suffer from ischemic stroke have some degree of reperfusion either spontaneously or as a result of thrombolytic therapy [10, 11]. A cascade of pathological events is associated with this sequence of ischemia followed by reperfusion, progressing through cerebral hypoperfusion, excitotoxicity, oxidative stress, blood brain barrier dysfunction, microvascular injury, hemostatic activation, post-ischemic inflammation, and cell death [12]. Within the ischemic core this cascade progresses quickly, resulting in a loss of neuronal function demonstrated by EEG flattening and irreversible cell death due to severe hypoperfusion. In contrast, within the surrounding tissue, or the ischemic penumbra, there is less severe hypoperfusion and the tissue remains viable. The penumbra is believed to be the primary target for treatment since it can be saved. In the penumbra there is a loss of neuronal function demonstrated by EEG flattening, but there is no cell death [13-16]. Tissue in this area can, however, progress to irreversible injury and expand the ischemic core depending on the severity and duration of ischemia [12].

Necrosis, the type of cell death involving energy depletion and loss of ionic gradients resulting in cellular swelling and membrane disruption, occurs during stroke. It occurs primarily in the ischemic core, where a lack of oxygen and glucose results in diminished ATP levels [17, 18]. This results in inhibition of the Na+-K+ ATPase causing cell depolarization and release of neurotransmitters, including glutamate, from neurons and astrocytes [19-21]. Excess glutamate activates ionotropic glutamate receptors on neurons and astrocytes that causes release of more glutamate in positive feedback fashion to increase intracellular calcium and cause excitotoxicty [22]. Furthermore, with decreased

oxygen levels there is electron leakage from the electron transport chain generation of reactive oxygen species [23]. Protons and lactate also accumulate due to glycolysis in the absence of oxidative phosphorylation [18]. These cells in the core undergo terminal depolarization as a result of the dramatic decrease in blood flow. Cells in the penumbra undergo transient ischemic depolarization as the reduction in blood flow is not as great. Still, transient depolarization can evolve into terminal depolarization and expand the core [24].

Apoptosis, parthanatos, and autophagy, types of programmed cell death, also occur during stroke. In contrast to necrosis, programmed cell death occurs primarily in the ischemic penumbra, but can also occur in the core to some extent [25]. The process of apoptosis differs from necrosis in that cell death occurs with minimal inflammation and energy must be expended during the process [12]. When mitochondria release cytochrome c, apoptotic cascades are activated that activate caspase 3, a common effector molecule in apoptosis. Parthanatos is programmed cell death that occurs independent of caspase activity. In parthanatos, ischemic reperfusion injury involves an increase in poly(ADP-ribose) (PAR) polymer from poly(ADP-ribose) polymerase-1 (PARP1) [26]. PAR polymer translocates from the nucleus to the cytoplasm and mitochondria, where it causes the release of apoptosis inducing factor (AIF) from mitochondria [27]. Parthanatos is believed to be very involved in ischemic penumbra injury [28]. AIF can also be released independent of parthanatos. The calcium-dependent protease calpain I can cleave an N-terminal fragment of AIF that results in its release from mitochondria. AIF and calpain I have been implicated as being important in cell death during stroke as inhibiting them is neuroprotective [28]. Autophagy is another

programmed cell death that can be triggered by endoplasmic reticulum stress and oxidative stress [29]. It is normally involved in the organelle and protein turnover, but can be involved in cell death during ischemia. Autophagy promoting beclin 1 and microtubule-associated protein 1 are upregulated in the penumbra, and inhibition of these has been shown to decrease cell death during ischemia [30-32].

Reperfusion injury also plays a big role in the pathophysiology of ischemic stroke. Reperfusion can occur after ischemia either spontaneously or due to thrombolytic therapy. It has the potential to create a paradoxical injury to brain tissue despite the improved cerebral blood flow that can occur. This is due primarily to the production of reactive oxygen species by NADPH oxidase [23]. Reperfusion also leads to the release of proinflammatory cytokines which activate inflammatory cascades. These can lead to breakdown of the blood brain barrier by matrix matalloproteinases and microvascular injury resulting in brain swelling and hemorrhagic transformation [12, 33]. Despite the risks of reperfusion injury, much evidence suggests that early reperfusion is associated with improved final outcomes compared to delayed reperfusion [10].

Excessive inflammation plays a significant role in the damage due to stroke, as well. During stroke, proinflammatory cytokines are released by astrocytes, microglia, smooth muscle cells, and endothelial cells [12]. These cytokines, including TNF-α, IL-1ß, and IL-6, are associated with an increase in inducible nitric oxide synthase (iNOS), activation of microglia, early invasion of neutrophils, and transmigration of adhesion molecules. Inflammation that occurs at the blood-endothelium interface, involving cytokines, adhesion molecules, chemokines, and leukocytes, is a major cause of the tissue damage in stroke [34]. After middle cerebral artery occlusion, TNF-α, IL-1ß, IL-6,

iNOS, and phosphorylated ERK1/2 are increased in smooth muscle cells of the middle cerebral artery and in associated intracerebral microvessels. Inhibiting the phosphorylation of ERK decreases the tissue damage and the cytokine and iNOS production after cerebral ischemia [35]. Inflammatory effects take place over a time course following the initial ischemic event (Figure 1-3). Early immediate genes are activated within a few hours. These include c-fos, c-jun, and zif-268. Soon after, the heat shock proteins, HSP70 and HSP72, are activated. Beginning after a few hours and peaking after a day, the cytokines and adhesion molecules are upregulated. Lastly, other late inflammatory mediators and apoptosis genes, such as iNOS, COX-2, and p53, are upregulated beginning around 12 hours and peaking at 2 days [36, 37].

The expression of iNOS has been shown to be dramatically upregulated in the brain following cerebral ischemia [38]. Furthermore, iNOS-specific inhibition and gene knockout has been shown to decrease infarct size and improve performance of neurological exams in a rat model of MCAO [39, 40]. The expression of iNOS has been confirmed in human cerebral infarcts [41]. It is important to point out that nitric oxide (NO), the product of NOS isozymes, plays an important physiological role in lower concentrations in the pM-nM range. At these levels, it is usually produced by endothelial NOS (eNOS) and is important for vasodilation and neurotransmission. However, at higher toxic levels in the μM-mM range, it is usually produced by iNOS and leads to nitrosylation of proteins and cell damage (Figure 1-4) [36, 37]. It should be stated that inflammation in general is not a bad process. There is much evidence about inflammatory injury after stroke, but inflammation can also be a protective process that attempts to limit damage and restore tissue architecture by eliminating damaged cells

and repairing extracellular matrix [42]. The damage occurs when inflammatory responses are uncontrolled.

## Pathophysiology of Hemorrhagic Stroke

Hypertension is the main risk factor for spontaneous hemorrhagic stroke. Increased blood pressure can result in the formation of microaneurysms at the bifurcation of arterioles. Persistent hypertension has been shown to damage the walls of small vessels [43, 44]. Hemorrhagic strokes most commonly occur in the putamen, caudate, and thalamus. They can also occur in the hemispheres (lobar), cerebellum, or pons. The key factor that determines outcome in hemorrhagic stroke is hemorrhage volume; bleeds that are greater 150 mL cause cerebral perfusion pressure to drop to zero, resulting in death. Most patients with bleeds smaller than 140 mL, however, will survive the initial ictus. Unfortunately, the hematoma itself can lead to secondary brain injury in these patients resulting in severe neurological deficits and possibly delayed death [45].

Early pathological changes and injuries of hemorrhagic stroke include hematoma expansion, midline shift, apoptosis, and necrosis. The physical disruption of adjacent tissue and mass effect of the resulting hematoma accounts for part of the injury during hemorrhagic stroke. More than two-thirds of patients stop bleeding shortly after the ictus [46] and about one-third experience hematoma enlargement [47-52]. This enlargement contributes to midline shift and hastens neurological deterioration [47, 53]. Most re-hemorrhage occurs within the first 24 hours, however the precise mechanism for this is unknown [50, 52]. Various models show that apoptosis takes place in the brain adjacent to a hemorrhage[45-50, 52-59]. Apoptosis has also been detected in the perihematomal zone in

humans [60] Necrosis, likely caused by mechanical forces and chemical toxicity, is also found adjacent to the hematoma [61].

Edema also develops almost immediately after hemorrhagic stroke and peaks a few days later [61-64]. Unfortunately, this increasing edema raises intracranial pressure and can result in herniation [65]. In animal models, perihematomal edema has been shown to be present primarily in white matter [15, 66]. Edema occurs in three phases. First, in the initial few hours, hydrostatic pressure increases and clot retraction occurs where serum moves from the clot into the surrounding tissue [62]. Second, in the first two days, the coagulation cascade is activated and thrombin production is increased. Third, erythrocytes lyse and hemoglobin toxicity occurs. The main form of edema in hemorrhagic stroke is vasogenic. This is primarily due to disruption of the blood-brain barrier following stroke. Although the blood-brain barrier remains intact to large molecules for the first several hours following hemorrhage [62], the permeability is dramatically increased by 8-12 hours [67].

A prolonged mass effect resulting in physical trauma and reduced cerebral blood flow also contributes to injury mechanisms that may account for damage in hemorrhagic stroke. A comparison of autologous whole blood to an oil-wax mixture showed that although edema was present following both injections, it was more severe around the clots formed from the blood [61]. This suggests that the edema observed in hemorrhagic stroke is not generated by a mass effect alone. In a rat model, microballoon inflation in the basal ganglia increased intracranial pressure, transiently reduced cerebral blood flow, and caused brain damage [68]. In patients, hematoma mass causes neurological deficits, but the mass alone induces little edema immediately after hemorrhage.

Controversy exists in the field about the role of secondary ischemia due to the mass effect. Rat studies have shown that cerebral blood flow near hematomas does decrease, but only partially and transiently [67, 69, 70]. A dog model demonstrated that no ischemic zone could be found in the first 5 hours. Furthermore, neither thrombin nor hemoglobin, two main causes of brain damage in hemorrhagic stroke, significantly decreases cerebral blood flow in animals [63, 71]. In studies of patients, oxygen extraction fraction was reduced in the perihematomal zone compared to the contralateral side due to decreased cerebral metabolic rate of oxygen and cerebral blood flow [72]. This suggests that, at least acutely, there is a zone of hypoperfusion without ischemia. MRI studies confirmed no cerebral ischemia in the area surrounding the hematoma [73]. Cerebral blood flow is reduced, however, as shown by single photon CT [74, 75]. General atrophy of the brain has been observed in patients with hemorrhagic stroke [76] and in rat models [64, 77]. In a rat model, ipsilateral striatum volume was reduced by 20% with an increased ipsilateral ventricular size 3 months after the hemorrhage was initiated [77].

Thrombin also plays a role in the mechanism of injury in hemorrhagic stroke. A serine protease essential to the coagulation cascade, thrombin is produced immediately in the brain following hemorrhagic stroke. Large dose infusions of thrombin into the brain cause inflammatory cell infiltration, mesenchymal cell proliferation, scar formation, edema formation, and seizures in animal models [71, 71, 78-83]. High concentrations of thrombin also induce apoptosis [84] and kill both astrocytes and neurons in vitro [85-87]. Further in vitro studies have demonstrated that thrombin can potentiate glutamate N-methyl-D aspartate receptor function [88] and activate microglia [89]. Two thrombin inhibitors, hirudin and argatroban, have been shown to inhibit edema formation in a rat

model of hemorrhagic stroke [82, 90]. Argatroban was also shown to reduce edema when given systemically to patients 24 hours after hemorrhage [91]. Interestingly, low concentrations of thrombin, however, are believed to be neuroprotective [85, 86, 92]. In addition to cleaving fibrinogen to fibrin, thrombin has receptor-mediated effects at three protease-activated receptors, PAR-1, PAR-3, and PAR-4 [93-95]. These receptors are expressed in both neurons and astrocytes [96, 97] and have been shown to mediate some of the pathological effects of thrombin in brain pathophysiology [98-100]. Human brain tissue has also been confirmed to possess thrombin receptor immunoreactivity [100].

Hemoglobin toxicity is another mechanism of injury resulting from hemorrhagic stroke. Erythrocyte lysis occurs several days after the initial hemorrhage in rats, dogs, and human patients [78, 101, 102]. Evidence exists to suggest that erythrocyte lysis may be related to delayed brain edema and associated midline shift [53]. In a dog model, hemoglobin concentrations in the cerebrospinal fluid peaked 2 days after blood injection into the subarachnoid space [103]. This demonstrated that erythrocyte lysis can occur remarkably early. Furthermore, hemoglobin and heme were present in the perihematomal zone one day after hemorrhagic stroke in a rat model [104]. This result is confirmed by other studies that erythrocyte lysis can occur within 24 hours [105, 106]. Experimental infusion of lysed erythrocytes to show the toxicity of their contents, when compared to whole packed erythrocytes, results in more edema formation, disruption of the blood-brain barrier, strong neuronal expression of heatshock protein 70, and DNA injury within 24 hours [63, 78, 107, 108]. In the brain, heme oxygenase degrades heme into iron, carbon monoxide, and biliverdin [109]. The infusion of hemoglobin and its degradation products directly has also been shown to cause brain damage [110, 111].

Furthermore, inhibitors of heme oxygenase and iron chelators reduce this injury and edema [106, 110, 112, 113]. Brain non-heme iron increases three fold after hemorrhagic stroke in rats, resulting in iron overload [105].

Inflammation and complement have a strong role in the mechanism of injury in hemorrhagic stroke, as well. The inflammatory response begins soon after hemorrhage and peaks several days later in humans and animal models [58, 101, 114, 115]. The infiltration of neutrophils occurs within 2 days, and the activation of microglia may continue for 1 month [114, 116]. Evidence supports a role of microglia in hemorrhagic stroke pathology because inhibiting their activation reduces damage [117, 118]. Inflammation is also associated with the production of matrix metalloproteinases, which have been shown to increase in collagenase-induced models of hemorrhagic stroke. These enzymes have been shown to disrupt the blood-brain barrier and cause secondary injury, but their precise role remains controversial [119-121]. In the healthy brain, complement is unable to cross the blood-brain barrier. In the hemorrhaged brain, however, it can enter the brain parenchyma through the extravasated blood or through the degraded barrier. Evidence supports that the complement cascade is activated in hemorrhagic stroke and that it contributes to edema; when the complement cascade is inhibited, there is decreased perihematomal edema in rats. One complement component in particular, the membrane attack complex (MAC), is hypothesized to lyse erythrocytes, neurons, glia, and endothelial cells [122]. MAC also causes the release of cytokines, oxygen radicals, and matrix proteins. There is believed to be a strong association between inflammation and edema, as evidenced by data that correlates plasma tumor necrosis factor alpha concentrations in patients with hemorrhagic stroke to the degree of brain edema [123].

## Renin Angiotensin System Components

The renin angiotensin system (RAS) (Figure 1-5) was first discovered as a circulating endocrine system. Its components are produced in various organs and secreted into the blood [124]. Renin is an enzyme produced in the kidneys that converts liver-derived angiotensinogen (ATG) to angiotensin I (Ang I). Another enzyme, angiotensin converting enzyme (ACE), is made in the pulmonary endothelium and converts Ang I to Angiotensin II (Ang II) [125]. Highly involved in blood pressure (BP) regulation, fluid balance, and electrolyte homeostasis, Ang II is one of the primary mediators of RAS activity [124, 126, 127]. It has been shown that several Ang II receptor types exist [128-130]. Most of the classically described physiological effects of Ang II are mediated through the Ang II type 1 receptor (AT1R). Together, these components make up what is referred to as the ACE/Ang II/AT1R axis of the RAS. Another receptor for Ang II, the Ang II type 2 receptor (AT2R) primarily opposes AT1R action [124, 131]. Several drugs have been developed that target the RAS for the treatment of hypertension, most aiming to block the ACE/Ang II/AT1R axis. At present, ACE inhibitors (ACEi) and AT1R blockers (ARBs) are among the first line drugs to treat hypertension [132]. Recent advances in the RAS field have demonstrated that this system is more ubiquitous than just a circulating endocrine system. In fact, there are several tissue specific paracrine RAS, which have been identified in the brain, heart, kidneys, pancreas, skin, intestines, and many other organs [133].

Ang II acting through AT1R is heavily implicated in the promotion of stroke and cardiovascular disease. Activation of AT1R in both the circulation and specific organs increases BP and promotes organ damage. In contrast, activation of AT2R opposes AT1R and counters the deleterious effects [134]. Another axis of the RAS also opposes

AT1R, known as the angiotensin converting enzyme 2 (ACE2)/angiotensin-(1-7) (Ang-(1-7))/Mas axis. ACE2 was recently discovered in 2000 and has been shown to convert Ang II to Ang-(1-7) with high efficiency [135-137]. The receptor for Ang-(1-7) was discovered to be a G protein-coupled receptor, Mas, which was initially identified as an orphan protooncogene in 2003 [138].

Although the primary way by which Ang-(1-7) is generated is through the action of ACE2 on Ang II, several other pathways for Ang-(1-7) production exist. These pathways can be either ACE dependent or ACE independent. ACE dependent pathways involve the conversion of either Ang I to Ang II by ACE then Ang II to Ang-(1-7) by ACE2 [135] or the conversion Ang I to Ang-(1-9) by ACE2 then Ang-(1-9) to Ang-(1-7) by ACE [136]. However, ACE2 is 400 times more efficient at catalyzing the conversion of Ang II to Ang-(1-7) than Ang I to Ang-(1-9), so the pathway involving Ang-(1-9) as an intermediate is likely not as important [139]. ACE independent pathways to generate Ang-(1-7) involve other enzymes, including neprilysin, prolyl-endopeptidase, prolyl-carboxypeptidase, chymase, and cathepsin A [140-143]. Each of these enzymes, however, lacks specificity for angiotensin peptide metabolism and is likely only a minor contributor to Ang-(1-7) synthesis under physiological conditions. They may become more relevant during pharmacological ACE inhibition. Therefore, the predominant theory in the RAS field is that ACE2 is the key regulator for the generation of Ang-(1-7).

As more is learned about the RAS, more components are being discovered making this system increasingly complex. The (pro)renin receptor ((P)RR), discovered in 2002, has been shown to be a receptor for both renin and its precursor prorenin. Binding of renin to (P)RR increases the conversion of ATG to Ang I, and ultimately

results in activation of ACE/Ang II/AT1R axis [144]. In addition, binding of either ligand can have Ang II independent effects through an intracellular signaling cascade that can trigger the expression of profibrotic genes [145]. Other more recently described RAS components, including Ang III and Ang IV, and the enzymes that produce them, aminopeptidase A and aminopeptidase N, have some pressor effects and also their own unique physiological and pathological actions such as memory function [146]. The RAS is a complex system, containing checks and balances to regulate many physiological actions, including cardiovascular function. Many pathways within this system provide good targets for cardiovascular disease and stroke drug development.

**Ang-(1-7)/Mas Opposes Ang II/AT1R Signaling**

AT1R activation has been shown to be involved in the pathophysiology of many cardiovascular diseases, including hypertension, cardiac hypertrophy, cardiac fibrosis, atherosclerosis, myocardial infarction, stroke and many others [137]. AT1R's involvement in these disorders is mediated through several functions, such as contraction growth, altering cell migration, endothelial dysfunction, expression of proinflammatory cytokines, and modification of extracellular matrix [147]. Interestingly, Mas activation has been shown to counteract much of these pathological functions (Figure 1-6) [148]. Targeting this interplay between AT1R and Mas signaling cascades may prove to have novel therapeutic potential.

The AT1R is a seven transmembrane G protein coupled receptor that mediates most of Ang II's well-known effects [149]. These effects are mediated through several signaling cascades, some G protein coupled and others non-G protein coupled. Phospholipase C (PLC), phospholipase D (PLD), and phospholipase $A_2$ ($PLA_2$) mediate the AT1R-induced G protein coupled pathways [150, 151]. AT1R-induced activation of PLC

converts phosphatidylinositol 4,5-bisphosphate ($PIP_2$) into inositol-1,4,5-triphosphate (IP3) and diacylglyerol (DAG). $IP_3$ can then bind to a receptor on the sarcoplasmic reticulum to increase intracellular $Ca^{2+}$ which binds to calmodulin and activates myosin light chain kinase (MLCK). In turn, MLCK phosphorylates the myosin light chain to cause smooth muscle cell contraction [152]. At the same time DAG activates Protein Kinase C (PKC) which stimulates the Ras/Raf/MEK/ERK pathway causing vasoconstriction and promoting cellular growth and proliferation [153]. Also, stimulation of AT1R and subsequent activation of PLD hydrolyzes phosphatidylcholine (PC) to choline and phosphatidic acid (PA) [147]. PA is then converted to DAG, which activates PKC to have the effects described above. Lastly, AT1R-induced activation of PLA2 cleaves arachidonic acid (AA) from PC. AA, through the actions of lipoxygenase (LO) and cyclooxygenase (COX), is converted to leukotrienes (LT) and prostaglandins (PG), respectively. LT and PG then influence smooth muscle contraction and inflammation [154].

In contrast, NAD(P)H oxidase (NOX), mitogen-activated protein kinases (MAPK), Src, JAK/STAT, FAK, Pyk2, and receptor tyrosine kinases mediate the AT1R-induced non-G protein coupled pathways [154]. Evidence suggests that non-G protein and G protein pathways may actually be closely integrated. For instance, AT1R stimulation can activate NOX *via* phosphorylation of Src/EGFR/PI3K/Rac-1 and PLD/PKC/p47phox. NOX then generates superoxide, hydrogen peroxide, and other reactive oxygen species (ROS). The phosphorylation of p38MAPK, Akt/PKB, Src, EGFR, and other messengers requires this activity [155]. These intracellular messengers and signaling molecules are heavily implicated in cell proliferation, endothelial dysfunction, inflammation, and atherosclerosis. In addition, AT1R stimulation activates MAPK signaling pathways.

ERK1/2, JNK, and p38MAPK are some examples that contribute to cell differentiation, proliferation, migration, and fibrosis in vessel walls. AT1R-induced activation of nonreceptor tyrosine kinases, such as c-Src, activate many downstream components, including Ras, JAK/STAT, PLC, and AP-1. JAK and STAT proteins can then dimerize and translocate to the nucleus, where they influence transcription. Lastly, AT1R stimulation can activate receptor tyrosine kinases, such as EGFR and PDGFR, and inhibit insulin receptor signaling [154]. Given the multitude of signaling pathways and redundancies, it is not surprising that other RAS receptors, namely AT2R and Mas, might have interacting/counteracting intracellular signaling cascades.

Similar to AT1R, Mas is a seven transmembrane G protein coupled receptor. In fact, there is evidence that Mas can directly dimerize and inhibit AT1R [156, 157]. In addition, Mas stimulation can have effects to counter signaling, such as inhibiting AT1R-mediated phosphorylation of p38MAPK, ERK1/2, and JNK [158, 159]. Furthermore, Mas-induced activation of SHP-2 can disrupt AT1R-mediated activation of c-Src, ERK1/2, and NOX [148, 160]. Where AT1R stimulation causes vasoconstriction, Mas stimulation causes vasorelaxation by inducing an increase in eNOS activity through the phosphatidylinositol 3-kinase (PI3K)/Akt pathway [148]. Stimulation of Mas also causes AA release and $PGI_2$ production to potentiate bradykinin signaling [161-164].

**Targeting the Renin Angiotensin System for Stroke Therapy**

Many factors are involved in the pathophysiology of stroke, yet the RAS appears to play a key role (Figure 1-7). As hypertension is one of the most important modifiable risk factors for both types of stroke and manipulating the RAS through the use of ARBs and ACEi is the standard of care for hypertension, there is much interest in the therapeutic potential of RAS manipulation in stroke. The classical ACE/Ang II/AT1R axis

has received the most attention for its potential involvement in stroke pathophysiology. Ang II levels have been shown to increase in the cortex and hypothalamus following stroke [165]. Blocking the effects of Ang II by ARB treatment has been shown to have therapeutic potential in both hemorrhagic and ischemic stroke. Many studies, utilizing both animal models and human clinical trials, have shown a decrease in cardiovascular risk and improvement in stroke prevention when blocking this axis [166-168]. The occurrence of hemorrhagic stroke is reduced in stroke-prone Spontaneously Hypertensive Rats (spSHR) when ARBs are administered systemically [169, 170]. Ischemic stroke is also a therapeutic target of ARBs as demonstrated by several studies in normal rats and spontaneously hypertensive rats (SHR) that undergo ischemia by middle cerebral artery occlusion (MCAO). ARBs were shown to reduce the infarct size by 40-50%, reduce the neurological deficits, and improve recovery [168, 171-175]. In addition, our lab has shown a robust cerebroprotective effect of the ARB candesartan in an endothelin (ET-1)-induced MCAO model in rats [176]. Interestingly, these therapeutic effects are, at least partly, independent of BP lowering effects [168, 175]. In addition, AT1R-deficient mice have smaller infarcts compared to controls after undergoing MCAO [177]. Further support that blocking AT1R has additional effects than simply lowering BP is provided by the fact that other antihypertensive drugs, such as β-adrenergic receptor blockers and Ca channel blockers, do not protect against ischemia [171, 172]. Also the cerebroprotective effects of ARBs are seen when given peripherally and centrally [168-175, 177, 178]. That the ARBs candesartan and valsartan cross the blood brain barrier readily and that systemic administration of these drugs for cerebroprotection has been utilized

in non-blood pressure lowering doses provides further evidence that these drugs have effects independent of BP lowering.

There are a few theories that have been proposed for the mechanism by which ARBs afford cerebroprotection. The two broad sites of action would have to be either the cerebrovasculature or the brain parenchyma. Examples of effects to the cerebral vessels in rat pretreatment models include increasing capillary density [179], improving cerebrovascular reserve [180], and improving cerebral endothelial function [181]. There are different proposed theories to how these cerebrovascular effects may occur, including AT1R blockade alone [182] or unopposed agonism of the AT2 or Ang II type 4 receptors [175, 183]. An example of a parenchymal effect is that agonism of the AT2R stimulates post stroke neurite outgrowth and improves neuron survival under hypoxic conditions [175]. Another is that AT1R blockade has been shown to protect neurons during hypoxia by decreasing oxidative stress [184]. As more evidence mounts, there is support for both theories working in concert.

In addition to many animal studies, many clinical trials show the therapeutic effects of ARBs. Interestingly, the Losartan Intervention For Endpoint (LIFE) clinical trial demonstrated that ARBs are more effective against stroke than β-adrenergic receptor blockers, common antihypertensive agents, in patients with hypertension and left ventricular hypertrophy [167]. The Study on Cognition and Prognosis in the Elderly (SCOPE) has demonstrated the effectiveness of ARBs in stroke prevention [185]. In the Captopril Prevention Project (CAPPP) study, ACE inhibitors were shown to be inferior to conventional therapy for stroke prevention [186]. This lead to the idea that perhaps increased levels of Ang II in response to ARBs, presumably acting at another receptor,

may play a role in their cerebroprotective effects [175, 186]. This and other studies lead to further investigation of the role of AT2R in stroke.

As mentioned above, there is debate about whether the cerebroprotective effects of ARBs occur because of decreased activation of AT1R or unopposed activation of AT2R [169, 170, 175, 178, 187, 188]. The role of AT2R in stroke has been the topic of many recent studies. The effects of Ang II at this receptor are often exactly opposite those at AT1R [189]. Furthermore, tissue levels of AT2R are increased following many injuries and disease states, including the heart after myocardial infarction, atherosclerotic blood vessels, wounded skin, and the peri-infarct region in the brain following ischemia [165, 175, 190-192]. There is also evidence that AT2R stimulation in neurons leads to differentiation/regeneration and plays a role in neurotrophic actions [193-195]. Because of this, it has been theorized that the increased expression of AT2R in the peri-infarct region can be activated by the raised endogenous levels of Ang II during ARB treatment to exert neuroprotective effects [175]. There is much support for this hypothesis. In an experiment utilizing an MCAO model of stroke where ARBs were given with an AT2R antagonist, the beneficial action was lost [175]. Also, ARBs have been shown to be more effective in stroke than ACEi in a rat model of ischemia and reperfusion [178]. When comparing AT2R knockout mice to wild-type controls using MCAO, the AT2R knockout mice show more brain damage [187]. Furthermore, central administration of an AT2R-specific agonist has cerebroprotective effects during ischemic stroke [188]. We have also shown that peripheral, post-stroke administration of the AT2R agonist C21 has robust cerebroprotective effects in MCAO, where infarct size is reduced and rats perform better on neurological exams (unpublished data).

Similar to activation of the AT2R, activation of the ACE2/Ang-(1-7)/Mas axis is just beginning to receive more attention for its therapeutic potential in cardiovascular disease [196]. Activating this axis has been demonstrated to be effective for the treatment of hypertension, hypertension-related pathology, myocardial infarction, and heart failure [197-203]. There is also evidence that activating this axis may have therapeutic potential in stroke. Peripheral administration of Ang-(1-7), both acutely and chronically, has been shown to increase cerebral blood flow [204-206]. Another study showed that central administration of Ang-(1-7), given shortly after stroke, increased bradykinin levels and upregulated bradykinin receptors in the brain [207]. Using this same model, Ang-(1-7) caused an increase in NO release and eNOS activity [208].

Furthermore, the components of the ACE2/Ang-(1-7)/Mas axis are present in the brain providing support that this axis may be targeted for stroke therapy. In fact, Mas was first characterized as a protooncogene found highly expressed in the brain [209]. It was originally thought to be present only in neurons [210]. In rats and mice, Mas mRNA was detected throughout the brain in areas such as the hippocampus, cortex, olfactory bulbs, and thalamus [209-212]. Mas has also been detected in rat endothelial cells in the brain [213]. Immunofluorescence studies have confirmed the mRNA studies, showing Mas immunoreactivity in both cardiovascular control areas and other areas of the brain [204]. Neurons were described as being the main cell type with Mas immunoreactivity in cardiovascular control regions of the brain, but there was no description of other brain areas. ACE2 has also been detected in the brain, including in human tissue where low levels of mRNA were present [214]. Furthermore, an immunofluoresence study using human brain showed positive staining in vascular smooth muscle and endothelial cells

[215]. Cell culture experiments have shown that glia have ACE2 [216]. In vivo mouse studies have shown ACE2 mRNA and protein to be predominantly located in neurons, however. It was shown to be present throughout the brain, in cardiovascular control regions, brainstem, raphe, motor cortex, and many other areas [217]. In summary, Mas and ACE2 are present throughout the brain, implying the possibility of a local ACE2/Ang-(1-7)/Mas axis.

We have recently demonstrated for the first time that ICV Ang-(1-7) affords cerebroprotection in an ET-1-induced MCAO model of ischemic stroke [218]. Ang-(1-7) had no effect on % baseline vessel diameter during stroke, nor on % baseline cerebral blood flow during stoke. ET-1 injection very significantly decreased both of these parameters. Treatment of Ang-(1-7) did decrease infarct size by more than 50% compared to control stroked animals. The decrease in infarct size was prevented by co-administration of the Mas antagonist, A-779, indicating a Mas dependent pathway. Ang-(1-7) also Mas-dependently improved performance of several neurological exams, including the Bederson exam, Garcia exam, and sunflower seed eating task. We also demonstrated that pharmacological activation of the ACE2/Ang-(1-7)/Mas by administration of the putative ACE2 activator diminazine aceturate (DIZE) had the same effects as exogenous Ang-(1-7). Further studies are indicated to determine the mechanism of this cerebroprotective action of stimulating the ACE2/Ang-(1-7)/Mas axis during stroke.

## Summary

Although the risk factors for stroke are well known, few effective preventative or acute therapies exist making it a leading cause of mortality and morbidity. In recent years, the RAS has been given more attention for its therapeutic potential (Figure 1-8).

Targeting the ACE2/Ang-(1-7)/Mas axis in stroke makes sense as the components are present within the brain, in both the cerebrovasculature and parenchyma. In addition, peripheral acute stimulation of Mas by Ang-(1-7) administration and chronic peripheral over-expression of ACE2 both increase cerebral blood flow. Central administration of Ang-(1-7) causes increases in bradykinin, eNOS activity, and NO production after stroke. Furthermore, we have shown a cerebroprotective effect of central stimulation of the ACE2/Ang-(1-7)/Mas axis in an ET-1-induced MCAO model of ischemic stroke. However, in this model we did not observe any effect on blood flow.

In summary, there is much evidence supporting a protective role for the ACE2/Ang-(1-7)/Mas axis in the cardiovascular system, including the ET-1 induced MCAO model of ischemic stroke. Therefore, we aim to uncover the mechanism of protection in this stroke model and also to examine if activation of this axis has any therapeutic potential in hemorrhagic stroke. Therefore, two Specific Aims were designed using a combination of in vivo, in vitro, and molecular approaches.

**Specific Aim 1: Investigate the mechanism of the cerebroprotective actions of Ang-(1-7) in ischemic stroke.** Hypotheses: Ang-(1-7) will modify the expression of some genes that will play a role in mediating the observed cerebroprotective effects. Furthermore, Mas will be present on certain cell types, indicating which cells are important in mediating the cerebroprotection.

**Specific Aim 2: Determine whether Ang-(1-7) also exerts cerebroprotective actions in hemorrhagic stroke.** Hypothesis: Since there is great overlap in the pathophysiology of both ischemic and hemorrhagic stroke, especially with regard to the

role of inflammation, Ang-(1-7) will also have a cerebroprotective effect in hemorrhagic stroke.

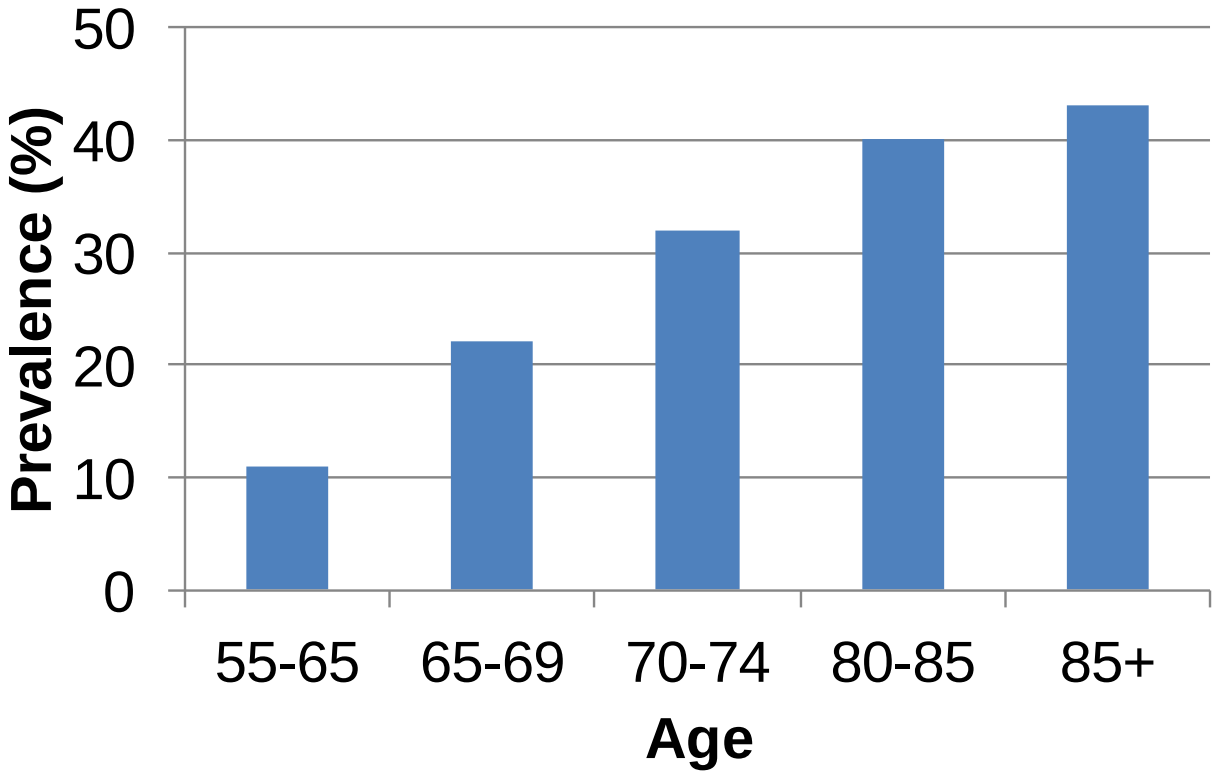


Figure 1-1. Prevalence of silent cerebral ischemia for age ranges. The prevalence of silent cerebral ischemia increases dramatically with respect to age. Data for this figure was adapted from the American Heart Association, Heart Disease and Stroke Statistics - 2009 Update.

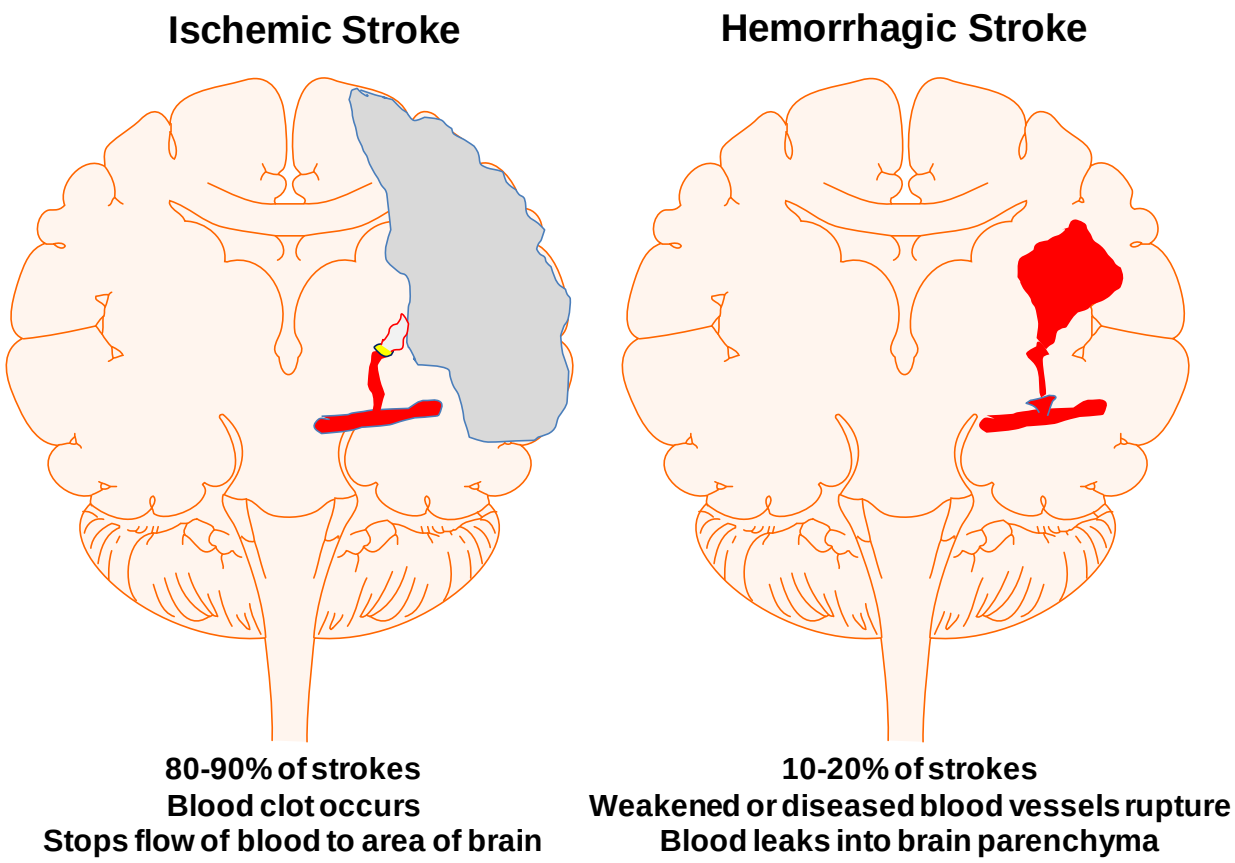


Figure 1-2. Two types of stroke. Hemorrhagic strokes occur when a blood vessel ruptures and blood leaks into the brain. Ischemic strokes occur when a clot prevents the flow of blood to an area of the brain. Figure was inspired by the Heart and Stroke Foundation of Canada.

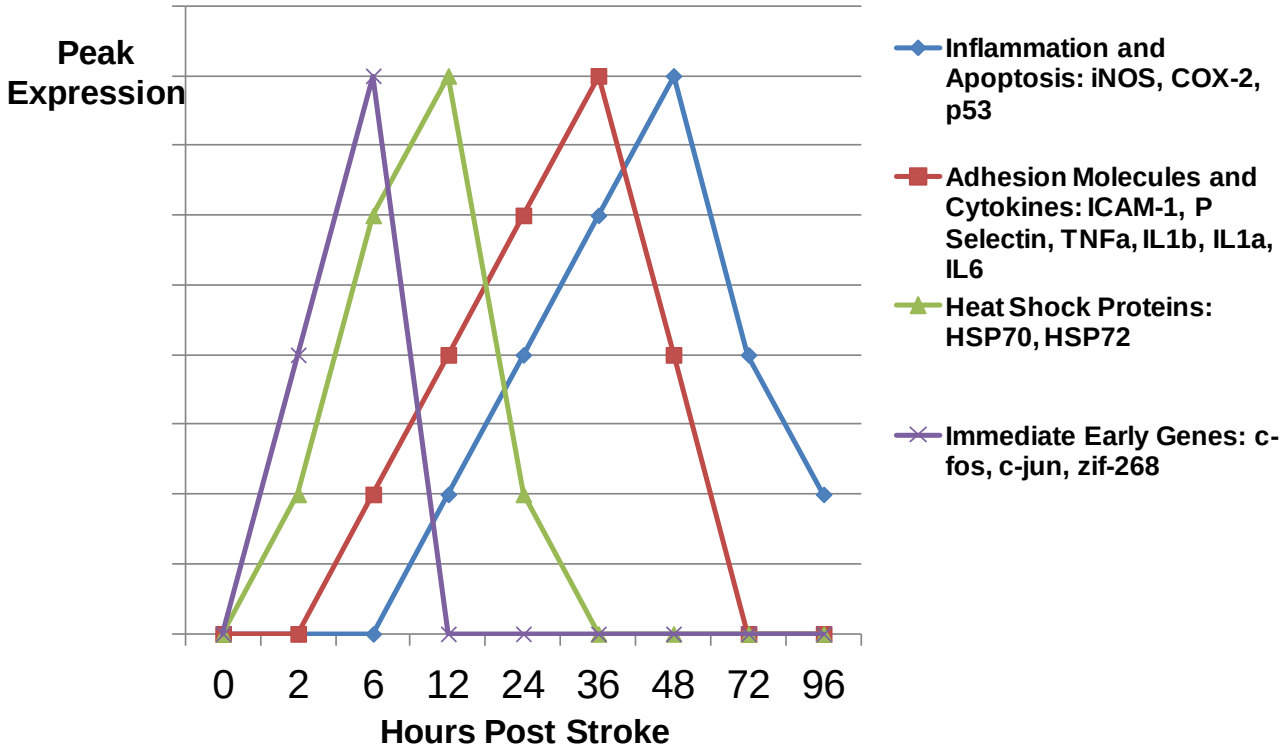


Figure 1-3. Time course of mediators in ischemic stroke damage. The early immediate genes peak at 6 h. Heat shock proteins peak at 12-20 h. The adhesion molecules and cytokines peak around 36 h. Lastly, genes involved in inflammation and apoptosis peak at around 48 h. Data for this figure was adapted from Iadecola, et al. 1997.

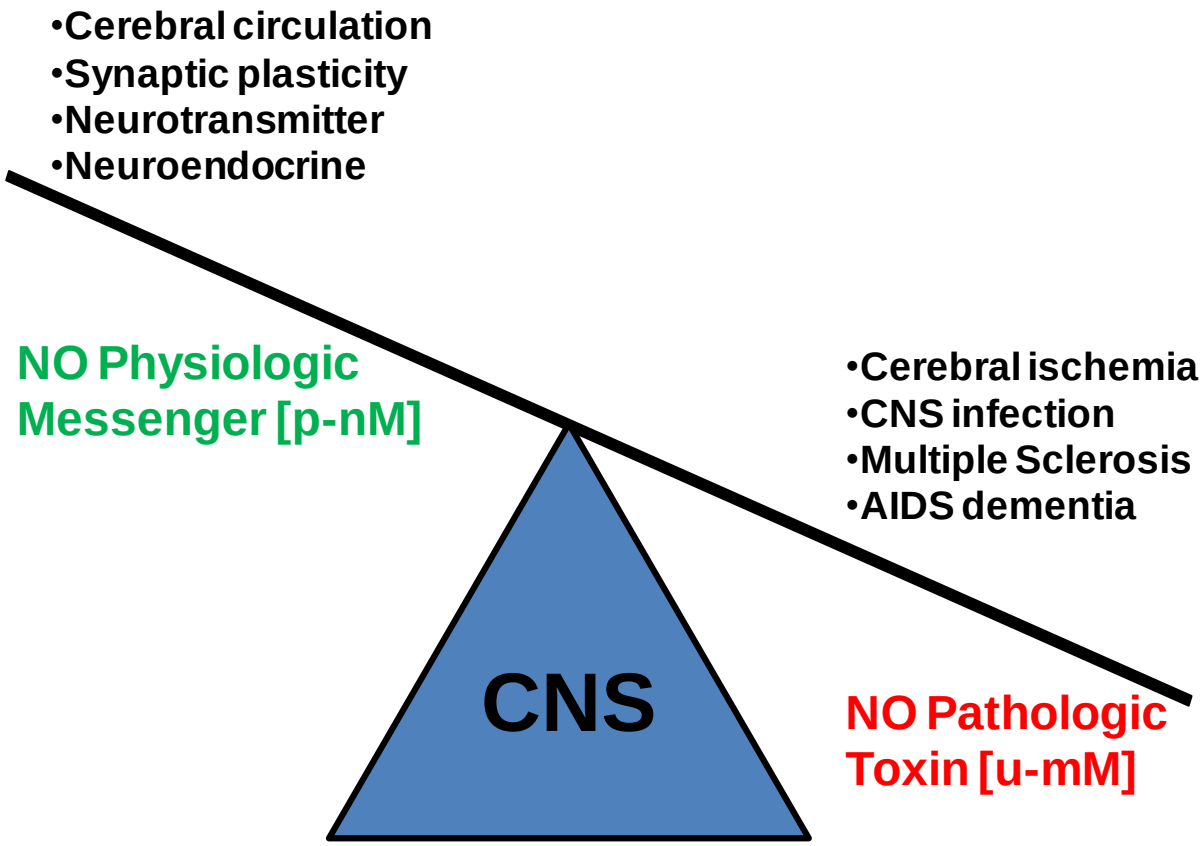


Figure 1-4. The two sides of NO. At low concentrations NO has physiological effects to cause vasodilation. At high concentrations, however, its effects are pathological resulting in nitrosylation of proteins and cell death. Figure was inspired from Iadecola, et al. 1997.

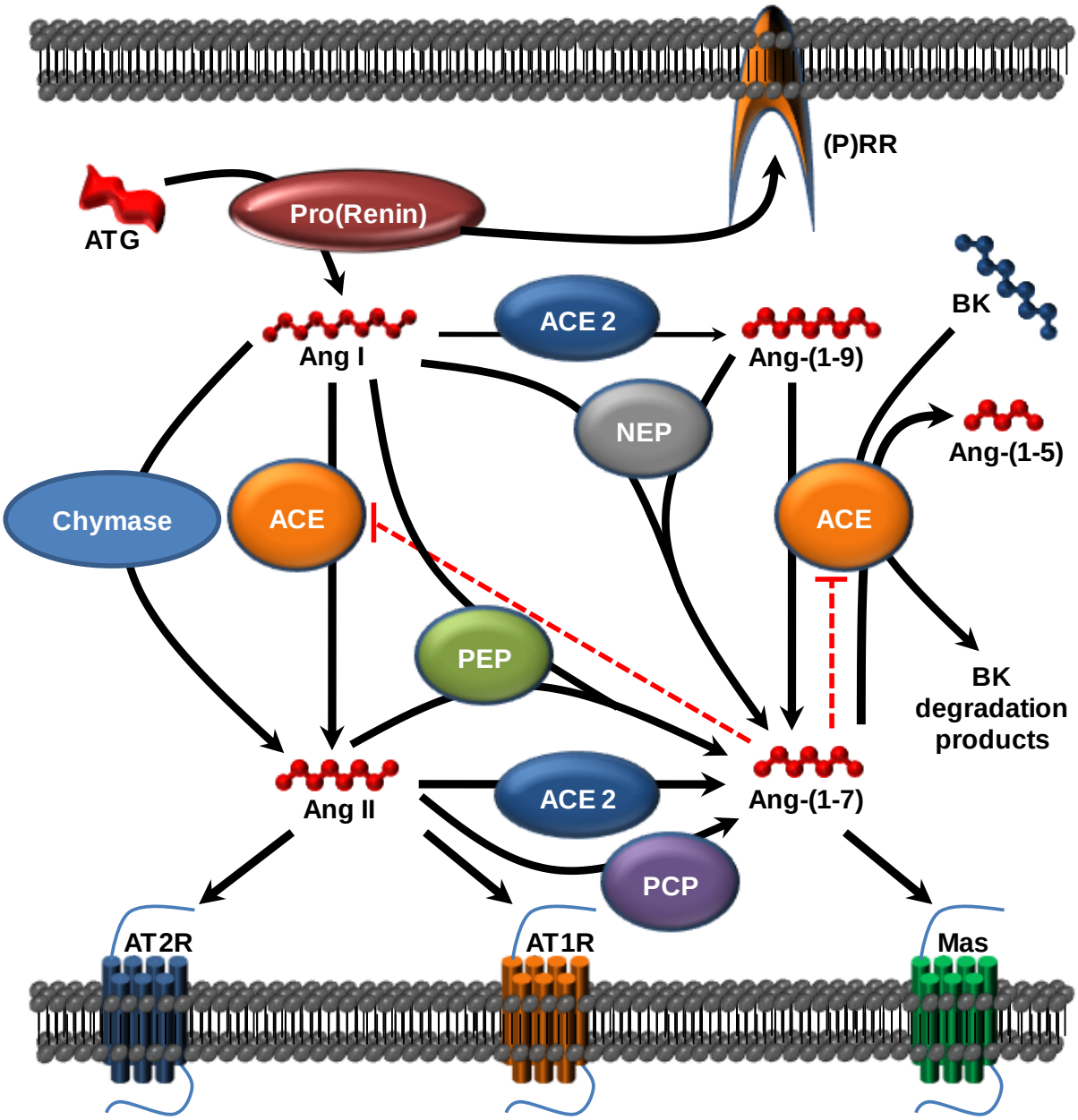


Figure 1-5. RAS components. ACE= Angiotensin Converting Enzyme, ACE2 = Angiotensin Converting Enzyme 2, ATG = Angiotensinogen, Ang = Angiotensin, AT1R = Ang II Type 1 Receptor, AT2R = Ang II Type 2 Receptor, BK = Bradykinin, NEP = Neprilysin, PEP = proyl-endopeptidase, PCP = proyl-carboxypeptidase, (P)RR = (Pro)Renin Receptor.

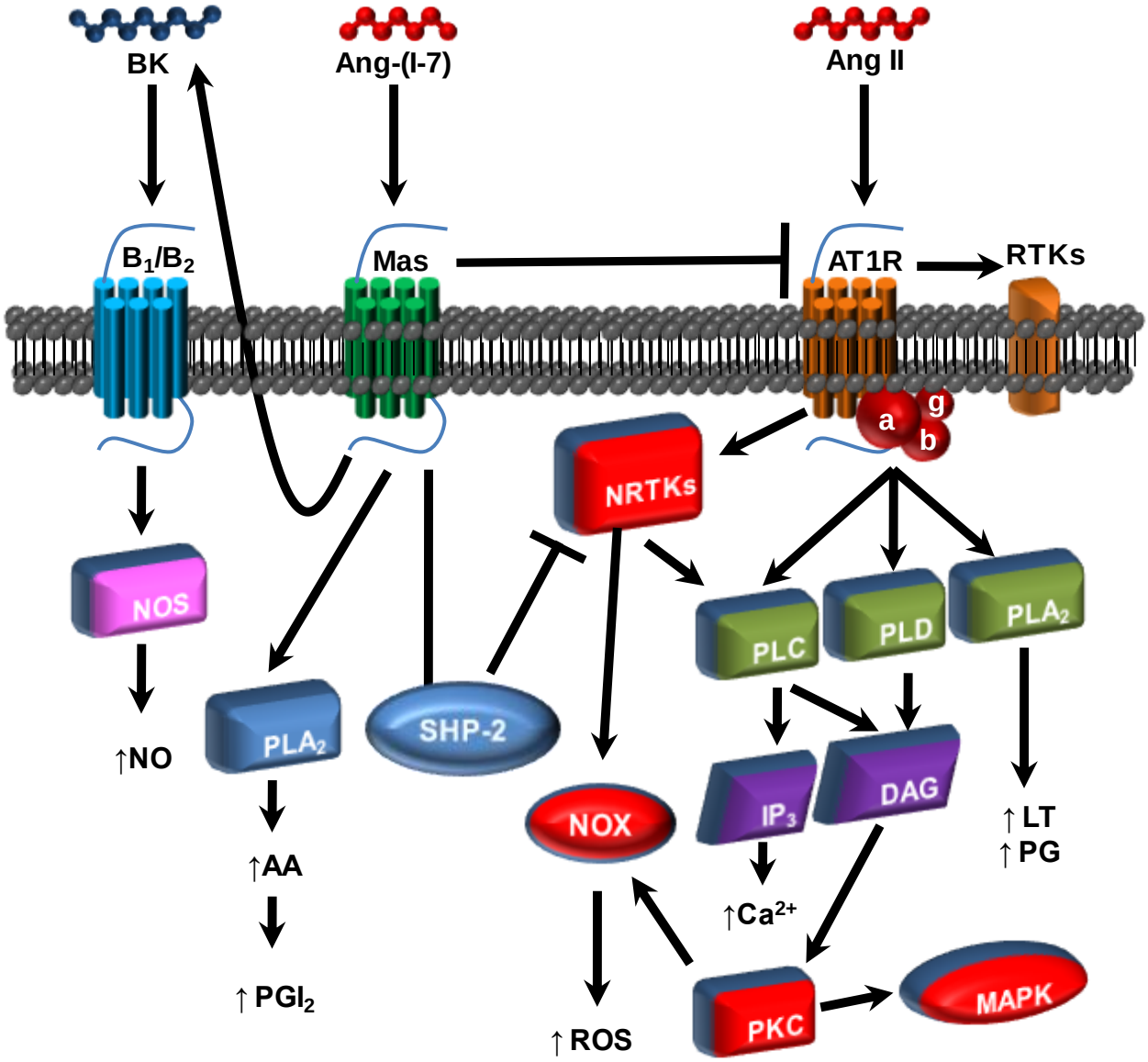


Figure 1-6. Ang-(1-7) opposes AT1R signaling. a/b/g = G protein subunits, Ang = Angiotensin, AA = Arachidonic Acid, AT1R = Ang II Type 1 Receptor, B1/B2 = Bradykinin Receptors, BK = Bradykinin, DAG = diacylglycerol, $IP_3$ = inositol-1,4,5-triphosphate , LT = Leukotrienes, MAPK = Mitogen-Activated Protein Kinase, NOS = Nitric Oxide Synthase, NO = Nictric Oxide, NOX = NAD(P)H Oxidase, NRTK = Nonreceptor Tyrosine Kinase, PG, Prostaglandins, PKC = Protein Kinase C, $PGI_2$ = Prostacyclin, PLC = phospholipase C, $PLA_2$ = phospholipase $A_2$, PLD = phospholipase D, ROS = Reactive Oxygen Species, RTK = Receptor Tyrosine Kinase.

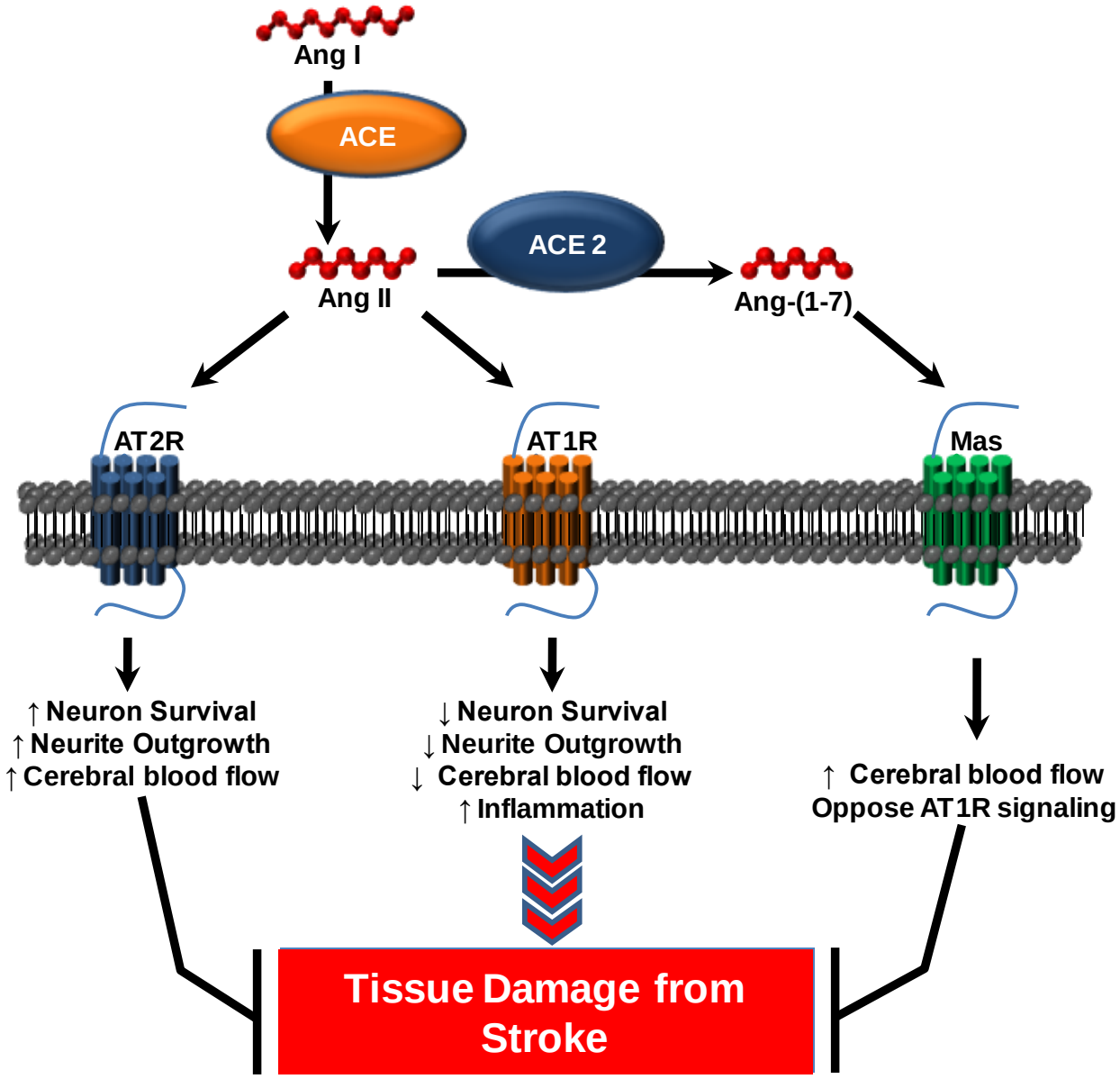


Figure 1-7. Renin Angiotensin System axes are involved in the pathophysiology of stroke. ACE= Angiotensin Converting Enzyme, ACE2 = Angiotensin Converting Enzyme 2, Ang = Angiotensin, AT1R = Ang II Type 1 Receptor, AT2R = Ang II Type 2 Receptor.

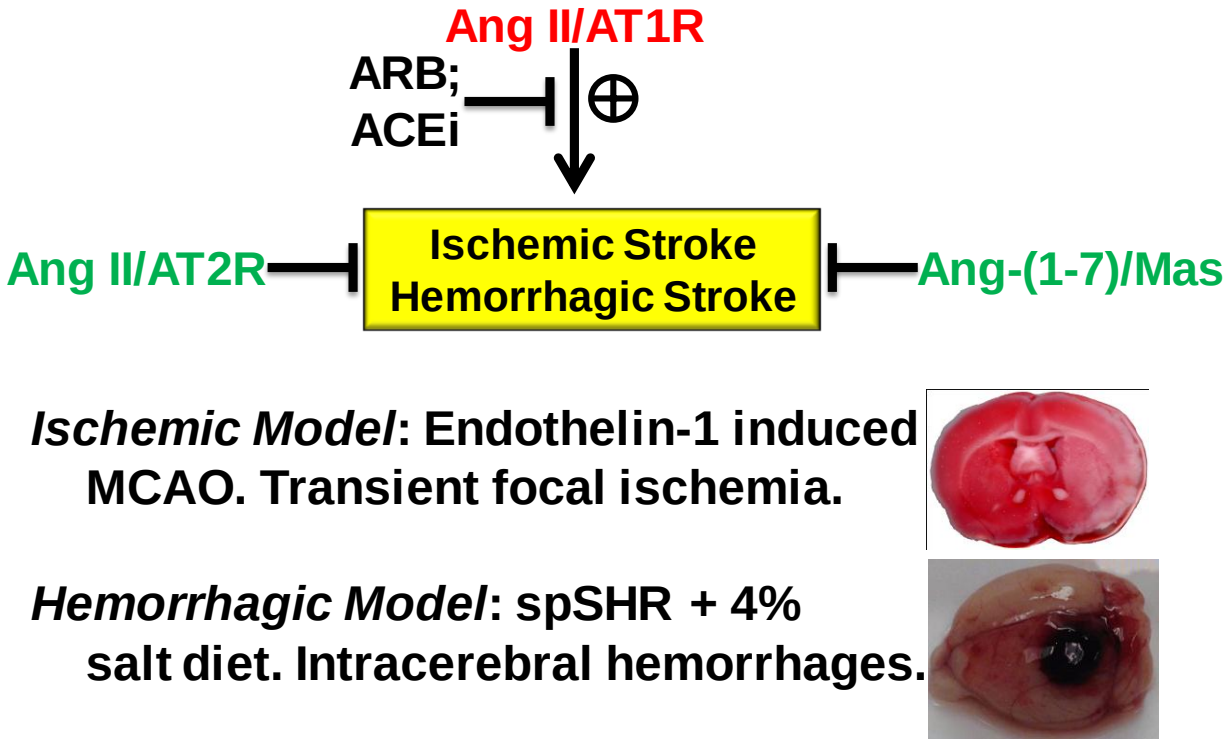


Figure 1-8. Summary of our focus on the therapeutic potential of the RAS. The effects of Ang II at AT1R are deleterious for both ischemic and hemorrhagic stroke. In contrast the effects of Ang II at AT2R and Ang-(1-7) at Mas can decrease the damage in both types of stroke. To study ischemic stroke we use and endothelin-1 induced model of middle cerebral artery occlusion. To study hemorrhagic stroke we use stroke-prone Spontaneously Hypertensive Rats.

# CHAPTER 2
# ANTI-INFLAMMATORY EFFECTS OF ANGIOTENSIN-(1-7) IN ENDOTHELIN-1 INDUCED MIDDLE CEREBRAL ARTERY OCCLUSION: POTENTIAL MECHANISM FOR CEREBROPROTECTION

## Introduction

Stroke is the fourth leading cause of death in the United States and a major cause of serious, long-term disability [219, 220]. While there have been many efforts to develop therapeutic approaches for stroke, very little progress has been made to counteract stroke damage and limit long-term disability. Mounting evidence indicates that the renin-angiotensin system (RAS) is a potential therapeutic target for ischemic stroke, as it is highly involved in the processes that induce cerebral damage following ischemia [165, 175, 177, 191]. Specifically, it is well known that over activation of the angiotensin converting enzyme/angiotensin II/angiotensin Type 1 receptor (ACE/Ang II/AT1R) axis of the RAS contributes to CNS damage following cerebral ischemia [176, 221]. In fact, numerous studies have shown that blocking the actions of Ang II at AT1R with AT1R antagonists (ARBs) decreases cortical/subcortical infarct size and the ensuing neurological deficits, in animal models of stroke [168, 171, 173]. Importantly, some human clinical trials have also indicated that ARBs can reduce cardiovascular risk and prevent stroke [167, 185, 186, 222].

A lesser known axis of the RAS, the angiotensin converting enzyme 2/angiotensin-(1-7)/Mas (ACE2/Ang-(1-7)/Mas) axis, has recently begun receiving more attention in the literature. There is accumulating evidence that activation of this axis exerts beneficial actions in several cardiovascular diseases [143, 223, 137, 223, 136, 222]. Activating the ACE2/Ang-(1-7)/Mas axis appears to have potential for treating hypertension, hypertension related pathology, pulmonary hypertension, myocardial infarction, and heart failure based on its ability to counteract the ACE/Ang II/AT1R axis [224]. In the brain,

Ang-(1-7) is primarily generated by the action of ACE2 on Ang II, and its effects are mediated by its receptor, Mas [138]. In recent studies, we demonstrated that the intracerebral damage and neurological deficits elicited by endothelin-1 (ET-1)-induced middle cerebral artery occlusion (MCAO), a model of ischemic stroke, are significantly reduced by intracerebroventricular (ICV) administration of either exogenous Ang-(1-7) or an activator of ACE2, prior to and during the stroke period [218].

Since we previously demonstrated a cerebroprotective effect of Ang-(1-7) treatment during ET-1-induced MCAO, our aim here was to uncover the mechanism of this protection. This will further support the rationale for activating the ACE2/Ang-(1-7)/Mas axis for stroke treatment and prevention. Furthermore, we believe that uncovering this mechanism will lead us to consider other diseases that may benefit from a treatment involving manipulation of the ACE2/Ang-(1-7)/Mas axis. We began by examining changes in gene expression during ET-1-induced MCAO that result from Ang-(1-7) treatment. For these experiments, we first tested for alterations in hypoxia related genes *in vivo* using a PCR Array. Changes were verified by quantitative reverse transcriptase polymerase chain resction (qRT-PCR) and Western blotting. Immunohistochemical analyses were also performed to examine which CNS cell types *in vivo* express Mas. Lastly, we measured the effects of Ang-(1-7) on isolated glia *in vitro*. The data suggest that Ang-(1-7) exerts a cerebroprotective action via a direct inhibitory action on microglia, as well as blunting the production of pro-inflammatory cytokines (PIC) and inducible nitric oxide synthase (iNOS).

## Methods

### Animals and Ethical Approval

For the experiments described here, we used a total of 127 adult male Sprague

Dawley rats (250-275 g) purchased from Charles River Farms (Wilmington, MA, USA). In addition, 20 Sprague Dawley pups were used to generate the cell cultures. All experimental procedures were approved by the University of Florida Institutional Animal Care and Use Committee. In addition, the principles governing the care and treatment of animals, as stated in the *Guide for the Care and Use of Laboratory Animals* published by the US National Institutes of Health (publication no. 85–323, revised 1996) and adopted by the American Physiological Society, were followed at all times during this study. Rats had *ad libitum* access to water and standard rat chow and were housed in a well-ventilated, specific pathogen-free, temperature-controlled environment (24 ± 1°C; 12 h–12 h light–dark cycle).

**Implantation of Intracranial Cannulae and Osmotic Pumps**

After a 7 day acclimation period, rats were anesthetized with a mixture of $O_2$ (1.5 L/min) and 4% isoflurane and placed in a Kopf stereotaxic frame. Anesthesia was maintained for the duration of the surgeries using an $O_2$/isoflurane (2%) mixture delivered through a nose cone attached to the frame. Animals then underwent intracranial surgeries, where two cannulae were implanted: one guide cannula for ET-1 injection and another cannula for ICV Ang-(1-7) [1.1 nM; 0.5 μL/h] or control artificial cerebrospinal fluid (aCSF; 0.5 μL/h) delivery via osmotic pumps, as detailed previously [218].

**ET-1 Induced Middle Cerebral Artery Occlusion (MCAO)**

Seven days after placement of intracranial cannulae, rats underwent MCAO via intracranial ET-1 (3 uL of 80 uM solution; 1 uL/min) injection through the guide cannula (17.2 mm below the top of the cannula), adjacent to the middle cerebral artery. Some groups of rats underwent sham MCAO via administration of 3 uL 0.9% saline instead of

ET-1. In previous studies we validated this procedure for investigating the role of the brain renin-angiotensin system in ischemic stroke [218].

**Post Mortem Analyses**

Following neurological testing, using forelimb flexion [176], to ensure that stroke had occurred, all rats were euthanized and their brains were removed at 6 h or 24 h post MCAO, depending on the experiment. Three coronal sections (2 mm each) were cut through the cerebrum ipsilateral to the ET-1 induced MCAO beginning caudally approximately 6 mm rostral to the top of the ventral pons, and ending rostrally just before the end of the prefrontal cortex and olfactory bulbs. To further confirm stroke, the rostral-most brain section from each rat was stained with 0.05% 2,3,5-triphenyltetrazolium chloride (TTC) for 30 minutes at 37°C [176, 218]. Tissue ipsilateral to the occlusion, which is unstained by TTC, was assumed to be infarcted. The coronal section immediately caudal to the section used for TTC staining was isolated and dissected so that left and right cortical and subcortical tissues were separated into four individual samples for protein analysis. They were immediately flash frozen in liquid nitrogen and stored at -80°C. Total protein was later extracted using a lysis buffer composed of the following: distilled water, 10X RIPA (Cell Signaling, Danvers, MA), protease inhibitor cocktail (Sigma, St. Louis, MO), two phosphatase inhibitor cocktails (Sigma), and PMSF (Sigma). Tissue was homogenized with a syringe, first using an 18 gauge needle then a 26 gauge until tissue was dissolved. Samples were allowed to incubate on ice for 30 min with occasional vortexing. Samples were then centrifuged at 4C for 30 min at 16.1g. Supernatant was saved for Western analysis at -20°C. The coronal section just caudal to this protein section was similarly separated into four

individual samples and saved for RNA at -80°C. Total RNA was isolated using an RNeasy Plus kit (Qiagen, Valencia, CA, USA). Isolated RNA underwent DNAse I treatment to remove genomic DNA. Different groups of rats were used for the Mas immunohistochemistry, where the same section described above that was saved for protein analysis was frozen in Tissue-Tek® Optimal Cutting Temperature OCT™ Compound (Sakura Finetech, Torrance, CA) to use for immunostaining.

**PCR Array Hypoxia Signaling Pathway**

RNA extracted from the ipsilateral (right) cortex at either 6 or 24 hr post MCAO was pooled (200 ng RNA/sample, N=5 samples per group) to make 1.0 ug total RNA for each pooled group. The pools were: aCSF+sham, aCSF+ET-1, and Ang-(1-7)+ET-1. cDNA was made from these pooled samples by using the RT² First Strand Kit (SABiosciences, Frederick, MD) as described by the manufacturer. RT² SYBR Green/ROX PCR Master mix (SABiosciences) and RT² Profiler™ PCR Arrays (SABiosciences, Rat Hypoxia Signaling Pathway PARN-032A) were used with the pooled samples. The array examined 84 hypoxia related genes, additional housekeeping genes, and appropriate controls. Data were first analyzed by comparing fold change in the stroked groups compared to sham. Ang-(1-7)+ET-1 fold change was then compared to control aCSF+ET-1 fold change.

**qRT-PCR**

Levels of iNOS, endothelial nitric oxide synthase (eNOS), neuronal nitric oxide synthase (nNOS), pentraxin-3 (Ptx3), interleukin-6 (IL6), interleukin 1 α (IL1α), interleukin 1 β (IL1β), tumor necrosis factor α (TNFα), cluster of differentiation molecule 11b (CD11b), glial fibrillary acidic protein (GFAP), myeloperoxidase (MPO), monocyte chemotactic protein-1 (MCP-1), chemokine receptor type 4 (CXCR4), and chemokine

(C-X-C motif) ligand 12 (CXCL12) mRNAs within the cerebral cortex were analyzed by quantitative real-time reverse transcriptase polymerase chain reaction (qRT-PCR). This was used to confirm all differences from the PCR array and examine other genes. A group where Ang-(1-7) was given to sham animals was also included. Extracted RNA was reverse transcribed with a high-capacity cDNA reverse transcription kit (Bio-Rad Laboratories, Hercules, CA) and then analyzed *via* qRT-PCR in a PRISM 7000 sequence detection system (Applied Biosystems, Foster City, CA) as detailed by us previously [225]. Oligonucleotide primers and TaqMan probes specific for rat iNOS, eNOS, nNOS, Ptx3, IL6, IL1α, IL1β, CD11b, MPO, and TNFα were obtained from Applied Biosystems (Carlsbad, California). Data were normalized to 18S rRNA.

**Western Blotting**

Extracted protein was added to an equal volume of 2x Laemelli's buffer (Bio-Rad, Hercules, CA) with β-mercaptoethanol (Bio-Rad). After heating for 5 min at 90°C, samples were loaded into a precast TGX Criterion gel (Bio-Rad). The gel was run at 200V using Tris Glycine SDS running buffer (Bio-Rad) and Dual Color MW markers (Bio-Rad). Transfer buffer was prepared using Tris base 25mM (Bio-Rad), Glycine 192mM (Fisher), and methanol 20% (Sigma). The protein was then transferred from the gel to a nitrocellulose membrane (Bio-Rad) at 80V for 1 hour. After transfer, the membrane was rinsed with Tris buffered saline (TBS), then TBS with Tween (TBST), and placed on a shaker in TBST+milk for 1 hour of blocking. The membrane was then incubated with primary antibodies [rabbit anti-iNOS (1:333) and rabbit anti-cofilin (1:10,000; used as a loading control)] overnight at 4°C with slow agitation on a shaker. The following day the membrane was washed six times with TBST (5 min each) on a

shaker with fast agitation. Then, the secondary antibody (goat anti-rabbit IgG horse radish peroxidase [HRP]; 1:2,000) was added to the membrane, which was then placed on a shaker for 1 h. The membrane was then washed with TBST six times (5 min each) on a shaker with fast agitation, exposed to ECL, and developed. Densitometry was used to quantify the blots using the integrated density (ImageJ, NIH). Samples were normalized to the housekeeping protein cofilin. A positive control, protein extracted from mixed cultured glia cells treated with LPS, was also used.

**Mas Immunohistochemistry**

Twenty-four hours following ET-1 or sham injections, a 2 mm coronal section of brain was sectioned and fresh frozen in Tissue-Tek® Optimal Cutting Temperature OCT™ Compound (Sakura Finetech, Torrance, CA) to be used for co- immunostaining of Mas with NeuN (neuronal specific nuclear protein), GFAP (glial fibrillary acidic protein), RECA-1 (rat endothelial cell antigen), OX-42 (CD11b), and MPO (myeloperoxidase), which are respective specific markers for neurons, astroglia, microglia, endothelial cells, and neutrophils. Procedures were as follows: Brain sections (at 5um) were cut from the 2 mm coronal section block and air dried at room temperature overnight. OCT was removed in a wash of 1X TBS for 5 minutes. Slides were drained and wiped, then blocked for 1 hour in 2% horse serum diluted in 1X TBS. Slides were wiped and blocking buffer was replaced with antibody cocktails (rabbit anti-Mas [1:400] combined with either mouse anti-NeuN [1:100], anti-GFAP [1:100], anti-OX-42 [1:100], anti-RECA [1:100] or anti-MPO [1:50] diluted in antibody diluent (Invitrogen, Carlsbad, CA), and incubated overnight at 4°C. Following two 5min washes in TBS, Alexafluor donkey anti-rabbit 594 and donkey anti-mouse 488 were added to the slides, both at 1:500. After a 45 minute room temperature incubation, slides were again double

washed in TBS. Sections were then post fixed for 5 minutes in 10% neutral-buffered formalin, washed twice, then wiped dry before mounting in DAPI vectashield (Vector Labs, Burlingame, CA).

**Nitric oxide Production by Primary Glial Cultures**

Primary mixed glial cultures were grown from newborn SD rat pups as previously described [226]. The cortex and striatum were dissected out and homogenized. Trypsin-dissociated brain cells, suspended in Dulbecco's modified Eagle's medium (DMEM) containing 10% fetal bovine serum (FBS), were filtered though sterile gauze, plated in poly-L-lysine coated dishes, and grown for 10-14 days at 37°C in 5% $CO_2$/ 95% air. Cells were then dissociated by mild treatment with trypsin (0.25%; 2 min, 37°C), re-plated in 35mm dishes at a density of 1 x $10^5$ cells/dish, and cultured for a further 7 days. At this time, cultures consisted of both astrocytes and microglia, but not neurons, as determined by immunostaining with GFAP, Iba-1, and NeuN antibodies. Cultures were treated as follows: control solution (PBS), lipopolysaccharide (LPS; 10 ng/mL), LPS + Ang-(1-7) [0.1 nmol/mL], and LPS + Ang-(1-7) + A779 (Mas inhibitor; 1.0 nmol/mL). Ang-(1-7) and A779 were applied 12 h before, at the time of, and 12 h after LPS treatment. Growth media was replaced with serum-free DMEM just before the first treatment. Twenty-four hours after the LPS treatment, the media was sampled for analysis of nitrite ($NO_2$, a stable breakdown product of nitric oxide) by the Greiss reaction, as previously described [226]. Media samples (100 ul) were added to 100 ul Greiss reagent consisting of 0.75% sulfanilamide in 0.5M HCl and 0.075% N-(1-naphthyl)ethylenediamine dihydrochloride, in water. The mixture was incubated for 10

min and the absorbance measured at 543 nm. $NO_2$ concentration was then calculated from a standard curve, using known concentrations of Na $NO_2$.

**HPLC Analysis of Ang-(1-7)**

Growth media was sampled at the following timepoints: 0 h, 14 h, 24 h, and 48 h. These samples were sent to a core facility for measurement of Ang-(1-7) by standard HPLC.

**Chemicals**

Ang-(1-7) and A779 were purchased from Bachem Bioscience (Torrance, CA, USA). ET-1 was from American Peptide Company, Inc (Sunnyvale, CA, USA). Rabbit anti-Ang-(1-7) Mas receptor antibody was from Alomone Labs (Jerusalem, Israel). Mouse anti-rat RECA-1 was from AbD Serotec (Raleigh, NC). Mouse anti- MPO, mouse anti-GFAP, rabbit anti-iNOS (ab15323), rabbit anti-Cofilin (ab11062) and goat anti-rabbit IgG HRP (ab6721) antibodies were from Abcam (Cambridge, MA). Mouse anti-OX-42 antibody was from BD Biosciences (San Jose, CA). Mouse anti-NeuN was from Millipore (Bedford, MA). Rabbit anti-Iba-1 (01919741) was from Wako (Richmond, VA). Alexafluor donkey anti-rabbit 594 and anti- mouse 488 were from Molecular Probes [Invitrogen] (Carlsbad, CA, USA). Vectashield mounting medium with DAPI (4',6-diamidino-2-phenylindole) was from Vector Labs (Burlingame, CA, USA). All other chemicals were purchased from Fisher Scientific (Pittsburgh, PA, USA).

**Data analysis**

Data are expressed as means ± SEM. Statistical significance was evaluated, as specified in the figure legends, with the use of a one-way ANOVA, Newman-Keuls test, Dunn's test, or t-test as appropriate. Differences were considered significant at $p<0.05$.

## Results

### Cerebroprotective Ang-(1-7) Reduces Infarct Size 24 h after ET-1-induced MCAO

In previous studies, we demonstrated a cerebroprotective effect of central treatment with Ang-(1-7) prior to and during induction of ischemic stroke via ET-1-induced MCAO 218. Ang-(1-7) treatment decreased the size of the intracerebral infarct and improved performance on several neurological exams 72 h after MCAO. Furthermore, Ang-(1-7) did not alter blood pressure, percent change in MCA branch vessel diameter or percent change in cerebral blood flow. Here we show the percent infarcted grey matter at 24 h after MCAO. Ang-(1-7) blunts the infarct size by 50% (Figure 2-1) in agreement with our previous results at 72 h 218.

### Increased Expression of Hypoxia-related Genes in the Ipsilateral Cerebral Cortex following ET-1-induced MCAO; Inhibitory Action of Ang-(1-7)

It is well-known that the expression of many genes, including PICs and some NOS isozymes, is increased in the cerebral cortical infarct zone following ischemic stroke, contributing to neurotoxicity [37, 40]. Therefore, we became interested in assessing changes in gene expression within the brain parenchyma to investigate potential mechanisms underlying the protective action of Ang-(1-7). We began by using a PCR array to examine the expression of hypoxia-related genes in pooled ipsilateral samples of cerebral cortex. Of the 84 hypoxia related genes on the array, five were up-regulated by more than 4-fold at 6 hours post MCAO stroke compared to sham (Table 2-1): heme oxygenase (9-fold increase in aCSF controls vs. 5-fold increase in Ang-(1-7) treated); the PICs interleukin 1α (ILα; 15-fold vs. 3-fold) and interleukin 6 (IL6; 24-fold vs. 4-fold); myosin light polypeptide 2 (6-fold vs. 2-fold); pentraxin related gene (Ptx3; 4-fold for both). At 24 hours post stroke, five genes were up-regulated by more than 4-fold (Table

2-2): heme oxygenase (34-fold vs. 40-fold); the PIC IL6 (45-fold vs 38-fold); iNOS (60-fold vs. 8-fold); plasminogen activator/urokinase (12-fold for both); and Ptx3 (72-fold vs. 42-fold). Ang-(1-7) appeared to blunt the increases in PICs (IL1α, IL6) and iNOS during stroke. Only those data that were increased in stroke by greater than four-fold are presented, as we believed these to be the most important and most reliable given the nature of PCR arrays.

**Effects of Ang-(1-7) on the Expression of Nitric Oxide Synthase (NOS) Isozymes, PICs, and Inflammatory Cell Markers in the Ipsilateral Cerebral Cortex following ET-1-induced MCAO**

The PCR array data presented in Tables 2-1 and 2-2 confirm the view that the expression of several inflammatory cytokines and iNOS is increased in the ipsilateral cerebral cortex following ischemic stroke, and also indicate potential loci of Ang-(1-7)'s protective action. Thus, in order to confirm the results of the PCR array, we performed qRT-PCR on individual ipsilateral cortical samples from rats that had undergone ET-1 induced MCAO or sham strokes in the absence or presence of ICV infusion of Ang-(1-7) as described in the Methods. Specifically, we were interested in determining the relative levels of mRNAs for NOS isozymes, PICs, chemokines and their receptors, and of inflammatory cell markers (MPO for neutrophils, CD11b for monocytes/microglia, and GFAP for astrocytes) under each treatment condition as a function of time following stroke. Levels of eNOS, IL1α, IL1β, CXCR4, and MPO mRNAs were all significantly increased at 6 hours post MCAO, whereas levels of iNOS, nNOS, CXCL12, CD11b (Figure 2-2) and IL6 (not shown) were unaltered. The data also demonstrate that Ang-(1-7) significantly decreased the levels of CXCL12 mRNA 6 h after MCAO, and also produced non-significant reductions in the post-MCAO expression of IL1α, MPO (Figure 2-2), and IL-6 (not shown). At 24 hours post MCAO there were dramatic increases in

the levels of iNOS, eNOS, Ptx3, IL1α, IL1β, IL6, TNFα, CXCR4, MCP-1, CD11b, and GFAP mRNAs by factors of 300, 7, 100, 10, 10, 80, 10, 40, 1200, 12, and 5 respectively, when compared with sham rats (Figures 2-3 and 2-4), whereas nNOS, CXCL12, and MPO mRNA levels were unaffected. Of the genes that were increased in stroke, the expression of iNOS, IL1α, CXCR4, and CD11b were all significantly blunted by ICV Ang-(1-7) administration, while Ptx3, IL6, IL1β, MCP-1, and GFAP exhibited non-significant reductions in the presence of this peptide. Ang-(1-7) alone had no effects on gene expression in sham animals that did not undergo MCAO (Figures 2-2 through 2-4). To control for ET-1 effects independent of stroke, we injected at a site 2 mm medial and 2 mm superior to the stroke coordinates and confirmed the absence of stroke by TTC staining. There was no effect of ET-1 at this site compared to saline on gene expression of several representative genes (iNOS, IL1α, CD11b). Since the inhibitory effects of Ang-(1-7) on iNOS mRNA levels were observed to be the most profound, we tested whether these changes were detectible at the protein level via Western blotting (Figure 2-5). Densitometry analysis showed that iNOS protein was increased by ~ 4-fold 24 h after MCAO. This increase was blunted by ICV Ang-(1-7) administration. As with the mRNA, Ang-(1-7) alone had no effect on the expression of iNOS protein in sham animals that did not undergo MCAO. These data corroborated our earlier finding where levels of iNOS mRNA in the cerebral cortical infarct zone were reduced by Ang-(1-7) at 24 hours post ET-1 induced MCAO [218], and also expanded our understanding of the potential mechanism of Ang-(1-7)'s cerebroprotective effects. No effect of stroke or Ang-(1-7) treatment was measured on Mas mRNA levels (not shown).

**Cellular Localization of Mas within Rat Cerebral Cortex**

Having demonstrated that Ang-(1-7) reduces the expression of various proinflammatory markers in the ipsilateral cortex during ischemic stroke, we used immunostaining to investigate the cellular location of the Ang-(1-7) receptor, Mas in the brains of normal, healthy rats and in those that had undergone ET-1 induced MCAO. The representative fluorescence micrographs presented in Figure 2-6 indicate that Mas immunoreactivity within normal rat cerebral cortex was primarily associated with neurons, as evidenced by co-localization with the neuron specific marker NeuN. However, it was clear that Mas immunoreactivity is also associated with non-NeuN positive cells. Further immunostaining experiments revealed the presence of Mas on macrophages/microglia, as illustrated by co-localization with immunoreactive CD11b (OX-42 immunostaining), a specific marker of these cells (Figure 2-6). Mas immunoreactivity was also observed within endothelial cells of small cerebral vessels (Figures 2-6), and was abundant within the endothelium of large vessels such as the MCA (not shown), as demonstrated by co-localization with immunoreactive RECA. In contrast, Mas immunoreactivity was not associated with astroglia or neutrophils (the latter present only within the blood vessel lumen in the normal brain), based on a lack of co-localization with immunoreactive GFAP and MPO, respectively (Figure 2-6). Similar localization of Mas immunoreactivity was observed in the subcortex of normal rats, i.e. presence of Mas on neurons, macrophages/microglia and endothelial cells, but not on astroglia nor on neutrophils (not shown). In comparison with the normal brains, stroked brains were also examined in the ipsilateral cortex at 24 hours following ET-1 induced MCAO (Figure 2-6). Consistent with the control brains, Mas immunoreactivity was associated with neurons and macrophages/microglia, but not with MPO-positive

neutrophils that invade the brain parenchyma (Figure 2-6). We have verified the specificity of the Mas antibody using brain sections from a Mas knockout mouse (Figure 2-6). We also confirmed that each immunopositive area was a cell by co-localizing with DAPI nuclear staining (not shown).

**Ang-(1-7) Blunts LPS Induction of NO in Primary Mixed Glial Cultures**

Considering that macrophages/microglia within the cerebral cortex contain immunoreactive Mas, and that ICV infusion of Ang-(1-7) decreases the stroke-induced expression of PICs, iNOS, and CD11b (indicating reduced activation of microglia), we wanted to test the *direct* effects of Ang-(1-7) on NO production by glia. As our hypothesis is that Ang-(1-7) is cerebroprotective by blunting inflammation, using an LPS-induced model of inflammation is relevant. This was achieved using primary glial cultures that contain a mixture of astrocytes and microglia, as evidenced by immunostaining using anti-GFAP and anti-Iba-1 antibodies (Figure 2-7). Incubation of cultures with LPS (10ng/mL), which is well known to elicit PIC production and secretion, produced a highly significant (3 fold) increase in NO production after 24 h, as demonstrated by accumulation of $NO_2$ (a stable breakdown product of NO) in the growth media (Figure 2-7). This increase in $NO_2$ was significantly blunted by Ang-(1-7) treatment (0.1 nmol/mL), administered 12 h before LPS, just before LPS, and 12 h after LPS (Figure 2-7). This multiple treatment model was designed to account for the breakdown of Ang-(1-7) as measured by HPLC (Table 2-3). Furthermore, this blunting was reversed by co-treatment with the Mas antagonist, A779 (1.0 nmol/mL), when administered at the same time points.

## Discussion

In previous studies we demonstrated a significant cerebroprotective action of the peptide Ang-(1-7) against ischemic stroke when administered centrally prior to and during the insult [218]. Here we have investigated the potential mechanisms that underlie this cerebroprotective action of Ang-(1-7). Our data suggest that the cerebroprotective action of Ang-(1-7) involves an anti-inflammatory effect, as evidenced by the following findings: (i) Ang-(1-7) blunts MCAO-induced increases in the levels of iNOS, PICs and CD11b (a marker of macrophage/microglial activation), that occur in the ipsilateral hemisphere following MCAO; (ii) Ang-(1-7) blunts the LPS-induced increases in NO production in cultured glia (mixed culture of microglia and astrocytes). Considering our immunostaining results which show that Mas is localized to microglia, our findings are consistent with the idea that the cerebroprotective action of Ang-(1-7) is mediated through reductions in microglial action and the intracerebral pro-inflammatory response that occurs following MCAO. Despite the above findings, the present study raises many important questions.

One of the major issues concerns the precise locus of action of Ang-(1-7) in reducing the damage due to stroke. Over-activation of microglia and increased iNOS expression have been shown to be detrimental in stroke [37, 40]. Furthermore, inhibiting iNOS and microglia has been shown to have a therapeutic effect in experimental models of stroke [40]. Based on our data we believe that Ang-(1-7) reduces the damage due to stroke through a reduction of an over-activated microglia response and an excessive production of iNOS. Evidence for this is as follows. First, Mas is present on microglia so Ang-(1-7) could have a direct action on this cell type. Furthermore, Ang-(1-7) blunts the increase in CD11b mRNA during stroke, implying that fewer activated

microglia are present in the ipsilateral cortex 24 h after MCAO. Lastly, downstream effects of microglia are also blunted by Ang-(1-7), namely the increases in iNOS and PICs during stroke. While direct actions of Ang-(1-7) on microglia are a possibility, we cannot conclusively rule out other indirect mechanisms. Other cell types, including neurons and endothelial cells, contain Mas immunoreactivity. Thus, it is possible that Ang-(1-7) has an effect on neurons, such as inhibition of monocyte chemotactic protein -1 (MCP-1) production and secretion, which normally recruits monocytes/microglia, astroglia, or other inflammatory cells towards neurons [227, 228]. There was a strong trend for Ang-(1-7) to blunt the increase in MCP-1 during stroke that almost reached significance. Although it has been reported that Mas stimulation increases cerebral blood flow through increasing bradykinin secretion and eNOS activity 3 hours after stroke [208], our previous measurements of cerebral blood flow with central Ang-(1-7) treatment during stroke do not support these alterations as a mechanism for cerebroprotection [218]. Further, our *in vitro* data with a cultured glial system support that Ang-(1-7) has a direct effect to blunt an LPS-induced increase in NO. Since the culture system lacked neurons or endothelial cells, it demonstrates that these cells are not required for an anti-inflammatory effect.

Many of the genes that were altered by MCAO on the PCR array have been discussed in the literature. Heme oxygenase, PICs, iNOS, myosin light polypeptide 2, Ptx3, and plasminogen activator/urokinase have been shown to be increased in several pathological conditions, including hypoxia, ischemia, and inflammation. Heme oxygenase gene expression is up-regulated in response to cerebral ischemia. Furthermore, it has been shown that over-expression of heme oxygenase is

neuroprotective in an MCAO model in mice [229]. In addition, PICs, such as IL1α and IL6, and iNOS have been shown to be increased in stroke models and to cause damage [40, 230, 231]. Myosin light polypeptide 2 has been reported to be upregulated during hypoxia or inflammation in several tissues, including the aorta in stroke-prone spontaneously hypertensive rats [232]. Ptx3, a gene believed to modulate the phagocytic activity of microglia [233], has been shown to increase in acute ischemic cardiomyopathy [234]. In an MCAO model in rats, mRNA levels of both tissue-type plasminogen activator and urokinase-type plasminogen activator were increased in the cerebral cortex and hippocampus 24 h post MCAO [235]. Confirming these changes further supported the validity of our stroke model.

The changes in gene expression due to Ang-(1-7) treatment, however, have not been previously reported to our knowledge. As stated in the methods, we verified changes with qRT-PCR. iNOS induction 24 h after MCAO was significantly blunted by Ang-(1-7), affirming our earlier study [218]. We focused much of our attention on iNOS, as there is substantial evidence in the literature to suggest it is highly involved in the pathology of stroke, by increasing NO levels [40]. Interestingly, while we did not see an effect of Ang-(1-7) on eNOS expression at 6 or 24 h post MCAO, it is still possible that Ang-(1-7) may have increased eNOS activation, but not gene expression, at least in the early post stroke time period as described previously [208]. Further support for the anti-inflammatory effect of Ang-(1-7) is shown by the significant blunting of IL1α and IL6 at 24 h post MCAO. There was also a trend for IL1β and TNFα to be blunted by Ang-(1-7) at 24 h, but these changes did not reach statistical significance. Furthermore, blunting of these PICs only reached statistical significance at 24 h post stroke and not 6 h post

stroke. This suggests that the effects of Ang-(1-7) may not be measurable early after stroke since there is not yet sufficient inflammation to reveal an effect. It is also worth mentioning that several of these trends may have reached statistical significance if we examined other time points, but we limited our examination to 6 and 24 h post stroke.

In addition to the above, CXCL12 and its receptor CXCR4 were examined. These molecules are involved in the trafficking of stem cells and are known to be upregulated in inflammation [236]. While CXCR4 was significantly increased 6 h and 24 h after stroke, CXCL12 showed only a trend to increase at these time points. Furthermore at 6 h, the increase in CXCR4 was significantly blunted by Ang-(1-7) treatment, as was the increase in CXCL12 at 24 h post stroke. CXCL12 has been shown to be upregulated in stroke in the ischemic penumbra [237]. It is possible that our samples contained less penumbra compared to the total tissue collected. It has been shown that the CXCL12/CXCR4 pathway stimulation can increase IL6 production in microglia, indicating a role for this pathway in activating microglia [237]. Interestingly, CD11b was increased by stroke at 24 h and found to be blunted by Ang-(1-7), as well. This suggests that fewer macrophages/microglia are becoming activated or fewer are migrating to the cortex in the stroked area after Ang-(1-7) treatment [238]. This was not observed at 6 h post MCAO, but CD11b levels were not observed to increase due to stroke until 24 h. It appeared that the early inflammatory response was mediated more by neutrophil invasion at 6 h, as there was a statistically significant increase in MPO at this time point due to stroke.

It should also be mentioned that all of the gene expression studies presented here, including the PCR array and the qRT-PCR, were performed using only cortex and

only from a precisely measured 2 mm coronal section determined to be in the stroked area (see Methods). It contained core, penumbra, and some healthy tissue. This same section was used for every rat. We believed that this was the most appropriate way to measure the expression of these genes in the tissue, since in a previous study [218] we showed no increases in iNOS, IL1α, or IL1β due to stroke when using the entire ipsilateral hemisphere (cortex and striatum/subcortex). Furthermore, we did not see nearly the same magnitude of increase in IL6 expression due to stroke looking at the entire hemisphere. We propose that the effects in the stroke region are diluted when excess healthy tissue is used in the analysis.

As much of our early attention was given to iNOS, we verified that this change in iNOS gene expression also existed at the protein level. Protein expression at 24 h post stroke was significantly increased, and this increase was significantly blunted by Ang-(1-7) treatment. In future experiments, it will be valuable to verify changes in protein translation for other genes with altered mRNA transcription due to Ang-(1-7) treatment.

We made several interesting observations with the Mas co-localization study. Interestingly, Mas immunoreactivity does not appear to co-localize with GFAP immunoreactivity. There is evidence in the literature to suggest that astroglia may have Mas, however these studies were performed in cultured astrocytes and brain slices from other brain regions [216, 239]. We cannot conclude with certainty that astrocytes do not have Mas, but we do feel that since the protein levels are below the detection threshold of immunostaining, astrocytes may not be as important in this Mas-mediated mechanism. Also, Mas staining is observed not only on the cellular membrane, but also in the nucleus and cytosol. This abundant presence of Mas in the nucleus is consistent

with its original discovery as an oncogene [240], perhaps being involved in cell cycle regulation. To control for any changes in Mas localization during stroke, we also performed a co-localization study on tissue that was collected from animals 24 h after MCAO. Mas immunoreactivity was present on neurons in the penumbra, as well as microglia within the ischemic core. Studying cerebral tissue from a rat that underwent stroke confirmed that infiltrating neutrophils were devoid of Mas.

We encountered several challenges while designing our *in vitro* experiments. Ang-(1-7) is broken down relatively rapidly in our cell culture system as measured by HPLC analysis (Table 2-3). Therefore, we designed a model with multiple treatments of a low dose given 12 h before LPS, at the time of LPS, and 12 h after LPS. This treatment model demonstrated that Ang-(1-7) could blunt the LPS-induced increase in $NO_2$. We interpret this as a proof of principle that there is a direct effect on glia.

This study provides further support that activating the ACE2/Ang-(1-7)/Mas axis has a therapeutic effect during stroke [218]. It also demonstrates for the first time an anti-inflammatory effect of Ang-(1-7) in CNS tissue. This supports the theory that activation of the ACE2/Ang-(1-7)/Mas axis could prove to be a novel therapeutic target for other diseases where the underlying pathology involves inflammation, such as other cardiovascular diseases, type 2 diabetes, chronic kidney disease, and cancer [241]. There is more evidence accumulating that the activation of this axis has anti-inflammatory effects in many tissues, such as the heart [242], aortic valve [243], joints [244], and kidneys [245]. Since we demonstrate a central effect here, it also may prove to be therapeutic for other brain diseases that involve inflammation, such as Alzheimer's disease [241]. Further

studies will be needed to determine other potential direct effects of Ang-(1-7) and also the intracellular signaling involved.

Table 2-1. PCR array data showing fold changes in gene expression in ipsilateral (right) cerebrocortical tissue 6 h after endothelin-1 (ET-1)-induced middle cerebral artery occlusion (MCAO) stroke compared to sham controls (0.9% saline instead of ET-1).

| Gene – 6 Hours | aCSF+ET-1 Fold Change | Ang-(1-7)+ET-1 Fold Change |
|---|---|---|
| Heme oxygenase | 9 | 5 |
| Interleukin 1α | 5 | 3 |
| Interleukin 6 | 24 | 4 |
| Myosin light polypeptide 2 | 6 | 2 |
| Pentraxin related gene | 4 | 4 |

Only those genes that showed a fold change from MCAO greater than 4 are presented. Seven days of Ang-(1-7) (1.1 nM; 0.5 μL/h) treatment prior to MCAO blunts the increases in IL1α, IL6, heme oxygenase and myosin light polypeptide 2 when compared to control animals treated with artificial cerebrospinal fluid (aCSF; 0.5 μL/h). RNA samples were pooled (N=5) for each aCSF+sham, aCSF+ET-1, and Ang-(1-7)+ET-1 groups so that 3 arrays were used as described in the methods.

Table 2-2. PCR array data showing fold changes in gene expression in ipsilateral (right) cerebrocortical tissue 24 h after ET-1-induced MCAO stroke compared to sham controls.

| Gene – 24 Hours | aCSF+ET-1 Fold Change | Ang-(1-7)+ET-1 Fold Change |
|---|---|---|
| Heme oxygenase | 34 | 40 |
| Interleukin 6 | 45 | 38 |
| Inducible NO synthase | 60 | 8 |
| Plasminogen activator | 12 | 12 |
| Pentraxin related gene | 72 | 42 |

Only those genes that showed a fold change from MCAO greater than 4 are presented. Seven days of Ang-(1-7) (1.1 nM; 0.5 μL/h) treatment prior to MCAO blunts the increases IL6, iNOS, and pentraxin related gene when compared to control animals treated with aCSF (0.5 μL/h). RNA samples were pooled (N=5) for each aCSF+sham, aCSF+ET-1, and Ang-(1-7)+ET-1 groups so that 3 arrays were used as described in the methods.

Table 2-3. Degradation of Ang-(1-7) in media of primary mixed glial cultures. Cells cultured as described in the Methods.

| Ang-(1-7) Start Conc, μM | Ave Conc Time 0 h | Ave Conc Time 14 h | Ave Conc Time 24 h | Ave Conc Time 48 h |
|---|---|---|---|---|
| 100 | 112 | 82 | 69 | 5 |
| 10 | 14 | 2 | 8 | 0.04 |
| 1 | 1 | 0.41 | 0.39 | 0.00 |

Averages (N=2) of media samples were calculated from HPLC analysis at different time points after Ang-(1-7) was added to the media.

.

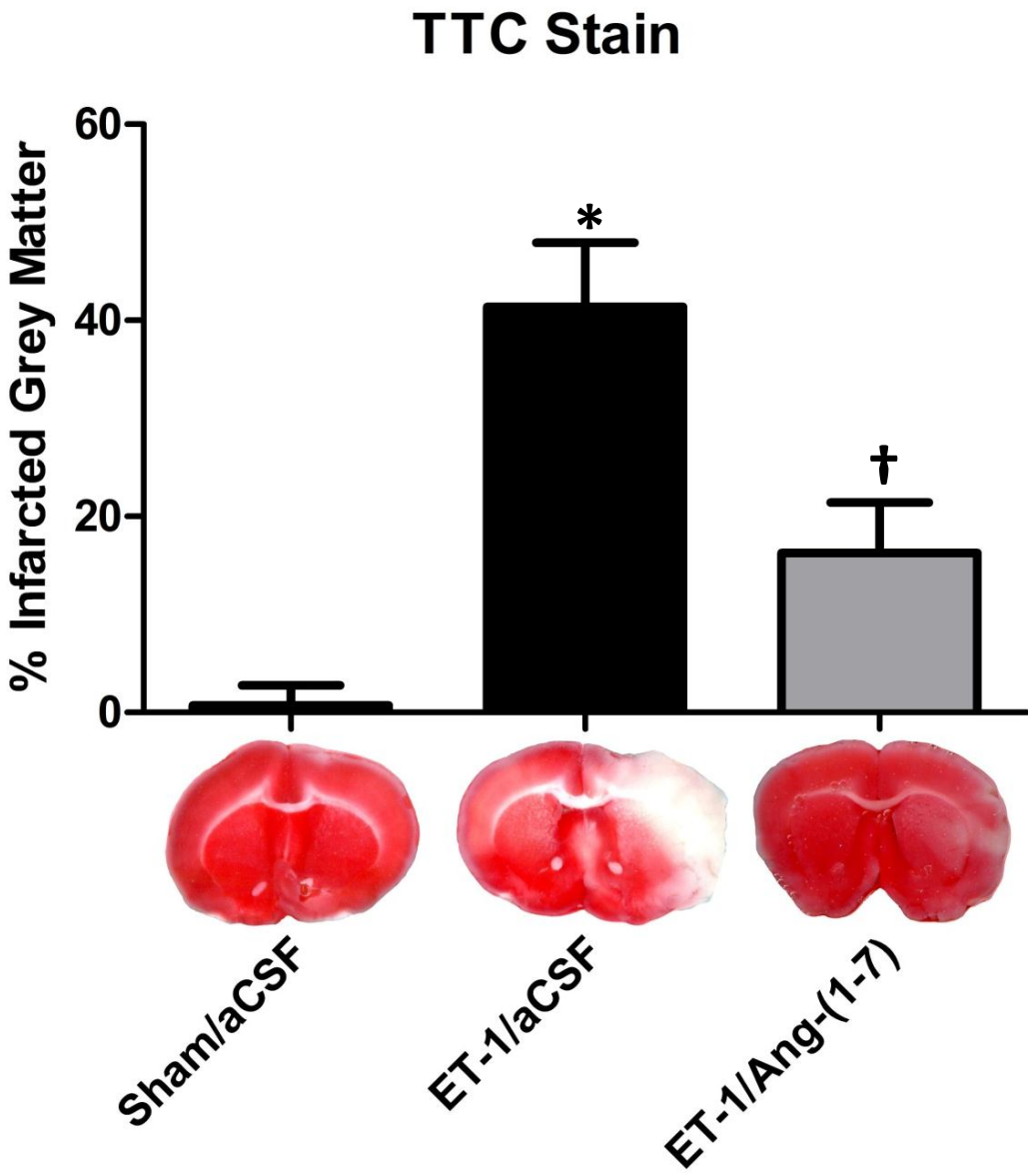


Figure 2-1. Intracerebral pretreatment with Ang-(1-7) reduces infarct size 24 h after ET-1-induced MCAO. Rats were pretreated via the ICV route with Ang-(1-7) (1.1 nM; 0.5 µL/h; n=8) or aCSF (0.5 µL/h; n=9) for 7 days prior to ET-1-induced MCAO as described in the methods. A control group of rats also underwent sham MCAO with 0.9% saline injection instead of ET-1 (n=5). Brains were removed for TTC staining 24 h after MCAO. Bar graphs are means + SEM showing the percentage infarcted grey matter in each treatment group. *P<0.05 compared to Sham/aCSF. †P<0.05 compared to ET-1/aCSF. Below are representative brain sections showing infarcted (white) and non-infarceted (red) grey matter.

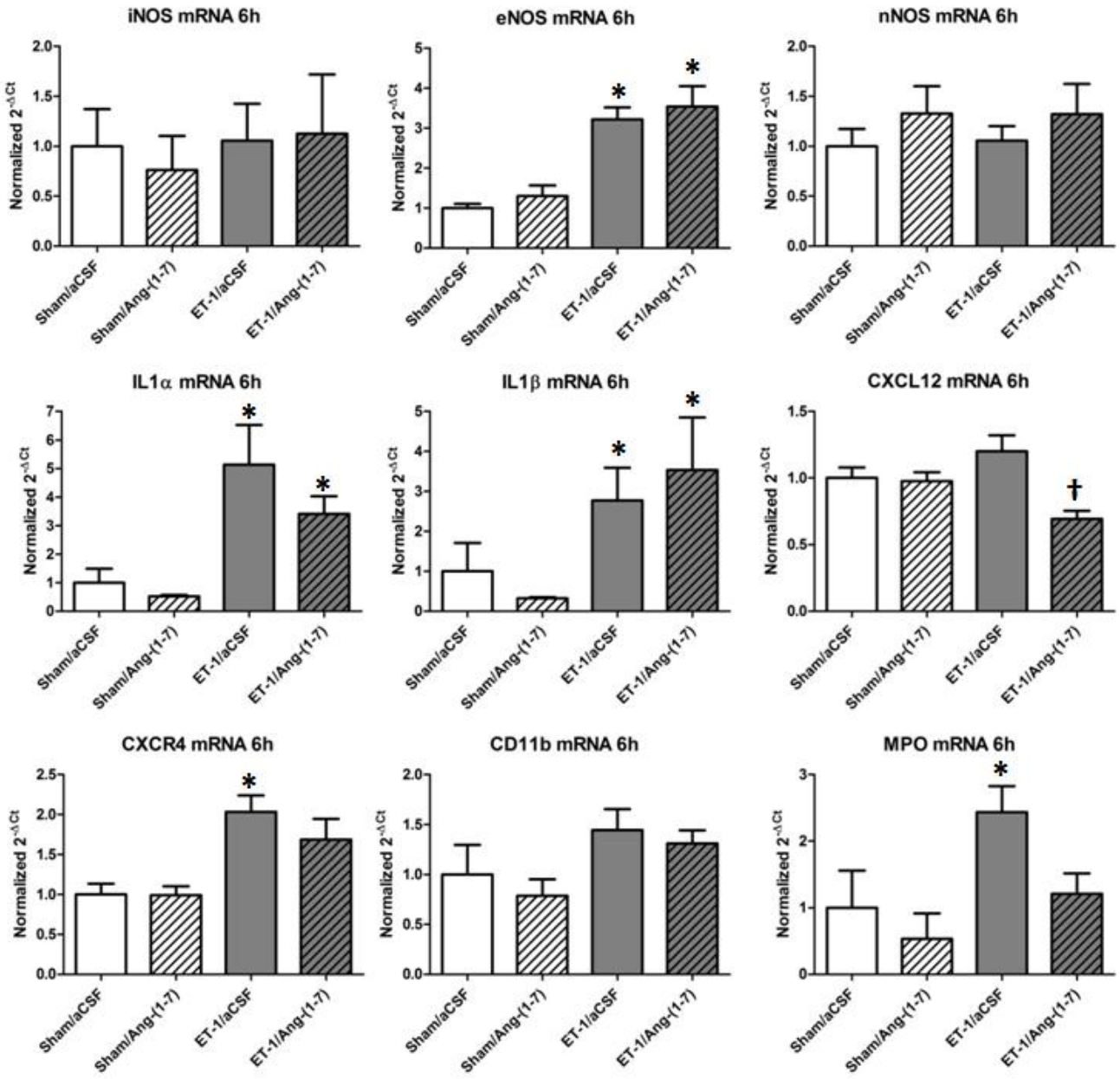


Figure 2-2. Gene expression in ipsilateral (right) cerebrocortical tissue 6 h after ET-1-induced MCAO. Rats underwent sham or ET-1 induced MCAO in the absence or presence of seven days infusion of Ang-(1-7) (1.1 nM; 0.5 μL/h) or aCSF (0.5 μL/h) via the ICV route. At 6 h post MCAO rats were euthanized and expression of the indicated genes in the ipsilateral cerebral cortex was assessed by qRT-PCR as detailed in the Methods. Bar graphs are means + SEM. N=6-11/group. *P<0.05 compared to Sham/aCSF. †P<0.05 compared to ET-1/aCSF.

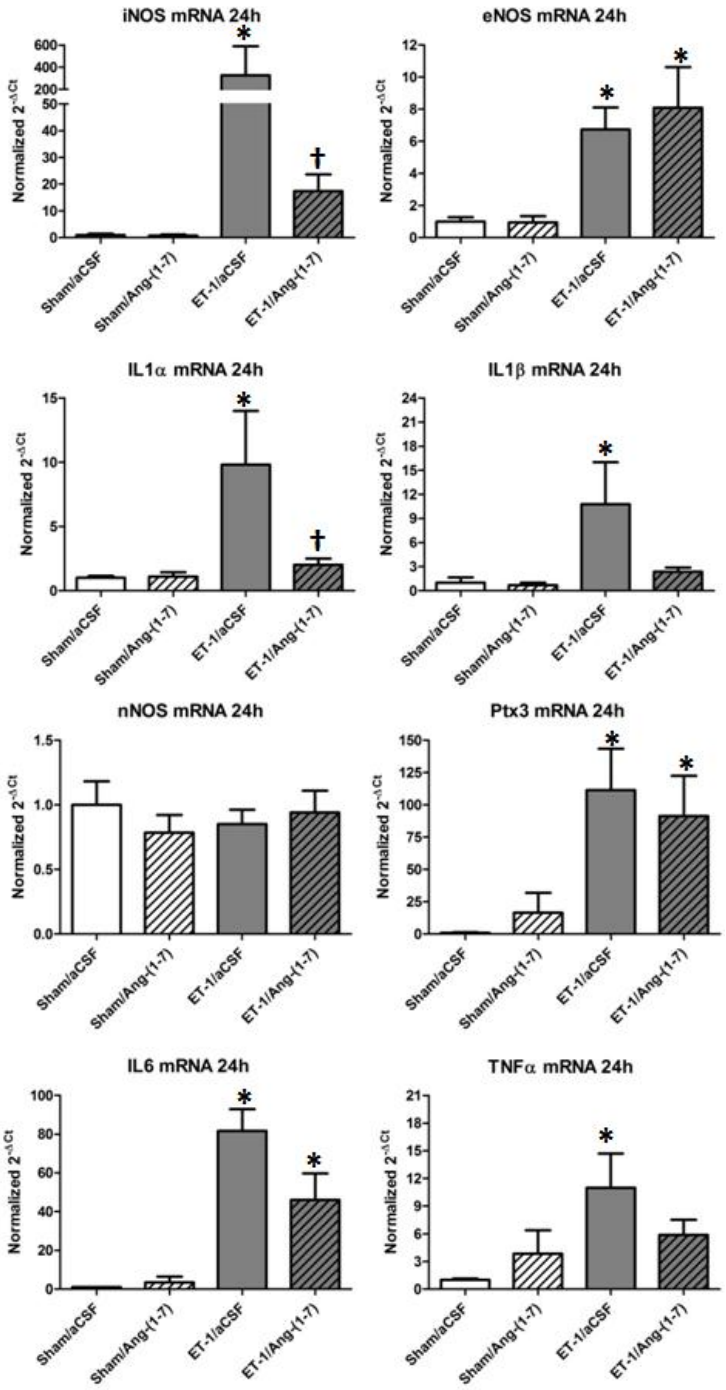


Figure 2-3. Gene expression of NOS isozymes and pro-inflammatory cytokines in ipsilateral (right) cerebrocortical tissue 24 h after ET-1-induced MCAO. Rats underwent sham or ET-1 induced MCAO in the absence or presence of seven days infusion of Ang-(1-7) (1.1 nM; 0.5 μL/h) or aCSF (0.5 μL/h) via the ICV route. At 24 h post MCAO rats were euthanized and expression of the indicated genes in the ipsilateral cerebral cortex was assessed by qRT-PCR as detailed in the Methods. Bar graphs are means + SEM. N=7-12/group. *P<0.05 compared to Sham/aCSF. †P<0.05 compared to ET-1/aCSF.

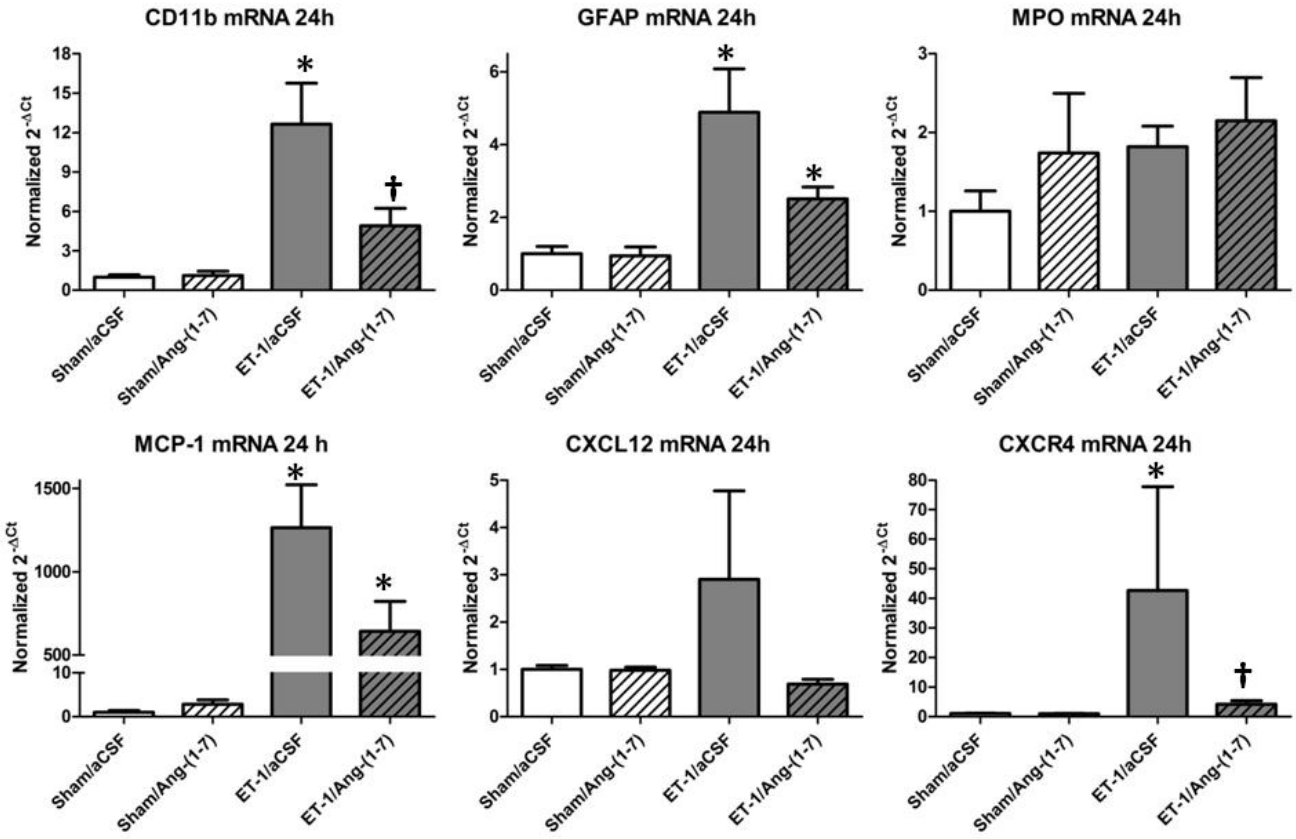


Figure 2-4. Gene expression of cell markers and migratory factors in ipsilateral (right) cerebrocortical tissue 24 h after ET-1-induced MCAO. Rats underwent sham or ET-1 induced MCAO in the absence or presence of seven days infusion of Ang-(1-7) (1.1 nM; 0.5 µL/h) or aCSF (0.5 µL/h) via the ICV route. At 24 h post MCAO rats were euthanized and expression of the indicated genes in the ipsilateral cerebral cortex was assessed by qRT-PCR as detailed in the Methods. Bar graphs are means + SEM. N=7-12/group. *P<0.05 compared to Sham/aCSF. †P<0.05 compared to ET-1/aCSF.

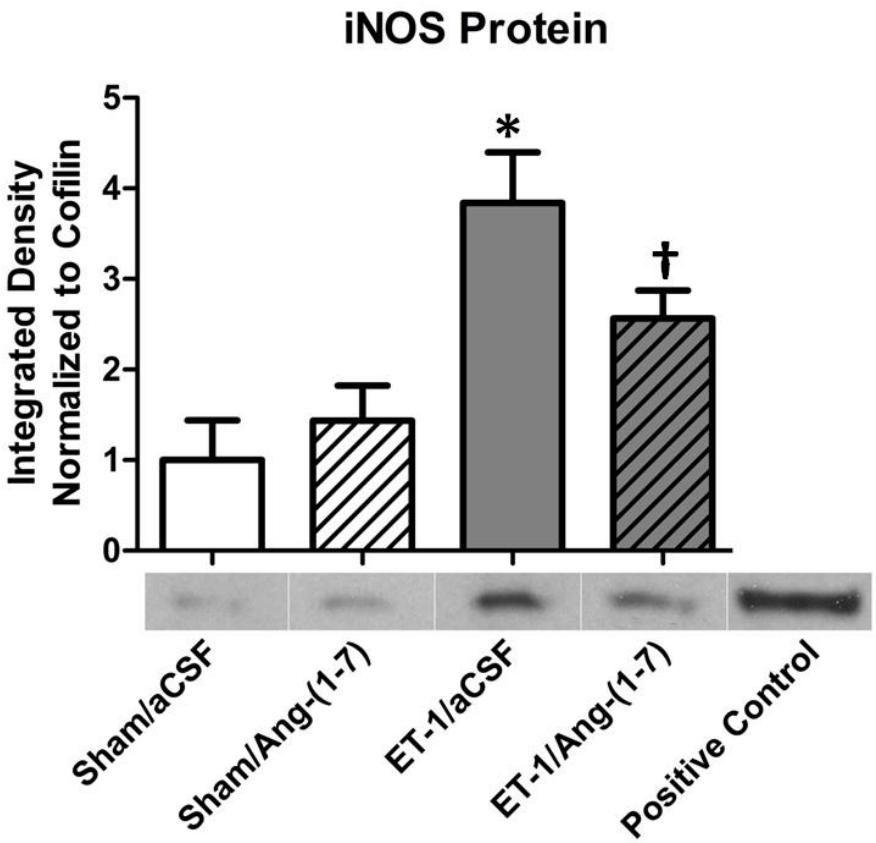


Figure 2-5. Levels of iNOS protein in ipsilateral (right) cerebrocortical tissue 24 h after ET-1-induced MCAO stroke or sham procedure. Rats underwent sham or ET-1 induced MCAO in the absence or presence of seven days infusion of Ang-(1-7) (1.1 nM; 0.5 µL/h) or aCSF (0.5 µL/h) via the ICV route. At 24 h post MCAO rats were euthanized and expression of iNOS protein in the ipsilateral cerebral cortex was assessed by Western blotting as detailed in the Methods. Bar graphs show levels of iNOS protein under each treatment condition, normalized against cofilin. Data are means + SEM. N=7-12/group. *P<0.05 compared to Sham/aCSF. †P<0.05 compared to ET-1/aCSF. Also shown are representative iNOS protein bands from each treatment, plus from a positive control (mixed cultured glial cells treated with LPS).

Figure 2-6. Previous page. Cellular localization of immunoreactive Mas in normal rat cerebral cortex and 24 h after ET-1-induced MCAO. Representative fluorescence micrographs taken at 40x magnification. A, B, C, D, and E) Panels from normal rat cerebral cortex and show respective co-localization of Mas (M; red fluorescence) with either NeuN (N), Ox-42 (Ox), Reca (Re), GFAP (G), or MPO [all green fluorescence]. F, G, and H) Panels from cortex 24 h after MCAO and show respective co-localization of Mas (M; red fluorescence) with either NeuN (N), Ox-42 (Ox) or MPO [all green fluorescence]. NeuN images (F) were taken in the penumbra. Ox-42 (G) and MPO (H) images were taken in the core of the stroke. Arrows indicate co-localization of Mas with neurons (NeuN), microglia (Ox-42) or endothelial cells (Reca). Panels I and J confirm Mas antibody specificity, showing no staining in knockout mouse brain tissue (KO, panel I) and staining in wildtype tissue (WT, panel J). N=3.

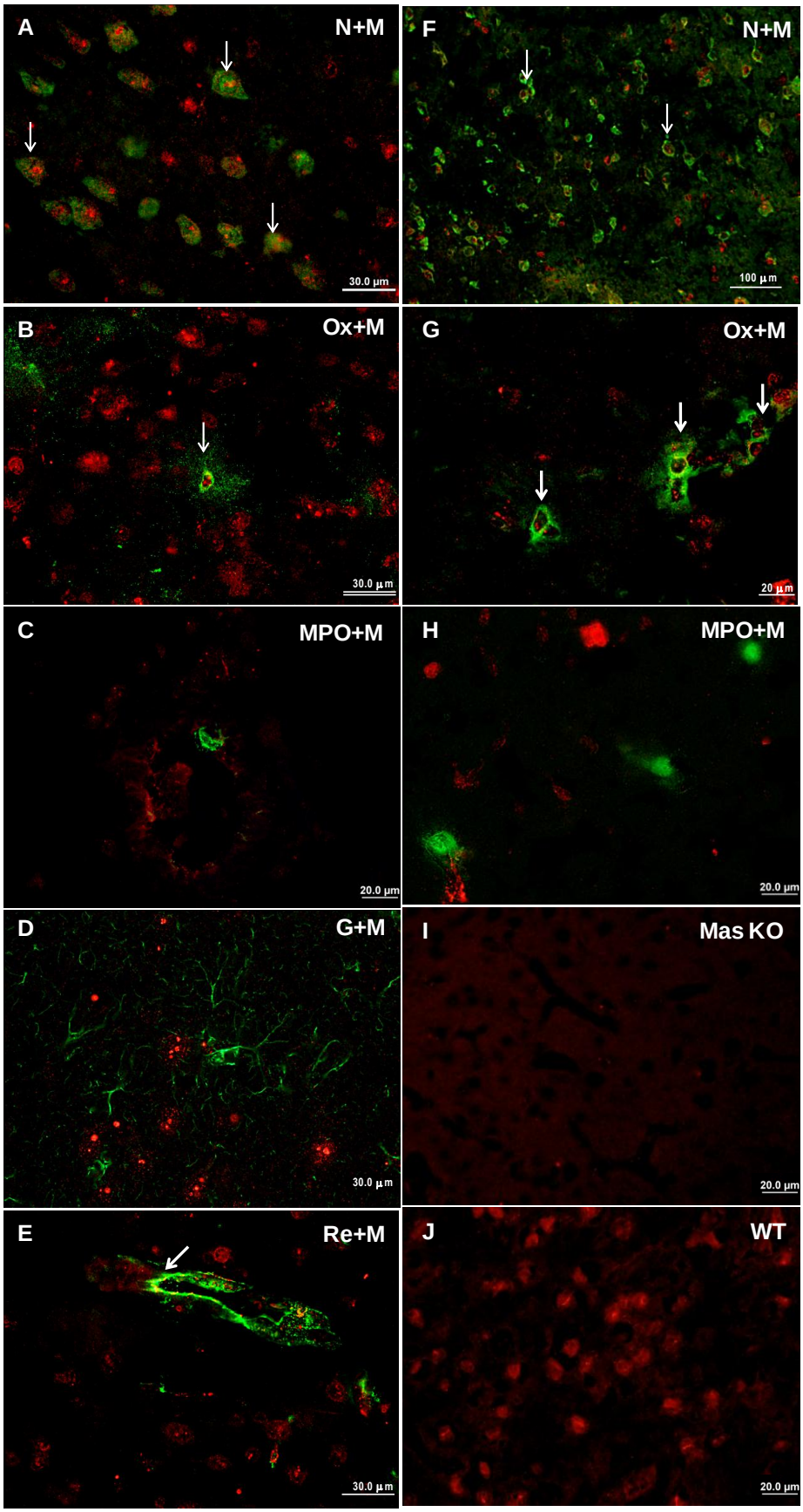
A
N+M
30.0 µm
F
N+M
100 µm
B
Ox+M
30.0 µm
G
Ox+M
20 µm
C
MPO+M
20.0 µm
H
MPO+M
20.0 µm
D
G+M
30.0 µm
I
Mas KO
20.0 µm
E
Re+M
30.0 µm
J
WT
20.0 µm

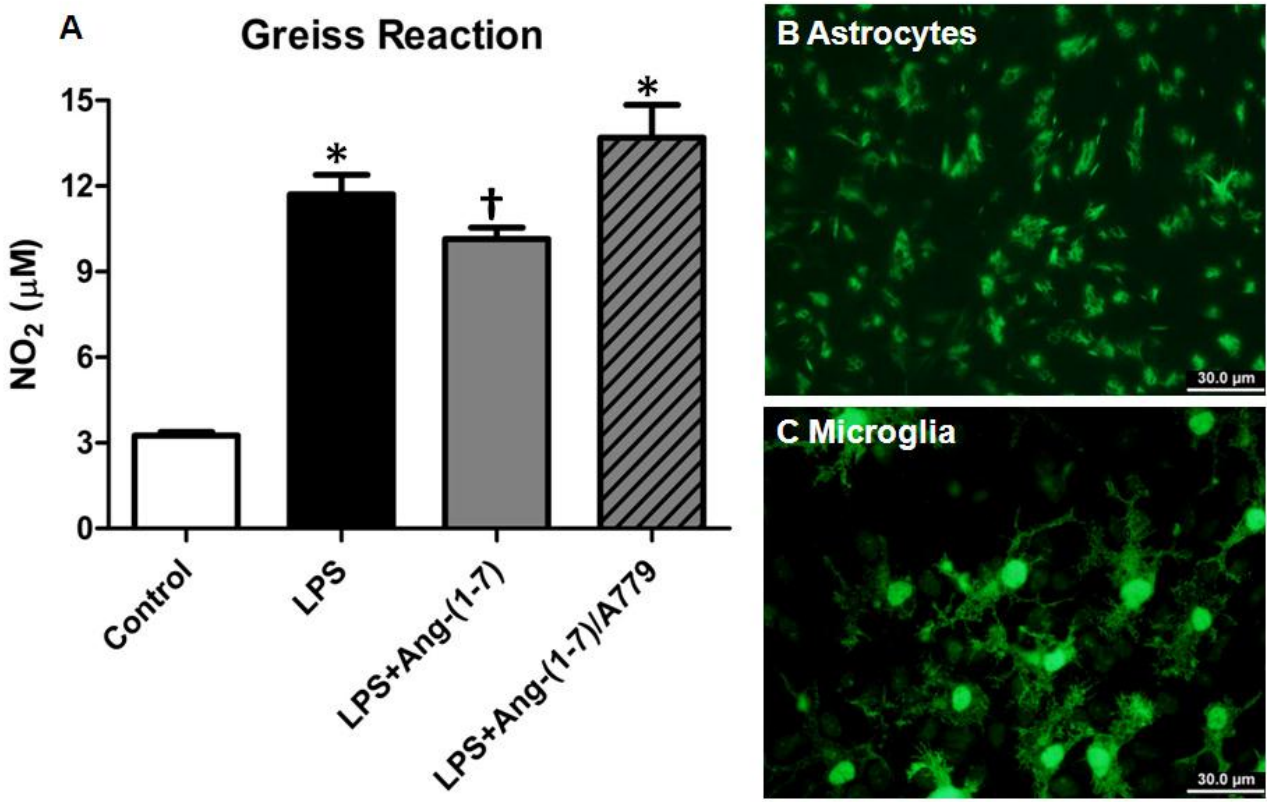


Figure 2-7. Ang-(1-7) blunts lipopolysaccharide (LPS)-induced increases in nitrite in the media of primary mixed glial cultures. Cells cultured as described in the Methods were treated as follows. Control solution (PBS), 24 h; LPS (10 ng/mL), 24 h; LPS (24 h) + Ang-(1-7) (0.1 nmol/mL), 24h. LPS (24 h) + Ang-(1-7) + A779 (1.0 nmol/mL). Note that Ang-(1-7) +/- A779 were administered 12 h before LPS, at the time of LPS treatment, and 12 h after LPS. Growth media were sampled 24 h after LPS treatment for analysis of nitrite ($NO_2$) via the Greiss reaction. A) Bar graphs are means + SEM showing the levels of $NO_2$ under each treatment condition. N=7 for control and N=10 for other treatment groups. *****P<0.05 compared to control. **†**P<0.05 compared to LPS. B and C) Fluorescence micrographs demonstrate the presence of immunoreactive GFAP (panel B) and immunoreactive Iba-1 (panel C) in the cultures used here, indicating the respective presence of astroglia and microglia.

# CHAPTER 3
# ANGIOTENSIN-(1-7) HAS CEREBROPROTECTIVE POTENTIAL IN HEMORRHAGIC STROKE AND INCREASES SURVIVAL OF STROKE-PRONE SPONTANEOUSLY HYPERTENSIVE RATS

## Introduction

In the United States, stroke is the fourth leading cause of death and a major cause of serious, long-term disability [220, 246]. There are two types of stroke: ischemic, where blood flow to the brain is reduced, and hemorrhagic, where persistent hypertension leads to vessel thinning and intracerebral bleeding. Very few therapies exist for both types, and the therapies that do exist can only be used in certain candidate patients. Hemorrhagic stroke, in particular, accounts for 10-20% of all strokes in Western populations [45], with a disproportionate affinity for Asians and African Americans [5]. Patients with hemorrhagic strokes that are most commonly induced by persistent hypertension have poor prognoses, often much worse than ischemic strokes of similar size. Furthermore, up to 30% of patients with ischemic stroke undergo hemorrhagic transformation [6], and many patients with ischemic strokes develop symptomatic hematomas following thrombolysis [54].

Both types of stroke are multifactorial, yet mounting evidence indicates that the renin-angiotensin system (RAS) is highly involved [165, 167-171, 173-175, 177, 185, 186, 191, 235]. The RAS has been implicated in many cardiovascular diseases. Primarily known for the effects of the angiotensin converting enzyme/angiotensin II/angiotensin type 1 receptor (ACE/Ang II/AT1R) axis, the RAS has been a target for the development of many potential therapies, including preventing the deleterious effects that lead to CNS damage following cerebral ischemia [247]. Numerous studies have shown that blocking the actions of Ang II at AT1R via angiotensin receptor blockers (ARBs) decreases

cortical/subcortical infarct size and the ensuing neurological deficits in animal models of stroke [168, 171, 173]. Human clinical trials have also shown that ARBs reduce cardiovascular risk and improve stroke prevention [167, 185, 186, 222]. Another axis of the RAS, the angiotensin converting enzyme 2/angiotensin-(1-7)/Mas (ACE2/Ang-(1-7)/Mas) axis, is receiving more attention in the literature for its therapeutic potential in cardiovascular disease and stroke diseases [137, 143, 223]. We demonstrated that intracerebroventricular treatment of Ang-(1-7) is cerebroprotective in endothelin-1-induced middle cerebral artery occlusion. Central Ang-(1-7) decreased the size of the infarct, improved rats' performance on neurological exams, and did not have any effect on cerebral blood flow [218]. Furthermore, we showed that this peptide has anti-inflammatory effects in the brain during stroke, preventing an over-activation of microglia and blunting pathological increases in pro-inflammatory cytokines and iNOS (Chapter 2).

Given Ang-(1-7)'s therapeutic potential in ischemic stroke and its anti-inflammatory effects, our aim here to determine if it also has any cerebroprotective effects in hemorrhagic stroke. Inflammation has a strong role in the mechanism of injury in hemorrhagic stroke. The inflammatory response begins soon after hemorrhage and peaks several days later in humans and animal models [58, 101, 114, 115]. The infiltration of neutrophils occurs within 2 days, and the activation of microglia may continue for 1 month [114, 116]. Evidence supports a role of microglia in hemorrhagic stroke pathology because inhibiting their activation reduces damage [117, 118, 120]. Furthermore, there is believed to be a strong association between inflammation and edema, as evidenced by data that correlates plasma tumor necrosis factor alpha concentrations in patients with

hemorrhagic stroke to the degree of brain edema [123]. For these experiments, we used stroke-prone Sponataneously Hypertensive Rats (spSHR). When fed a high salt diet, these rats spontaneously develop extremely high blood pressure resulting in hemorrhagic stroke and death. Here we show for the first time a cerebroprotective effect of Ang-(1-7) in spSHR, resulting in increased survival.

## Methods

### Ethical Approval and Animals

For the experiments described here, we used a total of 90 male stroke-prone Spontaneously Hypertensive Rats (spSHR) and 13 male Wistar Kyoto (WKY) rats purchased from Charles River Farms (Wilmington, MA, USA). All experimental procedures were approved by the University of Florida Institutional Animal Care and Use Committee. In addition, the principles governing the care and treatment of animals, as stated in the *Guide for the Care and Use of Laboratory Animals* published by the US National Institutes of Health (publication no. 85–323, revised 1996) and adopted by the American Physiological Society, were followed at all times during this study. Rats had *ad libitum* access to water and were housed in a well-ventilated, specific pathogen-free, temperature-controlled environment (24 ± 1°C; 12 h–12 h light–dark cycle). Rats were obtained at 35 days of age (weaning), and the spSHR were immediately started on a 4.0% high sodium diet (Research Diets). WKY rats were kept on standard chow.

### Implantation of Intracranial ICV Cannulae and Osmotic Pumps

ICV treatments were initiated when rats were 49 days old, except for the experiments involving direct blood pressure measurement (see below). Rats were anesthetized with a mixture of $O_2$ (1.5 L/min) and 4% isoflurane, placed in a Kopf stereotaxic frame, and anesthesia was maintained for the duration of the surgeries using

an $O_2$/isoflurane (2%) mixture delivered through a nose cone attached to the frame. Animals then underwent an intracranial ICV surgery essentially as detailed previously [176, 218]. This involved implantation into the left cerebroventricle (1.3 mm posterior to bregma, 1.5 mm lateral to bregma, and down through the cranium flush with the skull surface) of a stainless steel cannula (kit 1, ALZET, Cupertino, CA) coupled via vinyl tubing to a 6 week osmotic pump (model 2006, ALZET, Cupertino, CA) [197, 218, 248]. Osmotic pumps were implanted subcutaneously between the shoulder blades and were used to infuse Ang-(1-7) ± the Mas antagonist A779 (mixed in same pump) or control artificial cerebrospinal fluid (aCSF) into the left lateral cerebral ventricle. Infusion started at the time of ICV cannula placement and lasted for 6 weeks, until rats were 91 days old. Following this surgery, the wound was closed and each rat was administered an analgesic agent (buprenorphine; 0.05 mg/kg sc) before waking. Several studies were done, including a survival study, a study where animals were euthanized just before treatment ended (90 d old), and a study where animals were euthanized after the first spSHR died (108 d).

**Hemorrhage Number and Severity Assessment**

To compare the hemorrhages at the time of death, the brains were removed immediately after the rats were found dead. The whole brain for each rat was then photographed. Next, serial 2 mm sections were made throughout the entire brain to scan the subcortical regions. These sections were also photographed. The photographs were then analyzed by a research assistant who was blinded to the treatment groups. For each animal, the number of brain hemorrhages was counted. In addition, the severity of each hemorrhage was graded on a scale of 1 to 4, where 1 is minor and 4 most severe [249, 250]. Then the sum of the severity scores was calculated to give a global

assessment of severity called the “severity sum.” This was done for both the cortex using the whole brain and subcortex using the 2 mm sections. For the 2 mm sections, each section was counted, with no attempt to distinguish if a hemorrhage in one section had been counted in a previous section. We believe that this is the most objective and consistent way to count, as if a hemorrhage was counted more than once it would represent greater severity.

**Hermorrhage Volume**

For hemorrhage volume and hemoglobin content analysis [251], animals were euthanized at 108 days of age (when the first animal began to show signs of stroke) and transcardially perfused with normal saline. Brains were then taken from the skull, cerebellums and brainstems removed and discarded, and the remainder of the brain dissected into hemispheres. The right hemisphere was homogenized in 3 mL of PBS for 30 s and sonicated on ice for 1 min. 200 uL aliquots (15-fold dilution) were made. To prepare a standard curve, incremental volumes of homologous blood (0, 3, 6, 9, 12 uL) was added to 200 uL aliquots of homogenates from age matched WKY rats. These 200 uL aliquots were homogenized for 10 s and sonicated on ice for 20 s. Samples were then centrifuged at 13000 rpm for 30 min to allow collection of the hemoglobin containing supernatant. 50 uL of supernatant was added to 150 uL of Drabkin’s reagent (Sigma) and allowed to stand for 15 min at room temperature. The OD at 540 nm was then measured with a spectrophotometer. The concentrations of hemoglobin were then calculated using the standard curve of known volumes of blood. Then the dilution factor was used to calculate the amount of blood in the entire hemisphere.

**Brain Water Content**

For water content analysis, animals were euthanized at 108 days of age and

transcardially perfused with normal saline. Brains were then taken from the skull, cerebellums and brainstems removed and discarded, and the remainder of the brain dissected into hemispheres. The left hemisphere was weighed upon removal and again after 24 hours in a dryer oven to calculate the % water weight with the following formula: 100 x (wet weight – dry weight) / wet weight [251-253].

**Video Tracking and Locomotor Activity**

Rats were habituated to a circular open field (diameter 55 cm, height 42 cm) that was black in color. For acclimation, they were placed in the field for 10 min/day for three consecutive days before measurements were taken. Locomotor activity was monitored for 20 min on the fourth day (age 108 days old) and analyzed using Noldus Ethovision Software (Wageningen, The Netherlands) [254]. Immobility and rotation frequency were calculated. Immobility is the time that the running average mobility is below the immobile threshold. It is calculated by calculating the changed area of the rat, indicating movement. Rotation Frequency is the number of turns (either clockwise or counterclockwise) of 360 degrees. As rats are place in a circular field, we also interpret this result as a measure of activity.

**Sunflower Seed Task**

A sunflower seed eating task [176, 218, 255] was used that provides an index of fine motor function to assess the level of neurological deficits. In this test, the number of shell pieces that the rats leave after consuming 5 seeds is recorded. Rats with less neurological impairment open the five seeds more efficiently by breaking the shell into fewer pieces to accomplish the task. This task was performed from age 56 to 102 days old to monitor sensorimotor function.

**Morris Water Maze**

Rats underwent the Morris Water Maze task as previously described [256]. Briefly, each was placed in a 160-cm diameter black pool filled to a depth of 30 cm with clear water maintained at room temperature. Rats were required to locate a submerged platform using visual cues placed around the pool. They were placed in the pool at one of four different locations (N, S, E, W) and given 90 s to locate a 10-cm sided square platform submerged 2 cm below the surface of the water. Three trials of 5 d each were conducted, starting at 70, 77, and 84 days of age, respectively. For the first 4 d, the latency (s) to find the platform was recorded. On the 5$^{th}$ day, a probe trial was conducted in which rats were placed in the pool for 90 s without the platform. The time spent in the quandrant of the pool that previously had the platform was recorded.

**Mas Co-localization Immunohistochemistry**

For the Mas immunohistochemistry, control spSHR were euthanized at 90 days of age. The brains were fresh frozen in Tissue-Tek® OCT™ Compound (Sakura Finetech, Torrance, CA), as we previously determined the Mas antibody to work better with fresh frozen tissue (Chapter 2). Mas was co-stained with NeuN, GFAP, RECA, and OX-42, which are respective specific markers for neurons, astroglia, endothelial cells and microglia. Procedures were as follows. Brain sections were cut from the 2 mm coronal section block at 5um and air dried at room temperature overnight. OCT was removed in a wash of 1X TBS for 5 minutes. Slides were drained and wiped, then blocked for 1 hour in 2% horse serum diluted in 1X TBS. Slides were wiped and blocking buffer was replaced with antibody cocktails (rabbit anti-Mas [1:400] combined with either mouse anti-NeuN [1:100], anti-GFAP [1:100], anti-OX-42 [1:100], anti-RECA [1:100] or anti-MPO [1:50] diluted in antibody diluent (Invitrogen, Carlsbad, CA), and

incubated overnight at 4°C. Following two 5min washes in TBS, Alexafluor donkey anti-rabbit 594 and donkey anti-mouse 488 were added to the slides, both at 1:500. After a 45 minute room temp incubation, slides were again double washed in TBS. Sections were then post fixed for 5 minutes in 10% neural-buffered formalin, washed twice more, then wiped dry before mounting in DAPI vectashield (Vector Labs, Burlingame, CA). Furthermore, to verify Mas antibody specificity, it was tested in brain tissue from a Mas knockout mouse. There was no positive staining present in the knockout brain tissue, while staining was present in tissue from the wild type.

**Stereology and Immunostaining**

For stereology experiments, animals were euthanized just before the pumps ran out of treatment at 90 days of age. These animals were perfused transcardially (normal saline followed by 10% formalin), and the brains were removed. The brains were postfixed in 10% formalin for 24 h, and then cryoprotected in 30% sucrose in 0.1M phosphate buffer. Brains were then frozen in dry ice and stored at -80°C. Systematic uniform random sampling was achieved by exhaustively sectioning brains coronally on a calibrated freezing stage microtome (30 μm) through the full rostro-caudal extent of the striatum, beginning just caudal to the olfactory bulbs and ending at the rostral hippocampus. A registered 1-in-15 series of sections was obtained for each animal and separate series were randomly assigned for processing to detect total striatal microglia (IBA-1) or neurons (NeuN). Sections were collected into cold 0.1M TBS and stored at 4°C until stained immunohistochemically. Free-floating tissue sections were washed several times in Tris-buffered saline (TBS; 100 mM Tris-HCL, 150 mM NaCl, pH 7.5), pre-incubated in blocking solution containing 3% normal donkey serum (NDS) and 0.3% Triton X-100 in TBS for 1 hour, and incubated in blocking solution with the addition of

the appropriate primary antibodies for 72 hrs at 4°C. Specific antibody combinations and dilutions used were: rabbit anti-IBA-1 (Wako 019-19741, 1:500) and mouse anti-NeuN (Millipore MAB377, 1:1000). After primary incubation, sections were washed in 0.1M TBS, and incubated in TBS containing 3% NDS and appropriate secondary antibodies (Alexa 488 and 555; Molecular Probes, 1:300). Secondary incubations were performed for 2 h at room temperature in the dark. After secondary incubation, sections were washed in 0.1M TBS, and mounted onto Superfrost++ slides. Coverslips were applied with ProLong Gold (Invitrogen), sealed with clear fingernail polish, and stored in the dark at 4°C until analysis.

Quantification was done using the optical fractionator method [257, 258], implemented using a Zeiss AxioImager.M2 epiflourfescent microscope, equipped with the appropriate filter sets, a CCD camera, and a computer-driven X, Y and Z Ludl-motorized stage controlled with StereoInvestigator software (MBF Bioscience, Williston, VT). Initial z-plane analyses confirmed that each antibody penetrated the full section thickness. The boundaries of the striatum were delineated at low power magnification (2.5X) in a systematically random series of sections, spaced 450 µm apart (every 15$^{th}$ section), that extended rostrally from the emergence of the striatum in the corpus callosum and ended caudally at the disappearance of the striatum when the rostral hippocampus appeared. Cell estimates were derived from a minimum of 9 sections (per label). The motorized stage of the microscope was moved in evenly spaced x-y intervals under the computer control, surveying the regions of interest in each section according to a systematic random sampling scheme (see Table 3-1 for sampling details). Section thickness was measured at each sampling site using a 40X oil-immersion objective

(with 1.4 numerical aperture) and quantification was confined to a 20 μm optical disector height which was positioned 3 μm below the surface of the tissue. Cells were counted at each site if its top most nucleus first came into focus with the optical disector, provided it did not encroach on the exclusion lines of the counting frame [257, 259]. The total number of IBA-1 and NeuN immunopositive cells in the stratum were estimated using the optical fractionator method [258] in which the product of the cells counted in a known, uniformly random sample of the region of interest is multiplied by the reciprocal of the sampling fraction. Additional details, including stereological sampling parameters are provided in Table 3-1. The precision of the stereological estimates was determined by estimating the coefficients of error (CE) using methods previously described [257]. Equations used to generate the CEs are based on Gundersen's smoothness classification m=1, as the areas defined for the cell counts changed smoothly from the rostral entrance and caudal conclusion of the striatum.

**qRT-PCR**

For RNA, rats were euthanized just before the pumps ran out of treatment at 90 days of age. Fresh brains were taken from the skull, the cerebellum and olfactory bulbs were removed, and the remaining tissue was flash frozen in liquid nitrogen and saved at -80°C. Total RNA was extracted using TRIzol (Invirogen, etc) and purified using an RNeasy Plus kit (Qiagen, Valencia, CA, USA). Isolated RNA underwent DNAse I treatment to remove genomic DNA. Extracted RNA was reverse transcribed with a high-capacity cDNA reverse transcription kit (Bio-Rad Laboratories, Hercules, CA) and then analyzed *via* quantitative real-time reverse transcriptase polymerase chain reaction (qRT-PCR) in a PRISM 7000 sequence detection system (Applied Biosystems, Foster City, CA) as detailed by us previously [218, 225]. Oligonucleotide primers and TaqMan

probes specific for rat IL6, IL1α, IL1β, iNOS, MPO, GFAP, CD11b, and MCP-1 were obtained from Applied Biosystems (Carlsbad, California). Data were normalized to GAPDH expression.

**Direct Blood Pressure**

For direct blood pressure measurements, radiotelemetry transducers were implanted at 49 days of age. To allow time for recovery, the ICV cannulae and mini-osmotic pumps were not implanted until 63 days of age (procedure described above). For the telemetry transducer implantation, rats were anesthetized with a mixture of $O_2$ (1 L/min) and isoflurane (4%). Rat telemetry transducers (TA11PA-C40, DSI) were implanted into the abdominal aorta, as described by us previously [176, 260]. Rats were administered the analgesic (buprenorphine; 0.05 mg $kg^{-1}$ S.C.) following surgery, and were left to recover for 14 days before the implantation of subcutaneous mini-osmotic pumps. Data were collected every 2-3 days from age 49 d to age 72 d, when the sample sizes started to get small due to fewer animals surviving.

**Indirect Blood Pressure**

For indirect blood pressure measurements, we implanted the mini-osmotic pumps at 49 days of age to remain consistent with our other experiments. Blood pressure was recorded via an indirect tail-cuff plethysmography method as described previously [197, 218]. Briefly, blood pressure was non-invasively measured by determining the tail blood volume with a volume pressure recording sensor and an occlusion tail-cuff (CODA System, Kent Scientific, Torrington, CT). Rats were placed in the restraint and warmed on the warming plate for about 3 min until external temperature is 30°C. The pressure cuff was then cycled 5 times to acclimatize the rat followed by 15 cycles to collect blood pressure data. Data were collected every 2-5 days from age 70 d to age

129 d, when the sample sizes started to get small due to fewer animals surviving.

**Body weight**

Body weight was recorded using an analog Taconic Rat Scale Model YG-700 (Evanston, IL) just before rats were euthanized at 108 days old.

**Corticosterone**

At 108 days of age blood was collected prior to euthanasia. Serum was separated for corticosterone analysis using an enzyme immunoassay kit (K014-H1, Arbor Assays) as described by the manufacturer.

**Creatinine and BUN**

At 108 days of age blood was collected prior to euthanasia. Serum was separated for creatinine and BUN analyses. A University of Florida veterinary laboratory performed these standard analyses.

**Kidney and Heart Pathology**

Rats were euthanized at 90 days of age and perfused transcardially (normal saline followed by 10% formalin). Kidneys and hearts were removed and stored in 10% formalin until sectioned. Kidney sections were stained with H&E and PAS, and heart sections were stained with H&E and trichrome by the histology core at the University of Florida. Pathology was assessed in blinded fashion by a licensed veterinary pathologist. Glomerular and tubular alterations were evaluated by a lesion scoring system developed by our collaborator [261]. Specifically, glomeruli were evaluated for the presence or absence of tuft atrophy, Bowman's capsule changes, peri-glomerular fibrosis, membranoproliferative changes, degree of hypercellularity, thickening of Bowman's capsule, tuft adhesions, and sclerosis. This included all the glomeruli on the entire slide. Lesion scores were assigned as follows: 0 = no lesions, 1 = less than 10%,

2 = 10 to 25%, 3 = 25 to 50%, and 4 = greater than 50% of total slide area affected. Similarly, tubular lesions were scored from across the entire section, including interstitial fibrosis, cellular infiltrates, and tubular atrophy with thickening of the basement membrane. Lesion scores were assigned as follows: 0 = no lesions, 1 = <25%, 2 = 25 to 50%, and 3 = >50% of total slide area affected. Heart lesions were scored from across the entire section, including degenerative myofiber changes, interstitial fibrosis, and cellular infiltrates [262]. The severity of microscopic lesions observed was graded based on the degree and extent of tissue damage using a four-point scale of absent (0), minimal (1), mild (2), moderate (3), and marked (4). Minimal (grade 1) lesions involved less than 10% of the heart section. Mild (grade 2) lesions involved 11%–40% of the heart section. Moderate (grade 3) lesions involved 41%–80% of the heart section. Marked (grade 4) lesions involved greater than 81% of the heart section.

**Chemicals**

Ang-(1-7) and A779 were purchased from Bachem Bioscience (Torrance, CA, USA). ET-1 was from American Peptide Company, Inc (Sunnyvale, CA, USA). Rabbit anti-Ang-(1-7) Mas receptor antibody was from Alomone Labs (Jerusalem, Israel). Mouse anti-rat RECA-1 was from AbD Serotec (Raleigh, NC). Mouse anti- MPO, mouse anti-GFAP, rabbit anti-iNOS (ab15323), rabbit anti-Cofilin (ab11062) and goat anti-rabbit IgG HRP (ab6721) antibodies were from Abcam (Cambridge, MA). Mouse anti-OX-42 antibody was from BD Biosciences (San Jose, CA). Mouse anti-NeuN was from Millipore (Bedford, MA). Rabbit anti-Iba-1 (01919741) was from Wako (Richmond, VA). Alexafluor donkey anti-rabbit 594 and anti- mouse 488 were from Molecular Probes [Invitrogen] (Carlsbad, CA, USA). Vectashield mounting medium with DAPI (4',6-diamidino-2-phenylindole) was from Vector Labs (Burlingame, CA, USA). All other

chemicals were purchased from Fisher Scientific (Pittsburgh, PA, USA).

### Data Analysis

Data are expressed as means ± SEM. Statistical significance was evaluated, as specified in the figure legends, with the use of a one-way ANOVA, two-way row matched ANOVA, Newman-Keuls test, Dunn's test, t-test, or log rank as appropriate. Differences were considered significant at $p<0.05$.

## Results

### Ang-(1-7) Treatment Improves Survival of Stroke-prone Spontaneously Hypertensive Rats

In previous studies, we demonstrated that Ang-(1-7), administered ICV, had cerebroprotective effects in ischemic stroke [218]. Furthermore, our studies investigating underlying mechanisms showed that this cerebroprotection was likely due to an anti-inflammatory effect of Ang-(1-7) (Chapter 2). Therefore, we were motivated to examine any therapeutic effects of Ang-(1-7) in hemorrhagic stroke, as inflammation and edema contribute to its pathophysiology [58, 101, 114, 115]. Here we show that 6 weeks of central Ang-(1-7) treatment, infused from 49 to 91 days of age, increases the survival of stroke-prone Spontaneously Hypertensive Rats (spSHR) (Figure 3-1). The median survival is increased from 108 days in control aCSF treated spSHR to 154 days in Ang-(1-7) treated spSHR. Furthermore, this effect is reversed when the Mas antagonist A779 is co-administered with Ang-(1-7), indicating that this effect on survival is Mas dependent.

### Ang-(1-7) Treatment Decreases the Number and Severity of Hemorrhages in the Subcortex/Striatum, but not in the Cortex at the Time of Death of spSHR

Observational studies of spSHR have shown that they exhibit several cortical and subcortical hemorrhages when they die and that these hemorrhages are considered their primary cause of death in most cases [249, 250]. Here, both cortical and subcortical

hemorrhages were observed in brains removed from spSHR immediately after death (Figure 3-2A, 3-2B). Ang-(1-7) did not have an effect on the number or severity of hemorrhages counted in the cortex (Figure 3-2C, 3-2E) in these brains. There was, however, a significant decrease in the number of hemorrhages in the subcortex/striatum and a trend toward decreasing the severity of the hemorrhages in these regions (Figure 3-2D, 3-2F).

### Ang-(1-7) Treatment has no Effect on Brain Hemorrhage Volume (Hemoglobin Content) or Water Content

To more thoroughly investigate the severity of hemorrhages and edema, total hemorrhage volume (brain hemoglobin content) and water content. There was no effect of Ang-(1-7) on total hemorrhage volume when the rats were euthanized at 108 days old. This is likely because significant hemorrhagic strokes had yet to occur when rats were euthanized at 108 days old instead of waiting for rats' death. This is supported in that spSHR hemoglobin content was not significantly different from the hemorrhage volume of the control WKY rats. In addition, Ang-(1-7) treatment did not have an effect on water content of the brains when rats were euthanized at 108 days old. Similar to the hemorrhage volume data, the water content of spSHR brains was not different from that of the control WKY brains, suggesting that edema and other pathology had not yet occurred to a significant degree when rats were euthanized.

### Ang-(1-7) Treatment Improves the Neurological Status of spSHR, but has no Effect on Visuospatial Memory

The most obvious signs of neurological disease in spSHR are lethargy and general sensorimotor dysfunction [249]. We therefore chose to measure spontaneous movement using video tracking software and a sunflower seed eating task [218]. The video tracking software was used at 108 days of age. Ang-(1-7) decreased the mean

immobility of spSHR, or the duration of time that rats were immobile (Figure 3-4A). This suggests that the rats treated with Ang-(1-7) demonstrated less lethargic behavior. Also, Ang-(1-7) increased the rotation frequency within a circular arena, indicating that spontaneous movement is increased (Figure 3-4B). The sunflower seed eating task was performed repeatedly to track general sensorimotor function from 56 to 102 days of age. A significant improvement in the efficiency to shell seeds was observed in the Ang-(1-7) treated spSHR when analyzing both curves by repeated ANOVA with several time points showing very large differences (Figure 3-4C). They left fewer shell pieces behind, showing that they could better manipulate the seeds to eat them. Despite these improvements in neurological function observed in the Ang-(1-7) treated spSHR, no improvements were observed in visuospatial memory as measured by the Morris water maze task (Figure 3-5A, 5B).

**Cellular Localization of Immunoreactive Mas in spSHR Striatum**

Having shown that Ang-(1-7) has therapeutic potential in hemorrhagic stroke, we sought to examine potential mechanisms for these effects. We used immunostaining to investigate both the cell types that expressed the Ang-(1-7) receptor Mas and the cellular location of this receptor in the spSHR striatum to learn what cell types could be involved. Our results were in accordance with our previous study of Sprague Dawley cortical tissue (Chapter 2). Mas immunoreactivity is present in neurons (anti-NeuN, Figure 3-6A, 6B), microglia/macrophages (anti-OX-42, Figure 3-6C, 6D), and endothelial cells (anti-RECA, Figure 3-6E, 6F). However, Mas did not co-localize with astroglia (anti-GFAP, Figure 3-6G, 6H). It should be noted that we confirmed the specificity of the Mas antibody using Mas knockout mouse brain tissue. There is no staining in the knockout, where staining is obvious in the wild type (Figure 3-6I, 6J).

### Ang-(1-7) Decreases Microglia and Increases Neuron Survival in the Striatum

Since we previously demonstrated an effect of Ang-(1-7) on macrophage/ microglia activation in an ischemic model of stroke and in cell culture (Chapter 2), we aimed to quantify the number of microglia in the striatum in this spSHR model to determine their role in the mechanism of cerebroprotection. We focused on the striatum because it was the brain region where Ang-(1-7) significantly decreased the number of hemorrhages. Using stereology and Iba-1 immunostaining, Ang-(1-7) was shown to decrease the number of macrophages/microglia in the striatum (Figure 3-7). Ang-(1-7) appeared to blunt their over-activation and migration to this region. Furthermore, we also quantified neurons to determine if their survival was affected by Ang-(1-7) treatment. Using stereology and NeuN immunostaing, Ang-(1-7) was shown to increase the number of neurons in the striatum (Figure 3-7).

### Ang-(1-7) does not Alter the Expression of Genes Related to Inflammation in Whole Brain Homogenate

Our previous study investigating anti-inflammatory effects of Ang-(1-7) in ischemic stroke indicated that the expression of several key genes was altered by Ang-(1-7) (Chapter 2). Therefore, we examined the expression of IL6, IL1α, IL1β, iNOS, MPO, GFAP, CD11b, and MCP-1 in spSHR to see if a similar effect could be measured. IL6, IL1α, MPO, and CD11b were increased in spSHR compared to WKY controls, but there were no differences due to Ang-(1-7) treatment (Figure 3-8). Although there was a trend for IL1β and MCP-1 to be decreased by Ang-(1-7) treatment, none of the differences were statistically significant.

### Ang-(1-7) has no Effect on Mean Blood Pressure during Infusion in spSHR, but Rats Treated with Ang-(1-7) have Lower Mean Blood Pressure later in Life after Treatment Ends

Effects of central Ang-(1-7) on blood pressure would of course affect stroke, so we examined mean arterial pressure two different ways (Figure 3-9). Direct blood pressure measurements using telemetry transducers showed no effect of central Ang-(1-7) infusion on blood pressure. In another group of spSHR, indirect blood pressure measurements using tail cuff plethysmography showed no effect of Ang-(1-7) during the infusion. However, this technique allowed longer monitoring of animals after the pumps ran out of treatment. The spSHR that were previously treated with Ang-(1-7) had lower blood pressure later in life.

### Ang-(1-7) has no Effect on Body Weight, Corticosterone, Creatinine, BUN, or Kidney/Heart Pathology

We also aimed to rule out other peripheral effects of Ang-(1-7). Body weight was recorded just prior to euthanasia at 108 days old. There was no significant effect of Ang-(1-7). Furthermore, spSHR animals did not have different body weights compared to age-matched WKY rats. In addition, blood was collected at 108 days old, and serum was separated for corticosterone, creatinine, and BUN analysis. There were no significant effects of Ang-(1-7) on any of these analyses. Again, age matched WKY rats were not significantly different from spSHR either. We also scored the kidney and heart pathology at 90 days of age, as this is more sensitive than creatinine and BUN levels. A blinded licensed veterinary pathologist assessed tuft atrophy, Bowman's capsule thickening, periglomerular fibrosis, membranoproliferative changes, tubular interstitial fibrosis and cell infiltration, tubular degeneration/regeneration, heart degeneration, and

heart fibrosis and inflammation. For each metric, spSHR had more pathology that age matched WKY rats, but there was no effect of Ang-(1-7).

## Discussion

This present study demonstrates, for the first time, cerebroprotective effects of central Ang-(1-7) in spSHR. Perhaps the most convincing evidence is this peptide's ability to increase the survival of this rat strain. We believe this is a Mas dependent effect, since the survival time in spSHR treated with both Ang-(1-7) and A779 (Mas antagonist) is between spSHR treated with aCSF or Ang-(1-7) alone. Other evidence in support of Ang-(1-7)'s therapeutic potential in spSHR include an effect to decrease the number of hemorrhages in the striatum/subcortex at the time of death. There was a trend to decrease the number in the cortex, but it did not reach statistical significance. It is possible that the Ang-(1-7) could better diffuse to the striatum relative to the cortex, as it is infused into the lateral ventricle, which borders the striatum. We were surprised that there were no statistical differences in the hemoglobin content or water content when animals were euthanized at 108 days old. There are several experimental details that may provide an explanation. First, whole brain hemispheres were analyzed. If Ang-(1-7)'s effects were more localized to the striatum, the effects may be diluted. Also, the animals were all euthanized at 108 days old, the same age. This is the ideal way to compare groups, but it is possible that not enough hemorrhages and pathology/edema existed in many of the animals. This is supported by the data as the water content and hemoglobin content in WKY rats are not significantly different from both spSHR groups. There is, however, convincing neurological data at these ages. One of the most common neurological signs in spSHR as the pathology progresses is lethargy. Central Ang-(1-7) treatment reduces immobility and increases rotation frequency in a circular

open field designed to measure spontaneous activity. In addition, spSHR treated with Ang-(1-7) show improved performance on the sunflower seed eating task when analyzed by repeated ANOVA over a time course, which measured global sensorimotor function. We further hypothesized that because spSHR experience multiple microhemorrhages and edema as they age [249], visuospatial memory might decline. This was not observed when we subjected rats to the Morris water maze task, however. For each of these neurological exams we did not include a WKY control group, as it has been well documented that WKY are not good controls for spSHR, especially when it comes to behavioral studies [263, 264]. We believe these functional improvements add greatly to the evidence supporting a cerebroprotective effect of Ang-(1-7).

Previously, we performed an immunohistochemical co-localization study to determine what cell types in the brain of Sprague Dawley rats contain Mas (Chapter 2). We repeated this study with spSHR to confirm that the expression of Mas was the same. Indeed we found Mas immunoreactivity to be present on neurons, microglia, and endothelial cells. This affirmed our hypothesis that inflammation could be involved in the mechanism of cerebroprotection in spSHR. As previously stated, inflammation has a strong role in the mechanism of injury in hemorrhagic stroke. The inflammatory response begins soon after hemorrhage and peaks several days later in humans and animal models [58, 101, 101, 115]. The infiltration of neutrophils occurs within 2 days, and the activation of microglia may continue for 1 month [114, 116]. Evidence supports a role of microglia in hemorrhagic stroke pathology because inhibiting their activation reduces damage [117, 118, 120]. To observe changes in microglia and neurons in the striatum just before treatment ran out at 90 days of age, we used stereological techniques to count

cells. As stated, we focused on the striatum because it was this region where Ang-(1-7) had the greatest effect to reduce the number of hemorrhages. Ang-(1-7) decreases the number of microglia and increases the number of surviving neurons, providing further support of a neuroprotective action. Interestingly, we did not observe changes in gene expression that corroborated this. In an ischemic model of stroke, we saw Ang-(1-7) blunt pathological increases in iNOS, proinflammatory cytokines, and CD11b (Chapter 2). We did not observe any Ang-(1-7) effect here when rats were euthanized just before the end of treatment at 90 days old. This may be because not enough pathology had developed to cause measurable changes in gene expression at this time point. Alternatively, we have observed that some gene expression differences are not measurable when analyzing the entire brain [218], as we did here. However, we believe this is the only way to perform a gene expression study in this model because the hemorrhages occur throughout the brain. Furthermore, it would be difficult to consistently dissect out just one region, such as the striatum, for analysis.

Another major question we considered was whether or not centrally administered Ang-(1-7) could have any peripheral or systemic effects. We performed two studies to investigate mean arterial pressure. The first measured pressure directly using radiotelemetry transducers. There was no effect of Ang-(1-7) on blood pressure. The second measured pressure indirectly using tail cuff plethesmography. These animals that did not undergo the invasive telemetry transducer implantation surgery survived longer. Because of this, we could carry out the experiment after ICV pumps ran out of treatments. As with the direct measurements, we observed no effect of Ang-(1-7) during infusion. However, when the curve is separated into treatment and post-treatment

curves and analyzed separately, the animals that were previously treated with Ang-(1-7) have decreased mean arterial pressure later in life after the pumps run out of treatment. This suggests a protective effect of Ang-(1-7) that is not measureable later until pathology develops. Perhaps Ang-(1-7) is having some kind of effect on blood pressure control regions of the brain by decreasing inflammation there. Further experiments will need to be conducted to answer these questions. We also wanted to examine several other endpoints. At 108 days of age, there was no effect of Ang-(1-7) on body weight, serum corticosterone, BUN, or creatinine. Lastly, we could not measure any effect of centrally administered Ang-(1-7) on the histopathology of the heart or kidneys, although there were differences compared to the control WKY rats.

This study provides the first evidence that activating the ACE2/Ang-(1-7)/Mas axis may have therapeutic potential in hemorrhagic stroke. Ang-(1-7) given ICV is cerebroprotective in spSHR and increases their survival. This corroborates a cerebroprotective effect we have observed in a model of ischemic stroke [218]. The stereology data in this study also corroborates that Ang-(1-7) has anti-inflammatory effects (Chapter 2). We think the findings are robust as survival is improved, physical endpoints are improved, and behavioral endpoints are improved. The interesting observation that animals treated with Ang-(1-7) have lower blood pressure later in life after treatment ends merits further experiments. In addition, further studies will need to be performed to better understand the intracellular signaling and mechanism of protection of Ang-(1-7).

Table 3-1. Parameters used for stereology.

| Object | Sampling Grid (μM x μM) | Counting Frame (μM x μM) | Dissector Height (μM) | Mean Object Counted | Average CE |
|---|---|---|---|---|---|
| NeuN+ cells | 800 x 800 | 50 x 50 | 20 | 1460 | 0.04 |
| IBA-1+ cells | 800 x 800 | 50 x 50 | 20 | 503 | 0.05 |

Total cell numbers were estimated using the formula: *N* (Total number) = 1/ ssf (section sampling fraction) x 1/asf (area sampling fraction) x 1/hsf (height sampling fraction) x number of immunopositive cells counted. The total number of cells counted for each subject and the sampling grid and counting frame used to generate the asf for each label are provided above. The ssf is the current study equaled ¼ in every case. The hsf was calculated using the mean weighted thickness (with section thickness measured at each sampling site). SD=standard deviation**;** CE=coefficient of error, Gundersen's CE, m=1**;** N= 6/group.

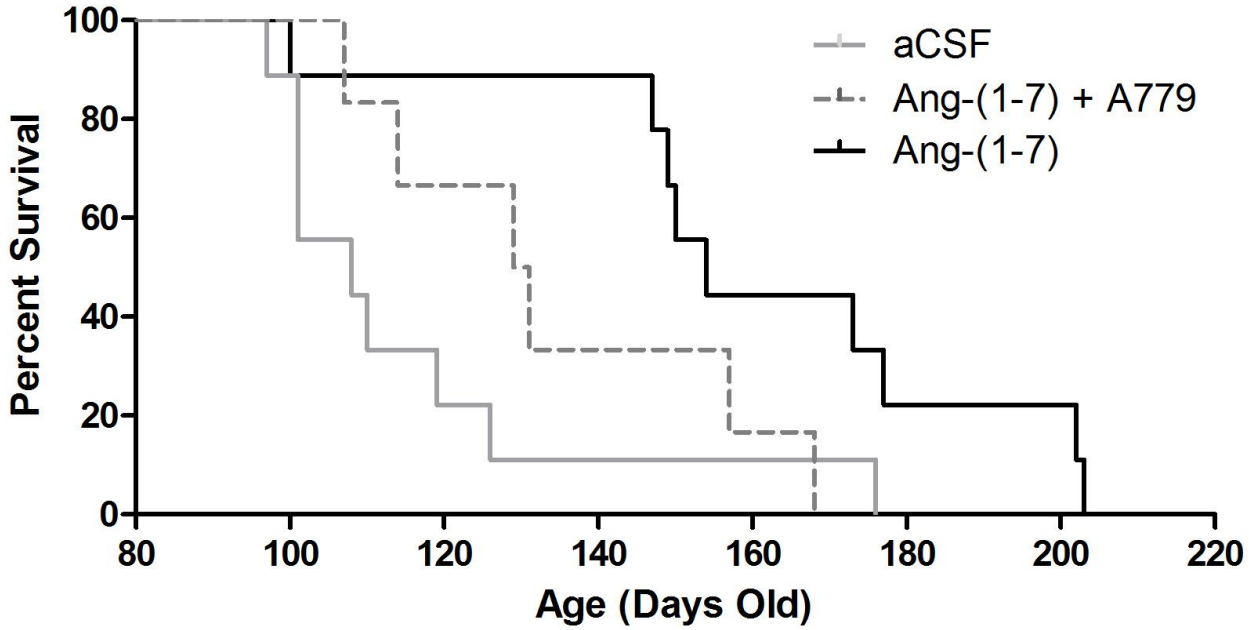


Figure 3-1. Ang-(1-7) treatment improves survival of stroke-prone Spontaneously Hypertensive Rats (spSHR). spSHR are fed a 4% sodium diet after weaning (35 days old). 6 wk Ang-(1-7) (1.1 nM; 0.5 μL/h), aCSF (0.5 μL/h), or Ang-(1-7) (1.1 nM; 0.5 μL/h) + A779 (2.75 nM; 0.5 μL/h) pumps implanted at 49 days old; 6-week old pumps ran out of treatment at 91 days old. Animals were monitored and maintained on high salt diet until death. N = 9 for aCSF, Ang-(1-7). N = 6 for Ang-(1-7) + A779.

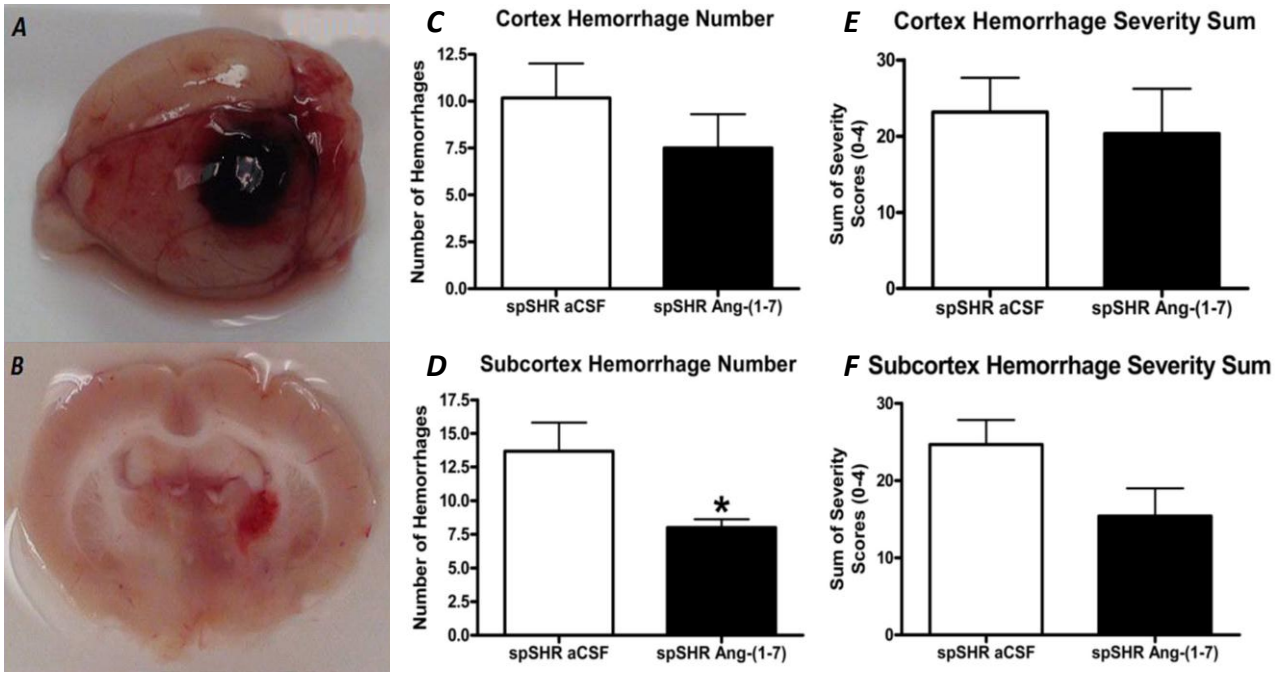


Figure 3-2. Ang-(1-7) treatment decreases the number of hemorrhages in the subcortex/striatum, but not in the cortex at the time of death of spSHR. spSHR are fed a 4% sodium diet after weaning (35 days old). 6 wk Ang-(1-7) (1.1 nM; 0.5 µL/h) or aCSF (0.5 µL/h) pumps implanted at 49 days old; 6-wk old pumps ran out of treatment at 91 days old. Animals were monitored and maintained on high salt diet until death, when their brains were removed. A) Representative cortex hemorrhages. B) Representative subcortex/striatum hemorrhages. C and D) Cortex/subcortex hemorrhage number was counted as described in the methods. E and F) Cortex/subcortex severity was assessed from 0-4 for each hemorrhage and these values were summed to calculate the “severity sum” as described in the methods. Bar graphs are means + SEM. N=6/group. *P<0.05 compared spSHR aCSF.

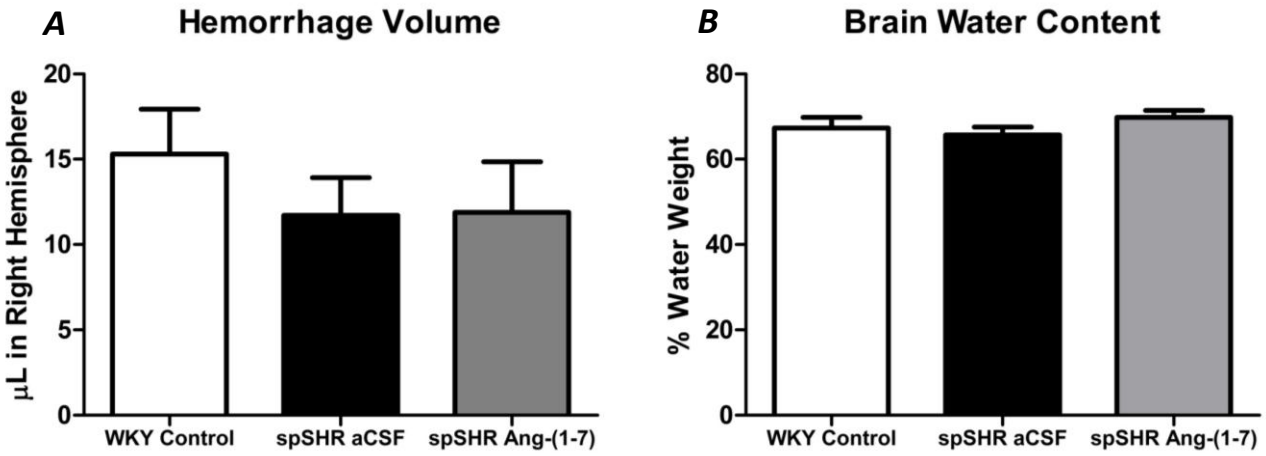


Figure 3-3. Ang-(1-7) has no effect on brain hemorrhage volume or water content. Ang-(1-7) (1.1 nM; 0.5 μL/h) or aCSF (0.5 μL/h) pumps were implanted in 49 day-old spSHR. aCSF (0.5 μL/h) pumps were also implanted in 49 day-old WKY controls. 6-week pumps ran out of treatment at 91 days old. Rats were euthanized at 108 days old and perfused with sterile saline. Brains were removed and dissected into hemispheres. For panels A and B, bar graphs are means + SEM. N=4, 9, and 7 for WKY, spSHR aCSF, and spSHR Ang-(1-7), respectively. A) Hemoglobin. The right hemisphere was homogenized and hemoglobin content was used to determine the hemorrhage volume as described in the methods. B) Water content. The left hemisphere was weighed upon removal and again 24 hours later to calculate the % water weight.

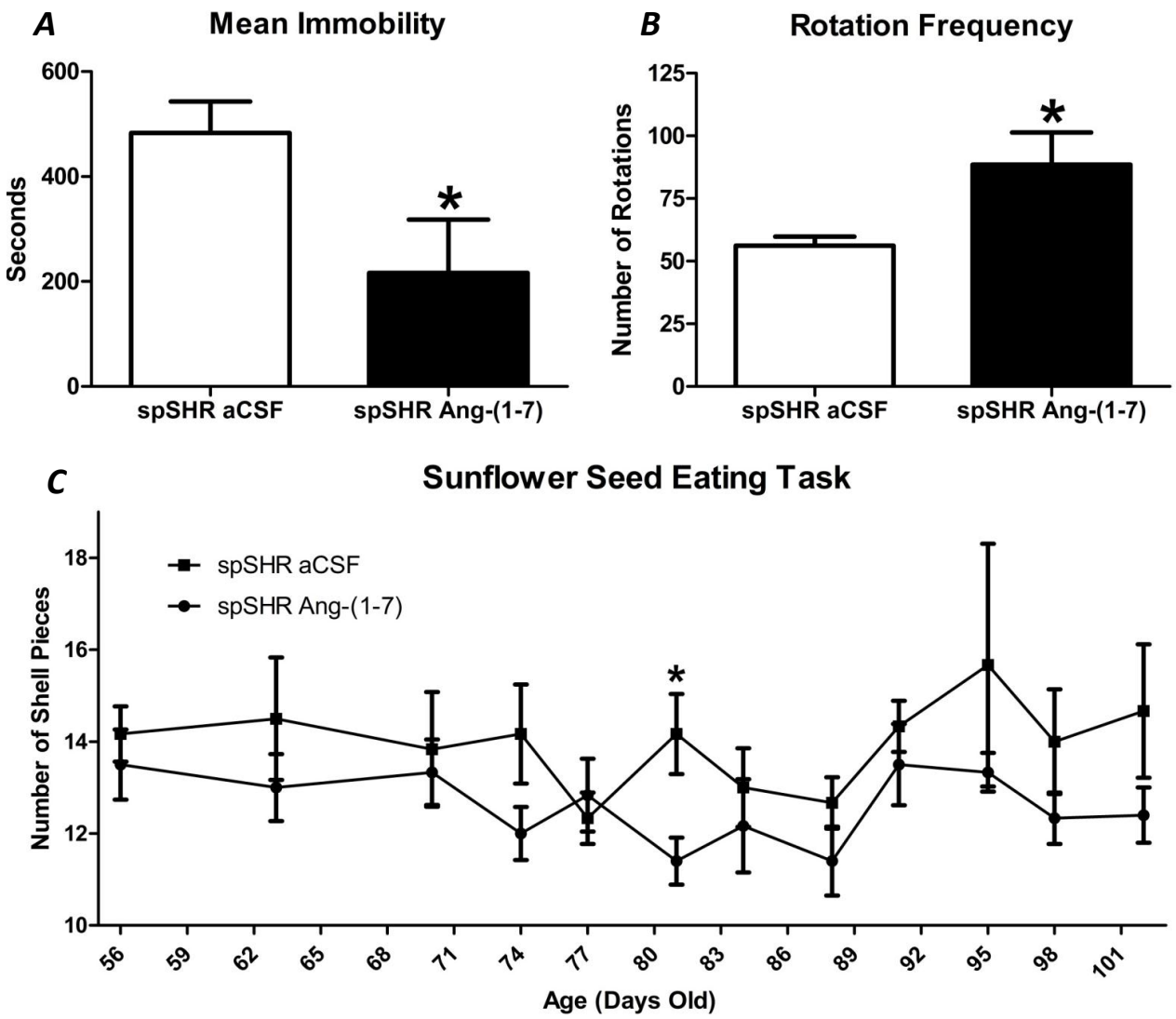


Figure 3-4. Ang-(1-7) treatment improves neurological status of spSHR. 6 wk Ang-(1-7) (1.1 nM; 0.5 µL/h) or aCSF (0.5 µL/h) pumps implanted at 49 days old; 6-week old pumps ran out of treatment at 91 days old. A) Ang-(1-7) decreases immobility showing a reversal of lethargy as assessed before euthanasia at 108 days old. Bar graphs are means + SEM. N=9 for spSHR aCSF and 7 for spSHR Ang-(1-7). B) Ang-(1-7) increases rotation frequency showing an increase in spontaneous movement within the circular arena as assessed before euthanasia at 108 days old. Bar graphs are means + SEM. N=9 for spSHR aCSF and 7 for spSHR Ang-(1-7). C) Ang-(1-7) improves performance of spSHR on the sunflower seed eating task allowing them more efficiently shell seeds. Timeline shows that the number of remaining shell pieces after eating 5 seeds is reduced, especially at age 81 days old. Data are means +/- SEM. N=6 per group. *P<0.05 compared to spSHR aCSF.

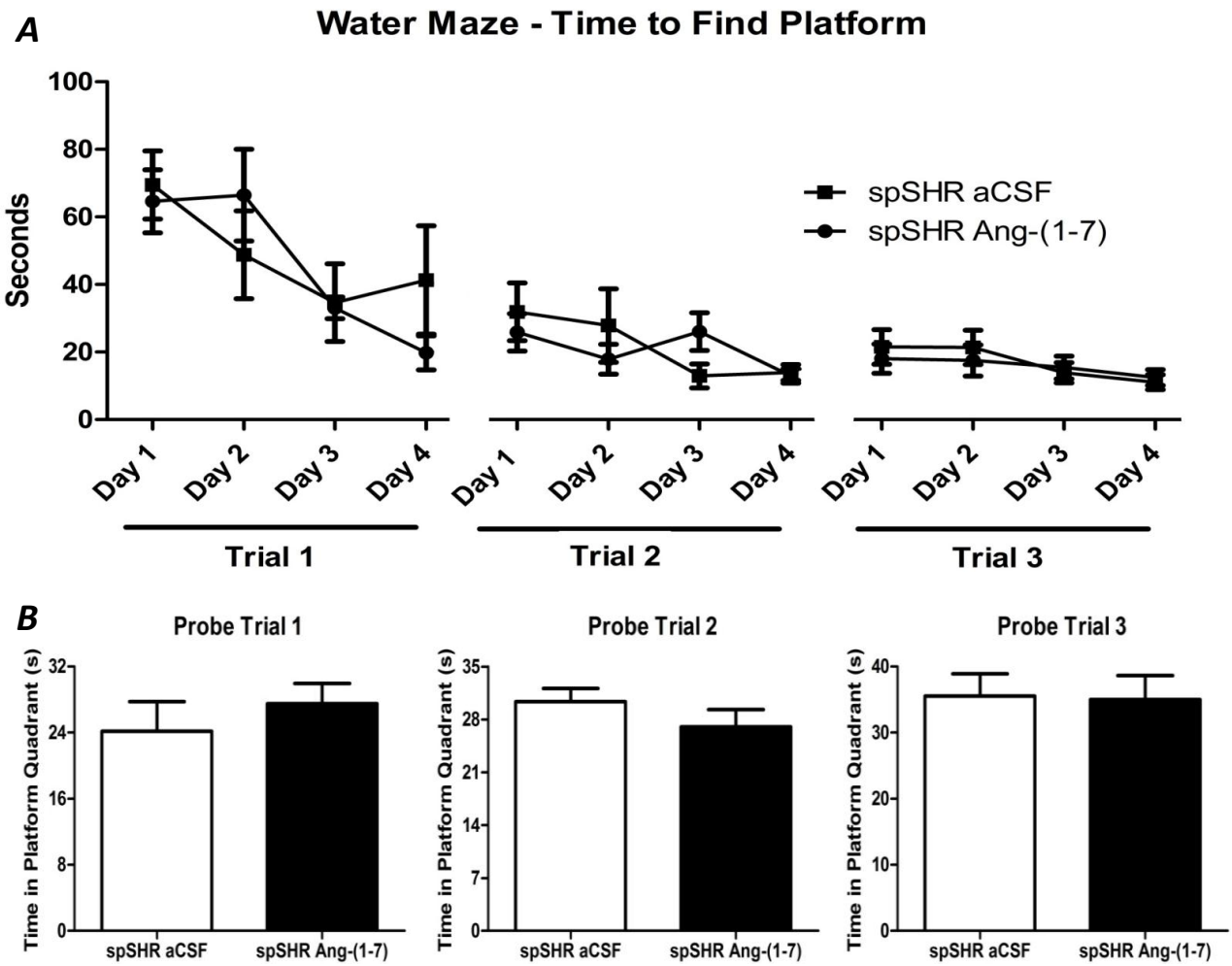


Figure 3-5. Ang-(1-7) does not improve performance visuospatial memory as assessed by the Morris Water Maze Task. Ang-(1-7) (1.1 nM; 0.5 μL/h) or aCSF (0.5 μL/h) pumps were implanted in 49 day-old spSHR. aCSF (0.5 μL/h) pumps were also implanted in 49 day-old WKY controls. 6-week pumps ran out of treatment at 91 days old. Trial 1, 2, and 3 were started at 70, 77, and 84 days of age, respectively. N=6/group. A) Time (s) it takes to find the platform. Three trials were performed, each lasting 4 d. B) Probe trials were conducted on the 5th day of every trial. Rats were placed in the maze and the time (s) spent in the quadrant where the platform was previously located was recorded.

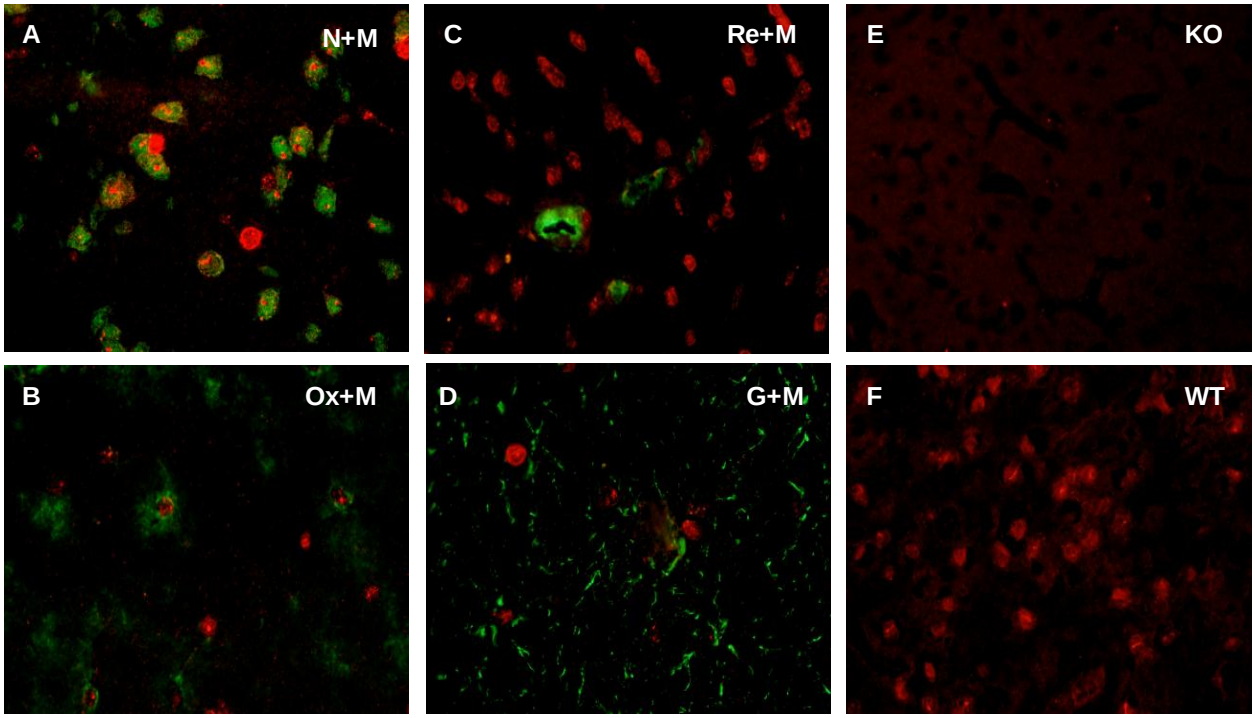


Figure 3-6. Cellular localization of immunoreactive Mas in spSHR striatum. Representative fluorescence micrographs taken at 40x magnification. N=3. Panels A, B, C, and D show respective co-localization of Mas (M; red fluorescence) with either NeuN (N), Ox-42 (Ox), Reca (Re), or GFAP (G) [all green fluorescence]. Panels E and F verify that the anti-Mas antibody is specific as staining is not present in the knockout mouse striatum (E; KO), but is in the wild-type mouse striatum (F; WT).

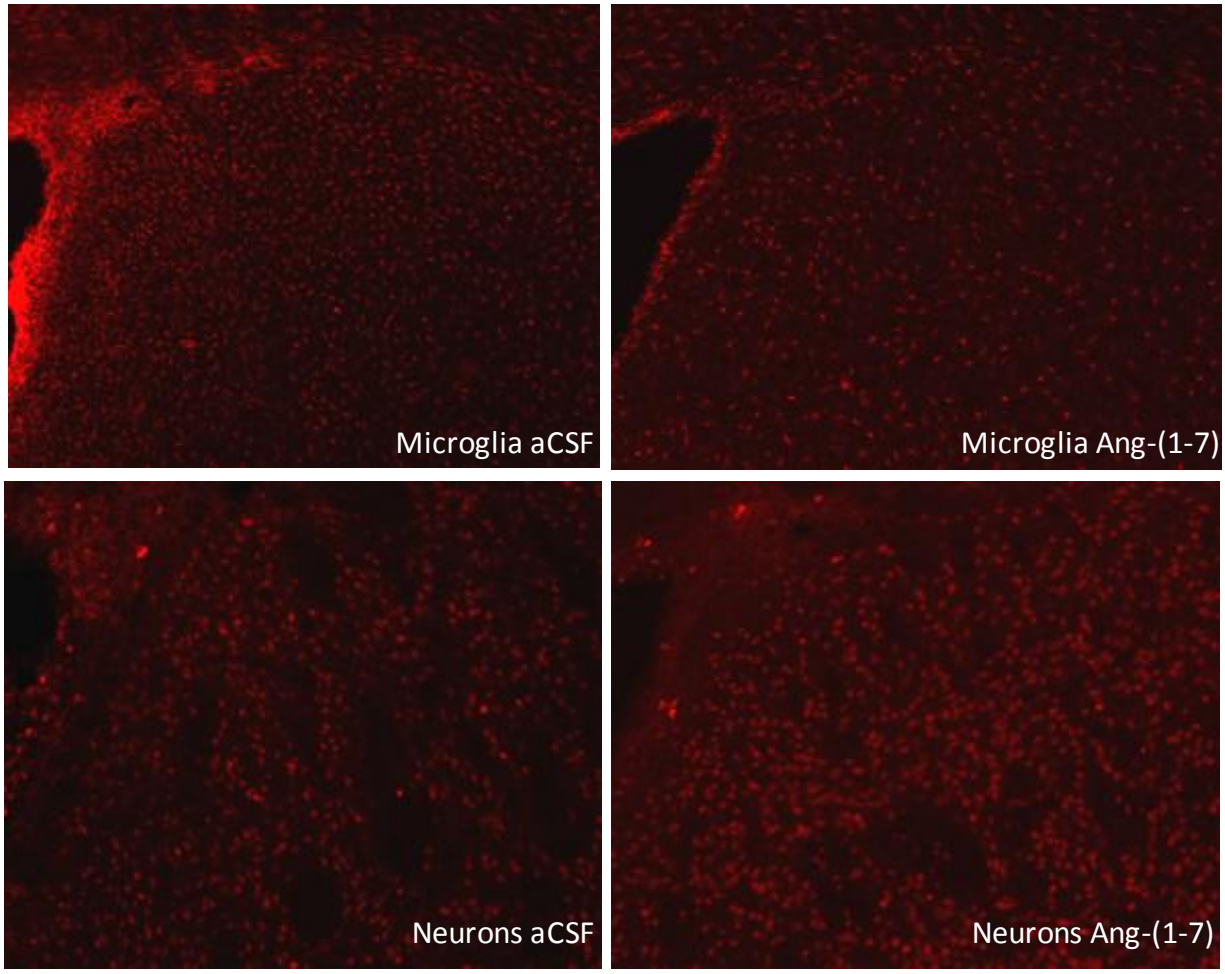


| | spSHR aCSF | spSHR Ang-(1-7) |
|---|---|---|
| NeuN+ cells (SD) | 3,801,013 (938,768) | 3,005,173 (935,436) |
| IBA-1+ cells (SD) | 5,093,099 (1,209, 808) | 6,335,407 (984,034) |

Figure 3-7. Ang-(1-7) decreases activated microglia and increases neuron survival in the striatum just before treatment ends. Ang-(1-7) (1.1 nM; 0.5 µL/h) or aCSF (0.5 µL/h) pumps were implanted in 49 day-old spSHR. Rats were euthanized at 90 days old, 1 day before treatment ran out of the 6 wk pumps, and perfused with saline and formalin. Brains were removed and fixed. Stereology was used to determine the number of cells in the striatum as described in the methods. N=3/group.

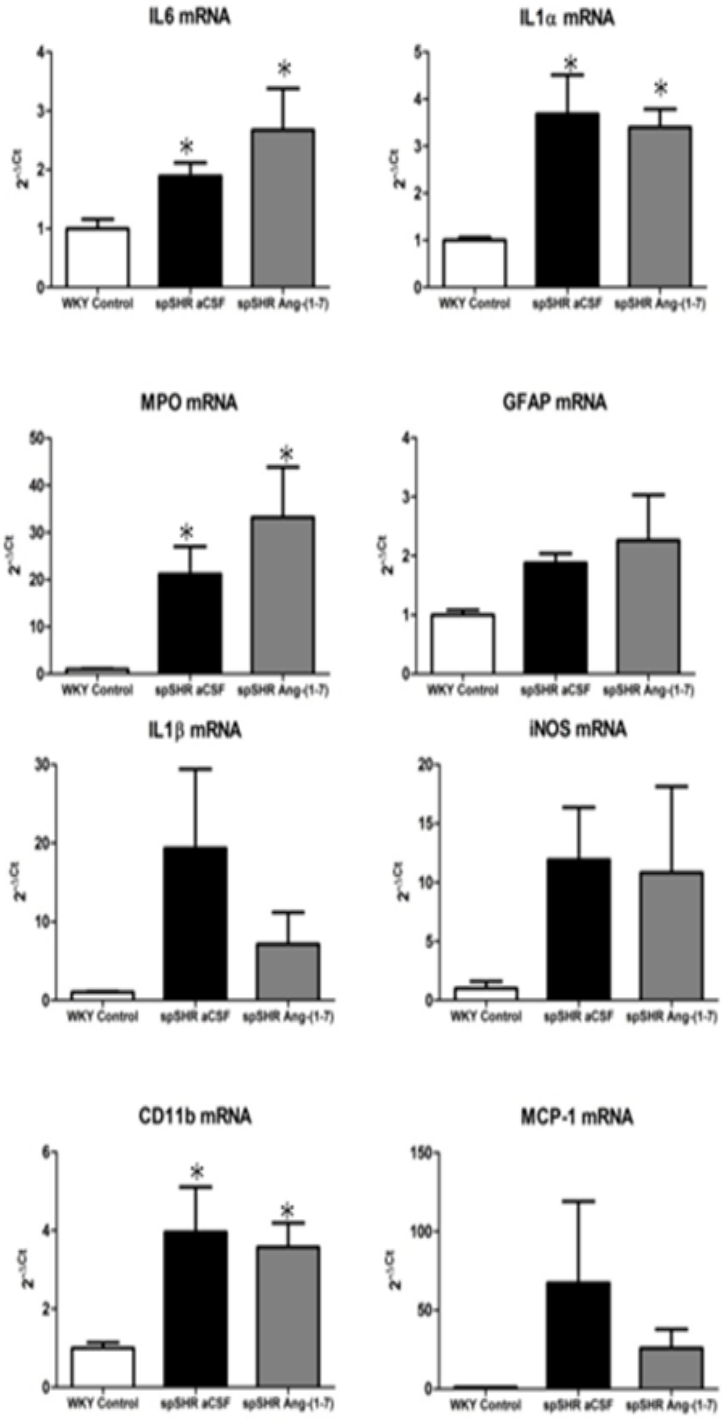


Figure 3-8. Ang-(1-7) does not alter the expression of genes related to inflammation in whole brain homogenate after treatment ends. Ang-(1-7) (1.1 nM; 0.5 µL/h) or aCSF (0.5 µL/h) pumps were implanted in 49 day-old spSHR. Rats were euthanized at 90 days old, 1 day before treatment ran out of the 6 wk pumps. Brains were removed and flash frozen to measure gene expression as detailed in the methods. Bar graphs are means + SEM. N=5/group. *P<0.05 compared to WKY Control.

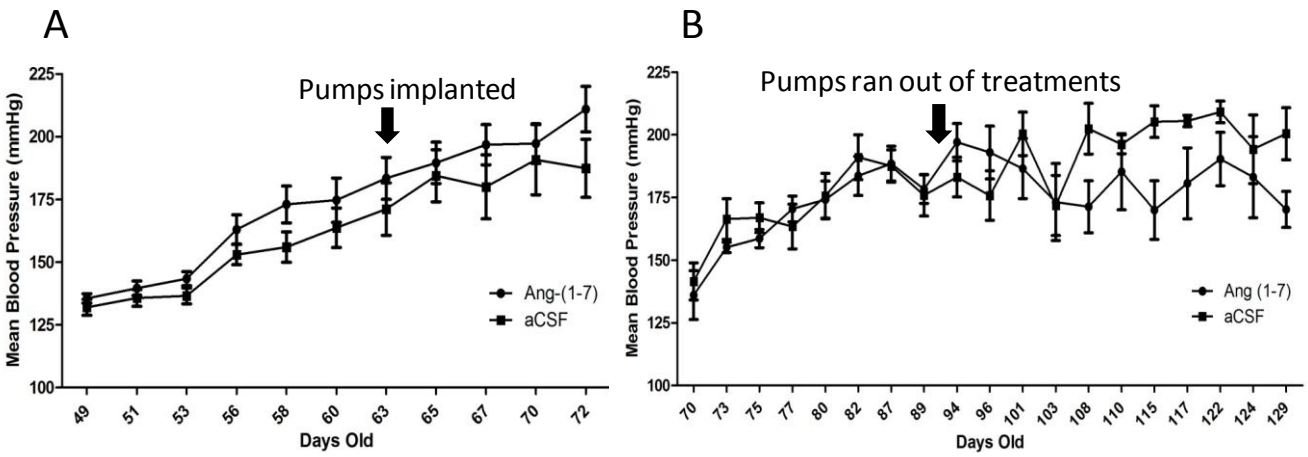


Figure 3-9. Ang-(1-7) administered intracerebroventricularly (ICV) has no effect on mean blood pressure during infusion in spSHR, but rats treated with Ang-(1-7) have lower mean blood pressure later after treatment ends. A) Direct blood pressure. Telemetry transducers implanted into the abdominal aorta at 45 days old. 6 wk Ang-(1-7) (1.1 nM; 0.5 µL/h) or aCSF (0.5 µL/h) pumps were implanted at 63 days old. N = 6 per group, Data are Means +/- SEM. B) Indirect blood pressure. 6 wk Ang-(1-7) or aCSF pumps implanted at 49 days old (not shown); 6-week old pumps ran out of treatment at 91 days old. Tail cuff plethysmography used after acclimation. N = 4-8 per group, Data are Means +/- SEM.

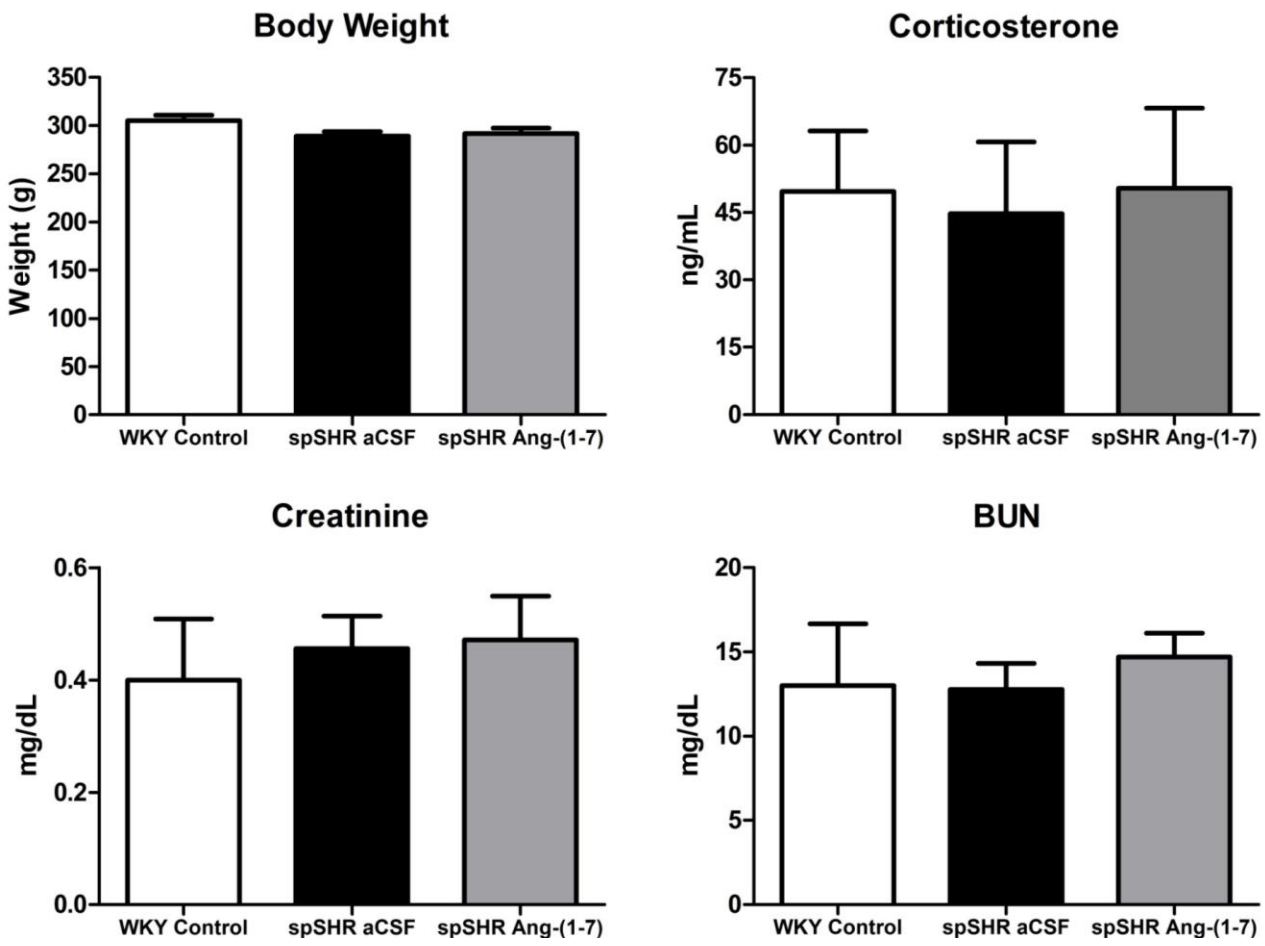


Figure 3-10. Ang-(1-7) has no effect on body weight, corticosterone, creatinine, or BUN. Ang-(1-7) (1.1 nM; 0.5 µL/h) or aCSF (0.5 µL/h) pumps were implanted in 49 day-old spSHR. aCSF (0.5 µL/h) pumps were also implanted in 49 day-old WKY controls. 6-week pumps ran out of treatment at 91 days old. Rats were euthanized at 108 days old. Bar graphs are means + SEM. N=4, 9, and 7 for WKY, spSHR aCSF, and spSHR Ang-(1-7), respectively. A) Body weight was recorded just prior to euthanasia. B, C, D) Blood was collected and serum was separated for corticosterone, creatinine, and BUN analysis as described in the methods.

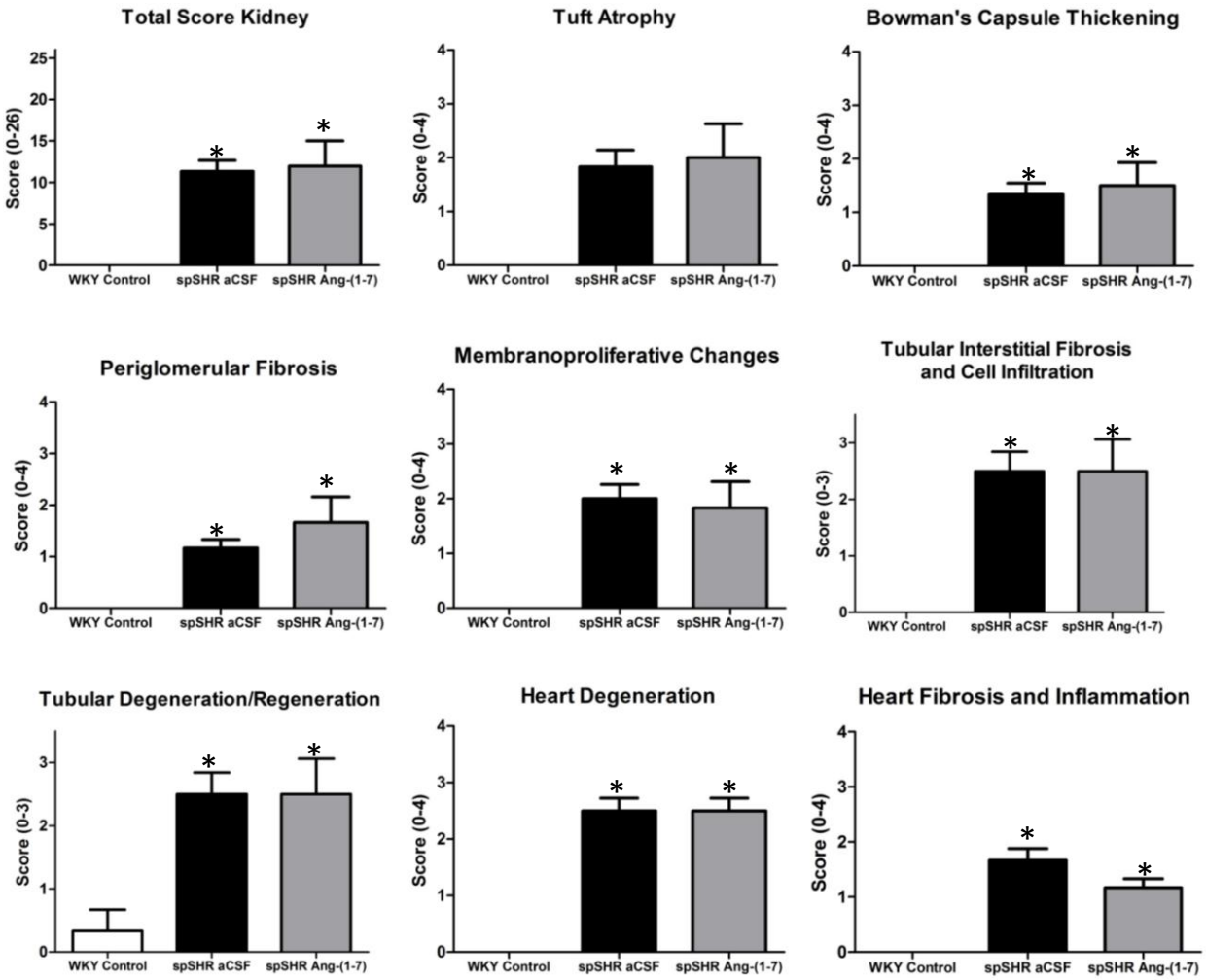


Figure 3-11. Ang-(1-7) has no effect on kidney or heart pathology just before treatment ends. Ang-(1-7) (1.1 nM; 0.5 µL/h) or aCSF (0.5 µL/h) pumps were implanted in 49 day-old spSHR. aCSF (0.5 µL/h) pumps were also implanted in 49 day-old WKY controls. Rats were euthanized at 90 days old, 1 day before treatment ran out of the 6 wk pumps, and perfused with saline and formalin. Tissues were dissected, removed, and fixed as detailed in the methods. Pathology was scored by a licensed veterinary pathologist. Bar graphs are means + SEM. N=4, 9, and 7 for WKY, spSHR aCSF, and spSHR Ang-(1-7), respectively. *P<0.05 compared to WKY Control.

# CHAPTER 4
# SUMMARY AND CONCLUSIONS

## Summary

### Specific Aim 1: Investigate the Mechanism of the Cerebroprotective Actions of Ang-(1-7) in Ischemic Stroke

In recent years, mounting evidence indicates that the renin-angiotensin system (RAS) is a potential therapeutic target for stroke, as it is highly involved in the processes that induce cerebral damage [165, 175, 177, 191]. Much of the work has focused on the angiotensin converting enzyme/angiotensin II/angiotensin type 1 receptor (ACE/Ang II/AT1R) axis of the RAS. This axis contributes to CNS damage following cerebral ischemia [176, 221]. Blocking this axis has been shown to be therapeutic in a number of animals and human studies [168, 171, 173 167, 185, 186, 222]. A lesser known axis of the RAS, the angiotensin converting enzyme 2/angiotensin-(1-7)/Mas (ACE2/Ang-(1-7)/Mas) axis, has recently begun receiving more attention in the literature. There is accumulating evidence that activation of this axis exerts beneficial actions in several cardiovascular diseases, including hypertension, hypertension related pathology, pulmonary hypertension, myocardial infarction, and heart failure [143, 223, 137, 223, 136, 222, 224]. In the brain, Ang-(1-7) is primarily generated by the action of ACE2 on Ang II, and its effects are mediated by its receptor, Mas [138]. In recent studies, we demonstrated that the intracerebral damage and neurological deficits elicited by endothelin-1 (ET-1)-induced middle cerebral artery occlusion (MCAO), a model of ischemic stroke, are significantly reduced by intracerebroventricular (ICV) administration of either exogenous Ang-(1-7) or an activator of ACE2, prior to and during the stroke period [218].

Since we previously demonstrated a cerebroprotective effect of Ang-(1-7) treatment during ET-1-induced MCAO, our aim here was to uncover the mechanism of this protection. This would further support the rationale for activating the ACE2/Ang-(1-7)/Mas axis for stroke treatment and prevention. Furthermore, we believed that uncovering this mechanism would lead us to consider other diseases that may benefit from a treatment involving manipulation of the ACE2/Ang-(1-7)/Mas axis. In previous

studies, we observed no effects of Ang-(1-7) on cerebral blood flow, percent vessel constriction, or systemic blood pressure (BP) [218]. Therefore, we hypothesized that Ang-(1-7) would modify the expression of certain genes that may play a role in mediating the observed cerebroprotective effects. Furthermore, we hypothesized that Mas would be present on certain cell types, indicating which cells are of potential importance in mediating the cerebroprotection. In this study a PCR array was used to identify several markers of inflammation that were increased in stroke and blunted by Ang-(1-7) therapy. It has previously been shown that damage due to stroke is a result of excessive inflammation. The findings from the array and changes in the expression of other genes, namely inducible nitric oxide synthase (iNOS), interleukin 1α (IL1α), chemokine receptor 4 (CXCR4), and a marker for monocytes/microglia (CD11b), were verified by quantitative reverse transcriptase real time PCR (qRT-PCR). Each was upregulated in stroke and significantly blunted by intracranial Ang-(1-7) infusion. A western blot was used to show that the changes in iNOS also existed at the protein level. To uncover which cell types were involved, we performed a co-localization study with the Ang-(1-7) receptor Mas and different cell markers. Microglia, endothelial cells, and neurons were shown to express Mas. Furthermore, we showed that Ang-(1-7) has a Mas dependent in vitro effect to blunt nitric oxide production in a mixed glia culture system. These findings indicate for the first time an anti-inflammatory property of Ang-(1-7) treatment in the CNS and provide a potential mechanism of cerebroprotection.

**Specific Aim 2: Determine whether Ang-(1-7) also Exerts Cerebroprotective Actions in Hemorrhagic Stroke**

There are two types of stroke: ischemic, where blood flow to the brain is reduced, and hemorrhagic, where persistent hypertension leads to vessel thinning and

intracerebral bleeding [45]. Both types of stroke are multifactorial, yet mounting evidence indicates that the renin-angiotensin system (RAS) is highly involved as described above [165, 167-171, 173-175, 177, 185, 186, 191, 235]. The peptide Ang-(1-7) has been shown to be therapeutic in many cardiovascular disease states, including ischemic stroke. In Aim 1, we demonstrated that this peptide had an *in vivo* anti-inflammatory effect during MCAO in rats and an *in vitro* anti-inflammatory effect in a mixed glia culture system. There is much overlap in the pathophysiology of ischemic and hemorrhagic stroke, especially regarding the role of excessive inflammation. Inflammation has a strong role in the mechanism of injury in hemorrhagic stroke. The inflammatory response begins soon after hemorrhage and peaks several days later in humans and animal models [58, 101, 114, 115]. The infiltration of neutrophils occurs within 2 days, and the activation of microglia may continue for up to 1 month [114, 116]. Evidence supports a role of microglia in hemorrhagic stroke pathology because inhibiting their activation reduces damage [117, 118, 120]. Furthermore, there is believed to be a strong association between inflammation and edema, as evidenced by data that correlates plasma tumor necrosis factor alpha concentrations in patients with hemorrhagic stroke to the degree of brain edema [123].

Given Ang-(1-7)'s therapeutic potential in ischemic stroke and its anti-inflammatory effects, our aim here was to determine if it also has any cerebroprotective effects in hemorrhagic stroke. For these experiments, we used stroke-prone Sponataneously Hypertensive Rats (spSHR). When fed a high salt diet from the time they are weaned, these rats will spontaneously develop extremely high blood pressure resulting in hemorrhagic stroke and death. We administered Ang-(1-7) centrally for six weeks starting at 49 days of age. Ang-(1-7) increased the survival of spSHR and

decreased the number of hemorrhages in the striatum. Furthermore, spSHR treated with Ang-(1-7) also showed less lethargy and improved neurological status as measured by a sunflower seed eating task. There was no effect on brain water content, however. We confirmed the presence of the Ang-(1-7) receptor Mas on neurons, microglia, and endothelial cells and showed that Ang-(1-7) decreases the number of microglia and increases the number of neurons striatum through the use of stereology. There was no effect of Ang-(1-7) on markers of peripheral disease, such as kidney pathology, heart pathology, body weight, corticosterone levels, or extent of hypertension. Interestingly, although BP was not altered by Ang-(1-7) during its administration, spSHR given Ang-(1-7) showed lower BP later in life after the treatment stopped. That the kidneys and hearts are not altered by Ang-(1-7) supports that the actions of this peptide are primarily central. These findings indicate for the first time Ang-(1-7) has cerebroprotective actions in hemorrhagic stroke and can increase the survival of spSHR.

## Discussion

The results of these studies provide further insight into the mechanism of cerebroprotection of activation of the ACE2/Ang-(1-7)/Mas axis of the RAS. Previous studies where Ang-(1-7) was administered centrally showed increases in bradykinin release, bradykinin receptor stimulation, endothelial nitric oxide synthase (eNOS) activity, and NO production [207, 208]. These findings raise the possibility of Ang-(1-7) having protective vascular effects in stroke, where it increases vasodilation through increasing NO availability. Other studies show that peripheral Ang-(1-7), administered both acutely and chronically, can increase cerebral blood flow [204-206]. Despite this, we doubt that the peripheral administration of Ang-(1-7) would deliver an effective dose to

cross the blood brain barrier (BBB) to have any central effects [265-267]. We have shown that our cerebroprotective dose given centrally has no effect on cerebral blood flow, percent vessel constriction, or systemic blood pressure [218].

Our data, presented in Chapter 2, demonstrate for the first time an anti-inflammatory effect of Ang-(1-7) when given centrally. This seems to be the most likely mechanism for cerebroprotection in our model. As stated above, inflammation plays a large role in the pathophysiology of stroke [37]. By blunting the expression of iNOS, CD11b, CXCR4, and IL1α, Ang-(1-7) can reduce the excess damage that occurs by an over activated inflammatory response. We showed that neurons, microglia, and endothelial cells have the Ang-(1-7) receptor Mas present. Therefore, we proposed that one of these cell types is most likely involved. To measure the effects of Ang-(1-7) on glia, in the absence of neurons or vessels, we used an LPS insult model with in vitro mixed glial cultures. We showed Ang-(1-7) decreased the concentration of released nitrite ($NO_2$), a stable breakdown product of NO. This verifies that Ang-(1-7) can have these anti-inflammatory effects independent of neurons and blood vessels.

Chapter 3 includes data that supports this idea and also poses further questions. Our stereology study indicated that Ang-(1-7) decreases numbers of microglia and increases numbers of neurons in the striatum. We believe that Ang-(1-7) decreases microglia and allows more neurons to survive. Interestingly, we did not observe an effect of Ang-(1-7) on the mRNA of iNOS or other pro-inflammatory cytokines (PICs) in the spSHR. This may be due to a technical challenge, where by homogenizing the whole brain there is too much healthy tissue from regions that have not undergone stroke/damage that the effects are diluted. We have previously observed this in the

MCAO model [218]. Another interesting observation related to mechanism of Ang-(1-7) action from the spSHR study is that while blood pressure was not affected during 6 wk of Ang-(1-7) infusion, the animals that were given Ang-(1-7) had lower BP later in life. This raises the possibility that maybe Ang-(1-7) had a protective effect where it decreased CNS inflammation/damage that can lead to the development of high BP. Perhaps this occurred at a BP control region of the brain. We think the effect is likely central because we observed no changes from Ang-(1-7) on heart/kidney pathology, corticosterone, or body weight. We believe that the primary effects are on microglia, but more work must be done to confirm this. By decreasing the excessive activation/migration of microglia in stroke, there would be less damage.

The next step in further understanding the mechanism of this cerebroprotective effect is to study the intracellular signaling responsible for this anti-inflammatory effect. If microglia are the primary cells involved, how is Mas signaling regulating their activation/migration? Is there a direct effect on regulating iNOS and PIC expression, or is that an indirect effect of fewer cells migrating to the region of damage? It is also important to consider that there could be multiple sites of action for the cerebroprotective effects. Perhaps in addition to the anti-inflammatory effects there is also a vascular effect that we just cannot measure in the ET-1 MCAO model with the dose of Ang-(1-7) that we used given centrally. Once more is known about intracellular signaling, we can better learn about commonalities between the stimulation of ACE2/Ang-(1-7)/Mas and ACE/Ang II/AT2R and the blockade of ACE/Ang II/AT1R.

As mentioned in Chapter 1, there is some overlap that is already understood in the signaling cascades of these RAS axes. A 7 transmembrane domain G protein

coupled receptor, the AT2R has 34% sequence homology to the AT1R [268]. AT2R stimulation results in the activation of signaling cascades that counteract many of the events mediated by AT1R [269]. AT2R stimulation activates several phosphatases, such as MAP Kinase Phosphatase-1 (MPK-1), SHP-1, and PP2A [131, 270], which serve to deactivate ERK1/2, STAT, JAK, and several other AT1R signaling molecules. Increasing these phosphatases can be both G protein dependent and independent. Stimulation of AT2R can also increase NO, cyclic GMP, and bradykinin [271-273]. Mas is also a 7 transmembrane domain G protein coupled receptor that similarly antagonizes the AT1R. Mas stimulation can block the phosphorylation of p38MAPK, ERK1/2, and JNK that is induced by AT1R activation [158, 159]. Mas signaling also activates SHP-2, which disrupts the AT1R mediated activation of c-Src, ERK1/2, and NOX [160]. Stimulation of Mas also increases eNOS activity via the phosphatidylinositol 3-kinase (PI3K) /Akt pathway [148]. It also causes AA release, production of $PGI_2$, and potentiates bradykinin signaling [161-164]. In summary, both stimulation of AT2R and Mas oppose AT1R, contributing to phosphatase activation, bradykinin receptor activation, and the release of NO. This common pathway of AT1R disruption hints that there may be common mechanisms of cerebroprotection.

The effects of Ang II at AT2R are in many cases very similar to those of Ang-(1-7) at Mas and opposite those of Ang II at AT1R [189] . There are many examples of studies where ARBs are cerebroprotective during stroke in both animals and humans [168, 171, 173 167, 185, 186, 222]. There is also an example of where an AT2R agonists was cerebroprotective in stroke [188]. Our own data show a novel AT2R agonist to be cerebroprotective in MCAO (unpublished). Interestingly, this agonist also had some anti-

inflammatory effects in vivo, blunting increases in iNOS and MCP-1 mRNA during stroke that parallel the anti-inflammatory effects of Ang-(1-7) discussed in Chapter 2.

It should be pointed out that developing pharmacotherapy targeted to the CNS can be difficult because the blood brain barrier (BBB) is impenetrable to many small molecules, limiting their activity centrally [265-267]. This results in only about 5% of drugs capable of central actions [274]. A molecule must meet certain specific requirements to across the BBB. Most must have a molecular weight less than 400 to 500 Da and have high lipophilicity [266]. Because Ang-(1-7) is 899 Da and hydrophilic, we designed the studies in Chapter 2 and 3 using transcranial central drug delivery directly into the left lateral ventricle. Disadvantages of this design are that this is more invasive and less sustainable long term compared to peripheral administration. This necessitates the exploration of alternative strategies to activating the central ACE2/Ang-(1-7)/Mas axis.

To increase BBB permeability, several strategies can be utilized. One is the use of medicinal chemistry to alter the molecule, making it more lipophilic or enabling it to utilize active transport mechanisms [266]. Because increasing lipophilicity increases a molecule's ability to cross in both directions, elimination is also increased. For this reason, taking advantage of active transport mechanisms is preferred. Another strategy is to disrupt the BBB. This can be accomplished though the use of poorly diffusible osmotic compounds, such as mannitol or lithium, to shrink endothelial cells or the use of detergents to destabilize membranes. A downside to this approach is that pathology is associated with both neurotoxic plasma proteins and the BBB disrupting compounds themselves [265, 266, 275]. Other more recent strategies include the use of transcranial ultrasound and liposome assisted delivery of drugs [276, 277]. We are currently undertaking

gene therapy approaches, as well, utilizing the viral delivery of ACE2 or a secretable form of Ang-(1-7). Another more sophisticated treatment strategy we are testing is the engineering of endothelial progenitor cells that over-express this secretable form of Ang-(1-7). These stem cells can be injected peripherally as they home to the sites of damage after stroke. It should also be mentioned that in stroke there is disruption of the BBB that occurs because of stroke-related damage. This may make crossing the BBB easier, allowing the passage of molecules that are administered acutely post stroke that would have otherwise been unable to cross. The difficulty with this approach is that there may be different degrees of BBB disruption in different stroke patients so dosage decisions may be difficult to make.

Within the stroke field, much emphasis is placed on developing acute therapies that are effective after the onset of stroke symptoms. We argue, however, that a preventative approach to stroke is not unrealistic. The major risk factors for stroke, including increasing age and high blood pressure, are well documented. It would be feasible to administer preventative drugs to patients exhibiting high risk. The experiments outlined in Chapters 2 and 3 were designed with a preventative chronic treatment approach where Ang-(1-7) was infused for over 1 wk or 6 wks, respectively. In the ET-1-induced MCAO model of ischemic stroke, Ang-(1-7) was given 1 wk before, during, and after stroke until the time of euthanasia. For the spSHR model of hemorrhagic stroke, Ang-(1-7) was given from 49 to 91 days of age during the development of pathology. In this way, we aimed to most efficiently explore the therapeutic potential of activating the ACE2/Ang-(1-7)/Mas axis. That being said, now that we show cerebroprotective effects with these designs, the potential for activating

this axis for acute, post-stroke therapy should be explored. As mentioned above, this may lessen the difficulty of designing drugs to cross the BBB.

Another step that should be made in pushing the translation of these findings to the clinic, is demonstrating the effectiveness of ACE2/Ang-(1-7)/Mas axis activation in other models of stroke and in other animals. For ischemic stroke, the intraluminal filament model of MCAO or the photoactivation model could be utilized [278]. Large animal models with more heterogeneity in stroke also demonstrate the likelihood of a treatment's effectiveness in the clinic [279]. For hemorrhagic stroke, the collagenase-induced model of intracerebral hemorrhage would prove useful. This model also allows for a more controlled, reproducible hemorrhage that may make many of the outcomes easier to measure and conclusions easier to draw [280]. After effectiveness in other models is established, clinical trials should be initiated to assess the potential of activating the ACE2/Ang-(1-7)/Mas axis in human patients.

In conclusion (Figure 4-1), these studies have increased the understanding of the mechanism by which activating the ACE2/Ang-(1-7)/Mas axis of the RAS is cerebroprotective in ischemic stroke. We demonstrate for the first time an *in vivo* anti-inflammatory property of central Ang-(1-7). We also show that Ang-(1-7) has anti-inflammatory effects in mixed glial cultures lacking neurons and vessels. Furthermore, we have demonstrated that activating this axis also has therapeutic potential in hemorrhagic stroke. It increases the survival of spSHR and improves their neurological status. We also demonstrated in 2 rat strains that Mas is present on microglia, neurons, and endothelial cells. Further work must be done to understand the intracellular signaling that results in these anti-inflammatory effects, and future studies must confirm

the therapeutic potential of activating this axis in other models and ultimately human patients.

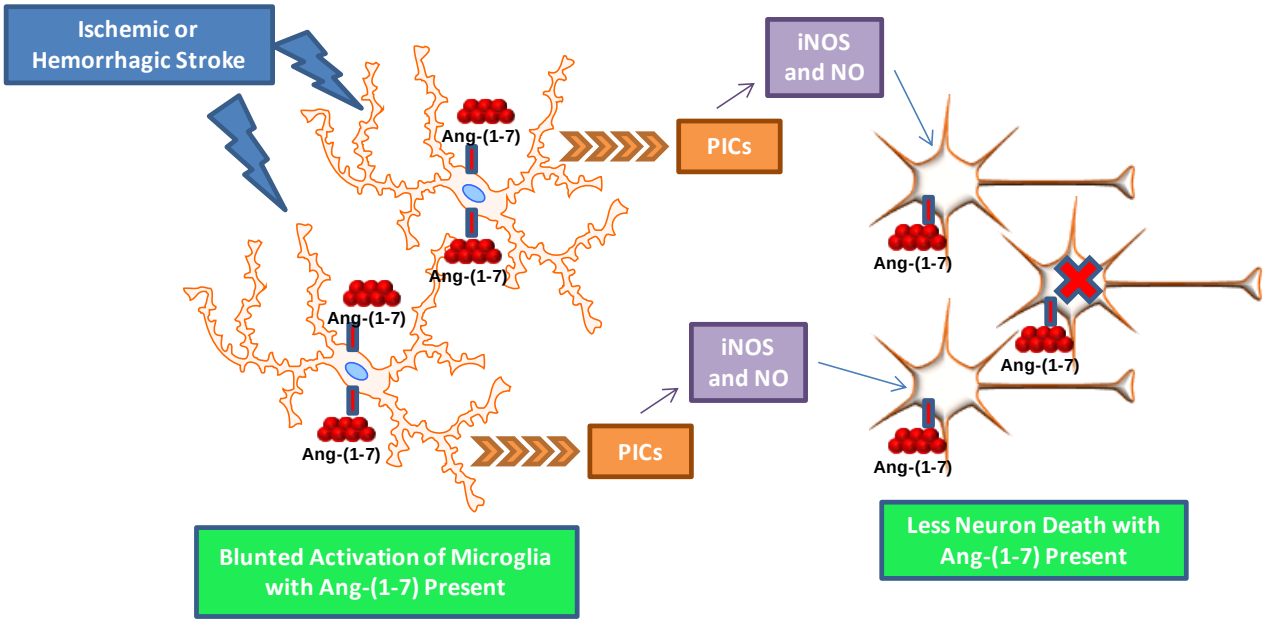


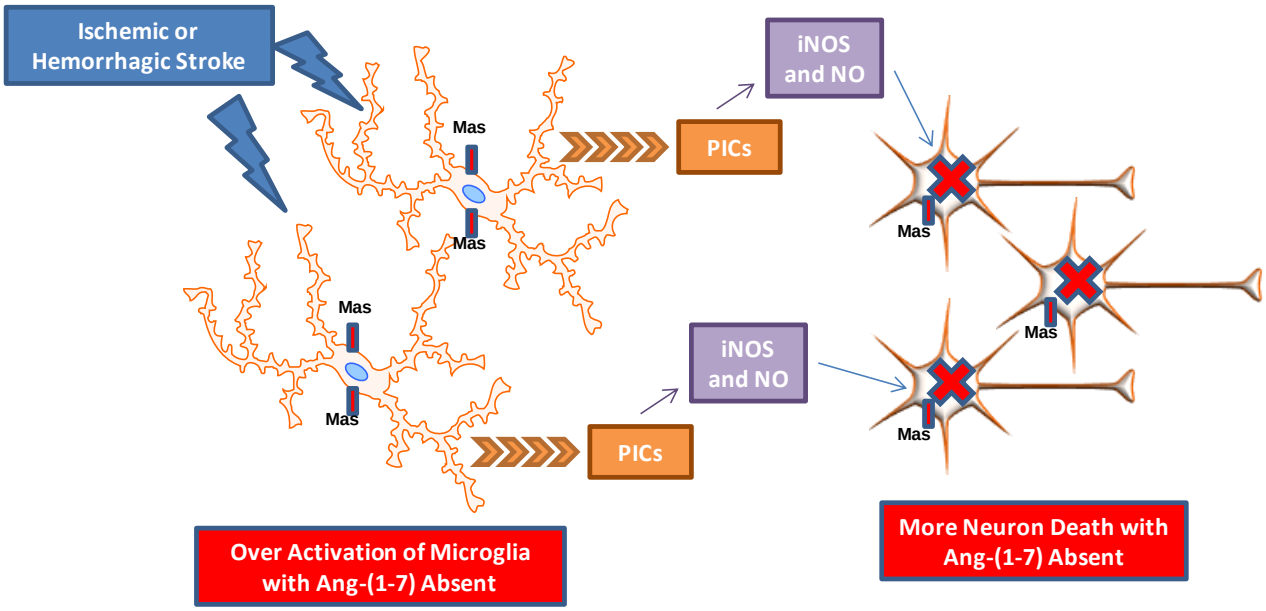


Figure 4-1. Schematic of proposed mechanism. Both ischemic and hemorrhagic stroke result in excessive inflammation that over-activates microglia. More microglia migrate to the area of damage and secrete proinflammatory cytokines which results in increased iNOS expression.

LIST OF REFERENCES


1 Roger, V. L. *et al*. Heart disease and stroke statistics--2012 update: a report from the American Heart Association. *Circulation* **125**, e2-e220 (2012).

2 Goldstein, L. B. *et al*. Primary prevention of ischemic stroke: a guideline from the American Heart Association/American Stroke Association Stroke Council: cosponsored by the Atherosclerotic Peripheral Vascular Disease Interdisciplinary Working Group; Cardiovascular Nursing Council; Clinical Cardiology Council; Nutrition, Physical Activity, and Metabolism Council; and the Quality of Care and Outcomes Research Interdisciplinary Working Group: the American Academy of Neurology affirms the value of this guideline. *Stroke* **37**, 1583-1633 (2006).

3 Sacco, R. L. *et al*. Guidelines for prevention of stroke in patients with ischemic stroke or transient ischemic attack: a statement for healthcare professionals from the American Heart Association/American Stroke Association Council on Stroke: co-sponsored by the Council on Cardiovascular Radiology and Intervention: the American Academy of Neurology affirms the value of this guideline. *Stroke* **37**, 577-617 (2006).

4 Lloyd-Jones, D. *et al*. Heart disease and stroke statistics--2009 update: a report from the American Heart Association Statistics Committee and Stroke Statistics Subcommittee. *Circulation* **119**, 480-486 (2009).

5 Lo, Y. K., Yiu, C. H., Hu, H. H., Su, M. S. & Laeuchli, S. C. Frequency and characteristics of early seizures in Chinese acute stroke. *Acta Neurol. Scand.* **90**, 83-85 (1994).

6 Lyden, P. D. & Zivin, J. A. Hemorrhagic transformation after cerebral ischemia: mechanisms and incidence. *Cerebrovasc. Brain Metab. Rev.* **5**, 1-16 (1993).

7 Intracerebral hemorrhage after intravenous t-PA therapy for ischemic stroke. The NINDS t-PA Stroke Study Group. *Stroke* **28**, 2109-2118 (1997).

8 Meschia, J. F. *et al*. Interobserver agreement in the trial of org 10172 in acute stroke treatment classification of stroke based on retrospective medical record review. *J. Stroke Cerebrovasc Dis.* **15**, 266-272 (2006).

9 Adams, H. P.,Jr *et al*. Classification of subtype of acute ischemic stroke. Definitions for use in a multicenter clinical trial. TOAST. Trial of Org 10172 in Acute Stroke Treatment. *Stroke* **24**, 35-41 (1993).

10 Tomsick, T. A. Intravenous thrombolysis for acute ischemic stroke. *J. Vasc. Interv. Radiol.* **15**, S67-76 (2004).

11 Olsen, T. S. & Lassen, N. A. A dynamic concept of middle cerebral artery occlusion and cerebral infarction in the acute state based on interpreting severe hyperemia as a sign of embolic migration. *Stroke* **15**, 458-468 (1984).

12 Brouns, R. & De Deyn, P. P. The complexity of neurobiological processes in acute ischemic stroke. *Clin. Neurol. Neurosurg.* **111**, 483-495 (2009).

13 Sharbrough, F. W., Messick, J. M.,Jr & Sundt, T. M.,Jr. Correlation of continuous electroencephalograms with cerebral blood flow measurements during carotid endarterectomy. *Stroke* **4**, 674-683 (1973).

14 Trojaborg, W. & Boysen, G. Relation between EEG, regional cerebral blood flow and internal carotid artery pressure during carotid endarterectomy. *Electroencephalogr. Clin. Neurophysiol.* **34**, 61-69 (1973).

15 Garcia, J. H. & Kamijyo, Y. Cerebral infarction. Evolution of histopathological changes after occlusion of a middle cerebral artery in primates. *J. Neuropathol. Exp. Neurol.* **33**, 408-421 (1974).

16 Astrup, J., Siesjo, B. K. & Symon, L. Thresholds in cerebral ischemia - the ischemic penumbra. *Stroke* **12**, 723-725 (1981).

17 Rossi, D. J., Brady, J. D. & Mohr, C. Astrocyte metabolism and signaling during brain ischemia. *Nat. Neurosci.* **10**, 1377-1386 (2007).

18 Silver, I. A., Deas, J. & Erecinska, M. Ion homeostasis in brain cells: differences in intracellular ion responses to energy limitation between cultured neurons and glial cells. *Neuroscience* **78**, 589-601 (1997).

19 Lipton, P. Ischemic cell death in brain neurons. *Physiol. Rev.* **79**, 1431-1568 (1999).

20 LOWRY, O. H., PASSONNEAU, J. V., HASSELBERGER, F. X. & SCHULZ, D. W. Effect of Ischemia on Known Substrates and Cofactors of the Glycolytic Pathway in Brain. *J. Biol. Chem.* **239**, 18-30 (1964).

21 Hansen, A. J. & Nedergaard, M. Brain ion homeostasis in cerebral ischemia. *Neurochem. Pathol.* **9**, 195-209 (1988).

22 Rossi, D. J., Oshima, T. & Attwell, D. Glutamate release in severe brain ischaemia is mainly by reversed uptake. *Nature* **403**, 316-321 (2000).

23 Abramov, A. Y., Scorziello, A. & Duchen, M. R. Three distinct mechanisms generate oxygen free radicals in neurons and contribute to cell death during anoxia and reoxygenation. *J. Neurosci.* **27**, 1129-1138 (2007).

24 Higuchi, T., Takeda, Y., Hashimoto, M., Nagano, O. & Hirakawa, M. Dynamic changes in cortical NADH fluorescence and direct current potential in rat focal ischemia: relationship between propagation of recurrent depolarization and growth of the ischemic core. *J. Cereb. Blood Flow Metab.* **22**, 71-79 (2002).

25 Harraz, M. M., Dawson, T. M. & Dawson, V. L. Advances in neuronal cell death 2007. *Stroke* **39**, 286-288 (2008).

26 Eliasson, M. J. *et al*. Poly(ADP-ribose) polymerase gene disruption renders mice resistant to cerebral ischemia. *Nat. Med.* **3**, 1089-1095 (1997).

27 Yu, S. W. *et al*. Mediation of poly(ADP-ribose) polymerase-1-dependent cell death by apoptosis-inducing factor. *Science* **297**, 259-263 (2002).

28 Andrabi, S. A. *et al*. Poly(ADP-ribose) (PAR) polymer is a death signal. *Proc. Natl. Acad. Sci. U. S. A.* **103**, 18308-18313 (2006).

29 Boland, B. & Nixon, R. A. Neuronal macroautophagy: from development to degeneration. *Mol. Aspects Med.* **27**, 503-519 (2006).

30 Rami, A., Langhagen, A. & Steiger, S. Focal cerebral ischemia induces upregulation of Beclin 1 and autophagy-like cell death. *Neurobiol. Dis.* **29**, 132-141 (2008).

31 Samara, C. & Tavernarakis, N. Autophagy and cell death in Caenorhabditis elegans. *Curr. Pharm. Des.* **14**, 97-115 (2008).

32 Adhami, F. *et al*. Cerebral ischemia-hypoxia induces intravascular coagulation and autophagy. *Am. J. Pathol.* **169**, 566-583 (2006).

33 Rosenberg, G. A., Estrada, E. Y. & Dencoff, J. E. Matrix metalloproteinases and TIMPs are associated with blood-brain barrier opening after reperfusion in rat brain. *Stroke* **29**, 2189-2195 (1998).

34 Huang, J., Upadhyay, U. M. & Tamargo, R. J. Inflammation in stroke and focal cerebral ischemia. *Surg. Neurol.* **66**, 232-245 (2006).

35 Maddahi, A. & Edvinsson, L. Cerebral ischemia induces microvascular pro-inflammatory cytokine expression via the MEK/ERK pathway. *J. Neuroinflammation* **7**, 14 (2010).

36 Iadecola, C. & Ross, M. E. Molecular pathology of cerebral ischemia: delayed gene expression and strategies for neuroprotection. *Ann. N. Y. Acad. Sci.* **835**, 203-217 (1997).

37 Iadecola, C. & Anrather, J. The immunology of stroke: from mechanisms to translation. *Nat. Med.* **17**, 796-808 (2011).

38 Iadecola, C., Zhang, F., Xu, S., Casey, R. & Ross, M. E. Inducible nitric oxide synthase gene expression in brain following cerebral ischemia. *J. Cereb. Blood Flow Metab.* **15**, 378-384 (1995).

39 Iadecola, C., Zhang, F. & Xu, X. Inhibition of inducible nitric oxide synthase ameliorates cerebral ischemic damage. *Am. J. Physiol.* **268**, R286-92 (1995).

40 Iadecola, C., Zhang, F., Casey, R., Nagayama, M. & Ross, M. E. Delayed reduction of ischemic brain injury and neurological deficits in mice lacking the inducible nitric oxide synthase gene. *J. Neurosci.* **17**, 9157-9164 (1997).

41 Forster, C., Clark, H. B., Ross, M. E. & Iadecola, C. Inducible nitric oxide synthase expression in human cerebral infarcts. *Acta Neuropathol.* **97**, 215-220 (1999).

42 Correale, J. & Villa, A. The neuroprotective role of inflammation in nervous system injuries. *J. Neurol.* **251**, 1304-1316 (2004).

43 Fisher, C. M. Pathological observations in hypertensive cerebral hemorrhage. *J. Neuropathol. Exp. Neurol.* **30**, 536-550 (1971).

44 Fisher, C. M. Cerebral miliary aneurysms in hypertension. *Am. J. Pathol.* **66**, 313-330 (1972).

45 Qureshi, A. I. *et al*. Spontaneous intracerebral hemorrhage. *N. Engl. J. Med.* **344**, 1450-1460 (2001).

46 Ojemann, R. G. & Mohr, J. P. Hypertensive Brain Hemorrhage. *Clin. Neurosurg.* **23**, 220-244 (1976).

47 Broderick, J. P., Brott, T. G., Tomsick, T., Barsan, W. & Spilker, J. Ultra-early evaluation of intracerebral hemorrhage. *J. Neurosurg.* **72**, 195-199 (1990).

48 Fujii, Y. *et al*. Hematoma enlargement in spontaneous intracerebral hemorrhage. *J. Neurosurg.* **80**, 51-57 (1994).

49 Fujii, Y., Takeuchi, S., Sasaki, O., Minakawa, T. & Tanaka, R. Multivariate analysis of predictors of hematoma enlargement in spontaneous intracerebral hemorrhage. *Stroke* **29**, 1160-1166 (1998).

50 Kazui, S., Naritomi, H., Yamamoto, H., Sawada, T. & Yamaguchi, T. Enlargement of spontaneous intracerebral hemorrhage. Incidence and time course. *Stroke* **27**, 1783-1787 (1996).

51 Kazui, S., Minematsu, K., Yamamoto, H., Sawada, T. & Yamaguchi, T. Predisposing factors to enlargement of spontaneous intracerebral hematoma. *Stroke* **28**, 2370-2375 (1997).

52 Brott, T. *et al*. Early hemorrhage growth in patients with intracerebral hemorrhage. *Stroke* **28**, 1-5 (1997).

53 Zazulia, A. R., Diringer, M. N., Derdeyn, C. P. & Powers, W. J. Progression of mass effect after intracerebral hemorrhage. *Stroke* **30**, 1167-1173 (1999).

54 NINDS ICH Workshop Participants. Priorities for clinical research in intracerebral hemorrhage: report from a National Institute of Neurological Disorders and Stroke workshop. *Stroke* **36**, e23-41 (2005).

55 Mayer, S. A. *et al*. Recombinant activated factor VII for acute intracerebral hemorrhage. *N. Engl. J. Med.* **352**, 777-785 (2005).

56 Hickenbottom, S. L., Grotta, J. C., Strong, R., Denner, L. A. & Aronowski, J. Nuclear factor-kappaB and cell death after experimental intracerebral hemorrhage in rats. *Stroke* **30**, 2472-7; discussion 2477-8 (1999).

57 Matsushita, K. *et al*. Evidence for apoptosis after intercerebral hemorrhage in rat striatum. *J. Cereb. Blood Flow Metab.* **20**, 396-404 (2000).

58 Xue, M. & Del Bigio, M. R. Intracerebral injection of autologous whole blood in rats: time course of inflammation and cell death. *Neurosci. Lett.* **283**, 230-232 (2000).

59 Gong, C. *et al*. Intracerebral hemorrhage-induced neuronal death. *Neurosurgery* **48**, 875-82; discussion 882-3 (2001).

60 Qureshi, A. I. *et al*. Apoptosis as a form of cell death in intracerebral hemorrhage. *Neurosurgery* **52**, 1041-7; discussion 1047-8 (2003).

61 Ohishi, H., Watanabe, T., Seki, H., Yoshimoto, T. & Suzuki, J. Sequential changes of experimental cerebral infarction--CT and histological studies. *No To Shinkei* **35**, 983-988 (1983).

62 Wagner, K. R. *et al*. Lobar intracerebral hemorrhage model in pigs: rapid edema development in perihematomal white matter. *Stroke* **27**, 490-497 (1996).

63 Xi, G. *et al*. Mechanisms of edema formation after intracerebral hemorrhage: effects of extravasated red blood cells on blood flow and blood-brain barrier integrity. *Stroke* **32**, 2932-2938 (2001).

64 Xi, G. *et al*. Intracerebral hemorrhage: pathophysiology and therapy. *Neurocrit Care.* **1**, 5-18 (2004).

65 Ropper, A. H. Lateral displacement of the brain and level of consciousness in patients with an acute hemispheral mass. *N. Engl. J. Med.* **314**, 953-958 (1986).

66 Tomita, H., Ito, U., Ohno, K. & Hirakawa, K. Chronological changes in brain edema induced by experimental intracerebral hematoma in cats. *Acta Neurochir. Suppl. (Wien)* **60**, 558-560 (1994).

67 Yang, G. Y., Betz, A. L., Chenevert, T. L., Brunberg, J. A. & Hoff, J. T. Experimental intracerebral hemorrhage: relationship between brain edema, blood flow, and blood-brain barrier permeability in rats. *J. Neurosurg.* **81**, 93-102 (1994).

68 Sinar, E. J., Mendelow, A. D., Graham, D. I. & Teasdale, G. M. Experimental intracerebral hemorrhage: effects of a temporary mass lesion. *J. Neurosurg.* **66**, 568-576 (1987).

69 Mendelow, A. D., Bullock, R., Teasdale, G. M., Graham, D. I. & McCulloch, J. Intracranial haemorrhage induced at arterial pressure in the rat. Part 2: Short term changes in local cerebral blood flow measured by autoradiography. *Neurol. Res.* **6**, 189-193 (1984).

70 Nath, F. P. *et al*. Effects of experimental intracerebral hemorrhage on blood flow, capillary permeability, and histochemistry. *J. Neurosurg.* **66**, 555-562 (1987).

71 Lee, K. R., Kawai, N., Kim, S., Sagher, O. & Hoff, J. T. Mechanisms of edema formation after intracerebral hemorrhage: effects of thrombin on cerebral blood flow, blood-brain barrier permeability, and cell survival in a rat model. *J. Neurosurg.* **86**, 272-278 (1997).

72 Zazulia, A. R. *et al*. Hypoperfusion without ischemia surrounding acute intracerebral hemorrhage. *J. Cereb. Blood Flow Metab.* **21**, 804-810 (2001).

73 Carhuapoma, J. R. *et al*. Diffusion-weighted MRI and proton MR spectroscopic imaging in the study of secondary neuronal injury after intracerebral hemorrhage. *Stroke* **31**, 726-732 (2000).

74 Mayer, S. A. *et al*. Perilesional blood flow and edema formation in acute intracerebral hemorrhage: a SPECT study. *Stroke* **29**, 1791-1798 (1998).

75 Tanaka, A., Yoshinaga, S., Nakayama, Y., Kimura, M. & Tomonaga, M. Cerebral blood flow and clinical outcome in patients with thalamic hemorrhages: a comparison with putaminal hemorrhages. *J. Neurol. Sci.* **144**, 191-197 (1996).

76 Skriver, E. B. & Olsen, T. S. Tissue damage at computed tomography following resolution of intracerebral hematomas. *Acta Radiol. Diagn. (Stockh)* **27**, 495-500 (1986).

77 Felberg, R. A. *et al*. Cell death in experimental intracerebral hemorrhage: the "black hole" model of hemorrhagic damage. *Ann. Neurol.* **51**, 517-524 (2002).

78 Xi, G., Keep, R. F. & Hoff, J. T. Erythrocytes and delayed brain edema formation following intracerebral hemorrhage in rats. *J. Neurosurg.* **89**, 991-996 (1998).

79 Xi, G. *et al*. Role of blood clot formation on early edema development after experimental intracerebral hemorrhage. *Stroke* **29**, 2580-2586 (1998).

80 Lee, K. R. *et al*. Edema from intracerebral hemorrhage: the role of thrombin. *J. Neurosurg.* **84**, 91-96 (1996).

81 Lee, K. R. *et al*. Intracerebral infusion of thrombin as a cause of brain edema. *J. Neurosurg.* **83**, 1045-1050 (1995).

82 Lee, K. R., Betz, A. L., Kim, S., Keep, R. F. & Hoff, J. T. The role of the coagulation cascade in brain edema formation after intracerebral hemorrhage. *Acta Neurochir. (Wien)* **138**, 396-400; discussion 400-1 (1996).

83 Nishino, A. *et al*. Thrombin may contribute to the pathophysiology of central nervous system injury. *J. Neurotrauma* **10**, 167-179 (1993).

84 Donovan, F. M., Pike, C. J., Cotman, C. W. & Cunningham, D. D. Thrombin induces apoptosis in cultured neurons and astrocytes via a pathway requiring tyrosine kinase and RhoA activities. *J. Neurosci.* **17**, 5316-5326 (1997).

85 Vaughan, P. J., Pike, C. J., Cotman, C. W. & Cunningham, D. D. Thrombin receptor activation protects neurons and astrocytes from cell death produced by environmental insults. *J. Neurosci.* **15**, 5389-5401 (1995).

86 Striggow, F. *et al*. The protease thrombin is an endogenous mediator of hippocampal neuroprotection against ischemia at low concentrations but causes degeneration at high concentrations. *Proc. Natl. Acad. Sci. U. S. A.* **97**, 2264-2269 (2000).

87 Jiang, Y. *et al*. Thrombin-receptor activation and thrombin-induced brain tolerance. *J. Cereb. Blood Flow Metab.* **22**, 404-410 (2002).

88 Gingrich, M. B., Junge, C. E., Lyuboslavsky, P. & Traynelis, S. F. Potentiation of NMDA receptor function by the serine protease thrombin. *J. Neurosci.* **20**, 4582-4595 (2000).

89 Moller, T., Hanisch, U. K. & Ransom, B. R. Thrombin-induced activation of cultured rodent microglia. *J. Neurochem.* **75**, 1539-1547 (2000).

90 Kitaoka, T., Hua, Y., Xi, G., Hoff, J. T. & Keep, R. F. Delayed argatroban treatment reduces edema in a rat model of intracerebral hemorrhage. *Stroke* **33**, 3012-3018 (2002).

91 Hamada, R. & Matsuoka, H. Antithrombin therapy for intracerebral hemorrhage. *Stroke* **31**, 794-795 (2000).

92 Xi, G., Keep, R. F., Hua, Y., Xiang, J. & Hoff, J. T. Attenuation of thrombin-induced brain edema by cerebral thrombin preconditioning. *Stroke* **30**, 1247-1255 (1999).

93 Dery, O., Corvera, C. U., Steinhoff, M. & Bunnett, N. W. Proteinase-activated receptors: novel mechanisms of signaling by serine proteases. *Am. J. Physiol.* **274**, C1429-52 (1998).

94 Coughlin, S. R. How the protease thrombin talks to cells. *Proc. Natl. Acad. Sci. U. S. A.* **96**, 11023-11027 (1999).

95 Coughlin, S. R. Thrombin signalling and protease-activated receptors. *Nature* **407**, 258-264 (2000).

96 Niclou, S., Suidan, H. S., Brown-Luedi, M. & Monard, D. Expression of the thrombin receptor mRNA in rat brain. *Cell. Mol. Biol. (Noisy-le-grand)* **40**, 421-428 (1994).

97 Weinstein, J. R., Gold, S. J., Cunningham, D. D. & Gall, C. M. Cellular localization of thrombin receptor mRNA in rat brain: expression by mesencephalic dopaminergic neurons and codistribution with prothrombin mRNA. *J. Neurosci.* **15**, 2906-2919 (1995).

98 Noorbakhsh, F., Vergnolle, N., Hollenberg, M. D. & Power, C. Proteinase-activated receptors in the nervous system. *Nat. Rev. Neurosci.* **4**, 981-990 (2003).

99 Xi, G., Reiser, G. & Keep, R. F. The role of thrombin and thrombin receptors in ischemic, hemorrhagic and traumatic brain injury: deleterious or protective? *J. Neurochem.* **84**, 3-9 (2003).

100 Junge, C. E. *et al*. The contribution of protease-activated receptor 1 to neuronal damage caused by transient focal cerebral ischemia. *Proc. Natl. Acad. Sci. U. S. A.* **100**, 13019-13024 (2003).

101 Enzmann, D. R., Britt, R. H., Lyons, B. E., Buxton, J. L. & Wilson, D. A. Natural history of experimental intracerebral hemorrhage: sonography, computed tomography and neuropathology. *AJNR Am. J. Neuroradiol.* **2**, 517-526 (1981).

102 Darrow, V. C., Alvord, E. C.,Jr, Mack, L. A. & Hodson, W. A. Histologic evolution of the reactions to hemorrhage in the premature human infant's brain. A combined ultrasound and autopsy study and a comparison with the reaction in adults. *Am. J. Pathol.* **130**, 44-58 (1988).

103 Marlet, J. M. & Barreto Fonseca Jde, P. Experimental determination of time of intracranial hemorrhage by spectrophotometric analysis of cerebrospinal fluid. *J. Forensic Sci.* **27**, 880-888 (1982).

104 Koeppen, A. H., Dickson, A. C. & McEvoy, J. A. The cellular reactions to experimental intracerebral hemorrhage. *J. Neurol. Sci.* **134 Suppl**, 102-112 (1995).

105 Wu, J. *et al*. Iron and iron-handling proteins in the brain after intracerebral hemorrhage. *Stroke* **34**, 2964-2969 (2003).

106 Nakamura, T. *et al*. Deferoxamine-induced attenuation of brain edema and neurological deficits in a rat model of intracerebral hemorrhage. *J. Neurosurg.* **100**, 672-678 (2004).

107 Matz, P. G., Weinstein, P. R. & Sharp, F. R. Heme oxygenase-1 and heat shock protein 70 induction in glia and neurons throughout rat brain after experimental intracerebral hemorrhage. *Neurosurgery* **40**, 152-60; discussion 160-2 (1997).

108 Wu, J. *et al*. Oxidative brain injury from extravasated erythrocytes after intracerebral hemorrhage. *Brain Res.* **953**, 45-52 (2002).

109 Kutty, R. K. & Maines, M. D. Purification and characterization of biliverdin reductase from rat liver. *J. Biol. Chem.* **256**, 3956-3962 (1981).

110 Huang, F. P. *et al*. Brain edema after experimental intracerebral hemorrhage: role of hemoglobin degradation products. *J. Neurosurg.* **96**, 287-293 (2002).

111 Hua, Y., Keep, R. F., Hoff, J. T. & Xi, G. Thrombin preconditioning attenuates brain edema induced by erythrocytes and iron. *J. Cereb. Blood Flow Metab.* **23**, 1448-1454 (2003).

112 Wagner, K. R. *et al*. Tin-mesoporphyrin, a potent heme oxygenase inhibitor, for treatment of intracerebral hemorrhage: in vivo and in vitro studies. *Cell. Mol. Biol. (Noisy-le-grand)* **46**, 597-608 (2000).

113 Koeppen, A. H., Dickson, A. C. & Smith, J. Heme oxygenase in experimental intracerebral hemorrhage: the benefit of tin-mesoporphyrin. *J. Neuropathol. Exp. Neurol.* **63**, 587-597 (2004).

114 Jenkins, A., Maxwell, W. L. & Graham, D. I. Experimental intracerebral haematoma in the rat: sequential light microscopical changes. *Neuropathol. Appl. Neurobiol.* **15**, 477-486 (1989).

115 Gong, C., Hoff, J. T. & Keep, R. F. Acute inflammatory reaction following experimental intracerebral hemorrhage in rat. *Brain Res.* **871**, 57-65 (2000).

116 Gong, Y., Hua, Y., Keep, R. F., Hoff, J. T. & Xi, G. Intracerebral hemorrhage: effects of aging on brain edema and neurological deficits. *Stroke* **35**, 2571-2575 (2004).

117 Wang, J., Rogove, A. D., Tsirka, A. E. & Tsirka, S. E. Protective role of tuftsin fragment 1-3 in an animal model of intracerebral hemorrhage. *Ann. Neurol.* **54**, 655-664 (2003).

118 Wang, J. & Tsirka, S. E. Tuftsin fragment 1-3 is beneficial when delivered after the induction of intracerebral hemorrhage. *Stroke* **36**, 613-618 (2005).

119 Lee, J. M. *et al*. Matrix metalloproteinase-9 and spontaneous hemorrhage in an animal model of cerebral amyloid angiopathy. *Ann. Neurol.* **54**, 379-382 (2003).

120 Wang, J. & Tsirka, S. E. Neuroprotection by inhibition of matrix metalloproteinases in a mouse model of intracerebral haemorrhage. *Brain* **128**, 1622-1633 (2005).

121 Tang, J. *et al*. Mmp-9 deficiency enhances collagenase-induced intracerebral hemorrhage and brain injury in mutant mice. *J. Cereb. Blood Flow Metab.* **24**, 1133-1145 (2004).

122 Hua, Y., Xi, G., Keep, R. F. & Hoff, J. T. Complement activation in the brain after experimental intracerebral hemorrhage. *J. Neurosurg.* **92**, 1016-1022 (2000).

123 Castillo, J. *et al*. Molecular signatures of brain injury after intracerebral hemorrhage. *Neurology* **58**, 624-629 (2002).

124 Steckelings, U. M., Rompe, F., Kaschina, E. & Unger, T. The evolving story of the RAAS in hypertension, diabetes and CV disease: moving from macrovascular to microvascular targets. *Fundam. Clin. Pharmacol.* **23**, 693-703 (2009).

125 SKEGGS, L. T.,Jr, MARSH, W. H., KAHN, J. R. & SHUMWAY, N. P. The existence of two forms of hypertensin. *J. Exp. Med.* **99**, 275-282 (1954).

126 Page, I. H. & Helmer, O. M. A Crystalline Pressor Substance (Angiotonin) Resulting from the Reaction between Renin and Renin-Activator. *J. Exp. Med.* **71**, 29-42 (1940).

127 Braun-Menendez, E., Fasciolo, J. C., Leloir, L. F. & Munoz, J. M. The substance causing renal hypertension. *J. Physiol.* **98**, 283-298 (1940).

128 Chiu, A. T. *et al*. Identification of angiotensin II receptor subtypes. *Biochem. Biophys. Res. Commun.* **165**, 196-203 (1989).

129 Whitebread, S., Mele, M., Kamber, B. & de Gasparo, M. Preliminary biochemical characterization of two angiotensin II receptor subtypes. *Biochem. Biophys. Res. Commun.* **163**, 284-291 (1989).

130 Speth, R. C. & Kim, K. H. Discrimination of two angiotensin II receptor subtypes with a selective agonist analogue of angiotensin II, p-aminophenylalanine6 angiotensin II. *Biochem. Biophys. Res. Commun.* **169**, 997-1006 (1990).

131 Stoll, M. *et al*. The angiotensin AT2-receptor mediates inhibition of cell proliferation in coronary endothelial cells. *J. Clin. Invest.* **95**, 651-657 (1995).

132 Sica, D. A. The evolution of renin-angiotensin blockade: angiotensin-converting enzyme inhibitors as the starting point. *Curr. Hypertens. Rep.* **12**, 67-73 (2010).

133 Paul, M., Poyan Mehr, A. & Kreutz, R. Physiology of local renin-angiotensin systems. *Physiol. Rev.* **86**, 747-803 (2006).

134 Widdop, R. E., Jones, E. S., Hannan, R. E. & Gaspari, T. A. Angiotensin AT2 receptors: cardiovascular hope or hype? *Br. J. Pharmacol.* **140**, 809-824 (2003).

135 Tipnis, S. R. *et al*. A human homolog of angiotensin-converting enzyme. Cloning and functional expression as a captopril-insensitive carboxypeptidase. *J. Biol. Chem.* **275**, 33238-33243 (2000).

136 Donoghue, M. *et al*. A novel angiotensin-converting enzyme-related carboxypeptidase (ACE2) converts angiotensin I to angiotensin 1-9. *Circ. Res.* **87**, E1-9 (2000).

137 Ferreira, A. J. *et al*. Therapeutic implications of the vasoprotective axis of the renin-angiotensin system in cardiovascular diseases. *Hypertension* **55**, 207-213 (2010).

138 Santos, R. A. *et al*. Angiotensin-(1-7) is an endogenous ligand for the G protein-coupled receptor Mas. *Proc. Natl. Acad. Sci. U. S. A.* **100**, 8258-8263 (2003).

139 Vickers, C. *et al*. Hydrolysis of biological peptides by human angiotensin-converting enzyme-related carboxypeptidase. *J. Biol. Chem.* **277**, 14838-14843 (2002).

140 Greene, L. J., Spadaro, A. C., Martins, A. R., Perussi De Jesus, W. D. & Camargo, A. C. Brain endo-oligopeptidase B: a post-proline cleaving enzyme that inactivates angiotensin I and II. *Hypertension* **4**, 178-184 (1982).

141 Welches, W. R. *et al*. Evidence that prolyl endopeptidase participates in the processing of brain angiotensin. *J. Hypertens.* **9**, 631-638 (1991).

142 Yamamoto, K., Chappell, M. C., Brosnihan, K. B. & Ferrario, C. M. In vivo metabolism of angiotensin I by neutral endopeptidase (EC 3.4.24.11) in spontaneously hypertensive rats. *Hypertension* **19**, 692-696 (1992).

143 Santos, R. A., Ferreira, A. J. & Simoes E Silva, A. C. Recent advances in the angiotensin-converting enzyme 2-angiotensin(1-7)-Mas axis. *Exp. Physiol.* **93**, 519-527 (2008).

144 Nguyen, G. *et al*. Pivotal role of the renin/prorenin receptor in angiotensin II production and cellular responses to renin. *J. Clin. Invest.* **109**, 1417-1427 (2002).

145 Raizada, M. K. & Paton, J. F. Recent advances in the renin-angiotensin system: angiotensin-converting enzyme 2 and (pro)renin receptor. *Exp. Physiol.* **93**, 517-518 (2008).

146 Zini, S. *et al*. Identification of metabolic pathways of brain angiotensin II and III using specific aminopeptidase inhibitors: predominant role of angiotensin III in the control of vasopressin release. *Proc. Natl. Acad. Sci. U. S. A.* **93**, 11968-11973 (1996).

147 Touyz, R. M. & Schiffrin, E. L. Signal transduction mechanisms mediating the physiological and pathophysiological actions of angiotensin II in vascular smooth muscle cells. *Pharmacol. Rev.* **52**, 639-672 (2000).

148 Sampaio, W. O. *et al*. Angiotensin-(1-7) through receptor Mas mediates endothelial nitric oxide synthase activation via Akt-dependent pathways. *Hypertension* **49**, 185-192 (2007).

149 Griendling, K. K., Lassegue, B. & Alexander, R. W. Angiotensin receptors and their therapeutic implications. *Annu. Rev. Pharmacol. Toxicol.* **36**, 281-306 (1996).

150 Ushio-Fukai, M. *et al*. Angiotensin II receptor coupling to phospholipase D is mediated by the betagamma subunits of heterotrimeric G proteins in vascular smooth muscle cells. *Mol. Pharmacol.* **55**, 142-149 (1999).

151 Baines, R. J., Brown, C., Ng, L. L. & Boarder, M. R. Angiotensin II-stimulated phospholipase C responses of two vascular smooth muscle-derived cell lines. Role of cyclic GMP. *Hypertension* **28**, 772-778 (1996).

152 Yan, C., Kim, D., Aizawa, T. & Berk, B. C. Functional interplay between angiotensin II and nitric oxide: cyclic GMP as a key mediator. *Arterioscler. Thromb. Vasc. Biol.* **23**, 26-36 (2003).

153 Vallega, G. A., Canessa, M. L., Berk, B. C., Brock, T. A. & Alexander, R. W. Vascular smooth muscle Na+-H+ exchanger kinetics and its activation by angiotensin II. *Am. J. Physiol.* **254**, C751-8 (1988).

154 Mehta, P. K. & Griendling, K. K. Angiotensin II cell signaling: physiological and pathological effects in the cardiovascular system. *Am. J. Physiol. Cell. Physiol.* **292**, C82-97 (2007).

155 Griendling, K. K., Sorescu, D. & Ushio-Fukai, M. NAD(P)H oxidase: role in cardiovascular biology and disease. *Circ. Res.* **86**, 494-501 (2000).

156 Kostenis, E. *et al*. G-protein-coupled receptor Mas is a physiological antagonist of the angiotensin II type 1 receptor. *Circulation* **111**, 1806-1813 (2005).

157 Castro, C. H. *et al*. Evidence for a functional interaction of the angiotensin-(1-7) receptor Mas with AT1 and AT2 receptors in the mouse heart. *Hypertension* **46**, 937-942 (2005).

158 Tallant, E. A., Ferrario, C. M. & Gallagher, P. E. Angiotensin-(1-7) inhibits growth of cardiac myocytes through activation of the mas receptor. *Am. J. Physiol. Heart Circ. Physiol.* **289**, H1560-6 (2005).

159 Su, Z., Zimpelmann, J. & Burns, K. D. Angiotensin-(1-7) inhibits angiotensin II-stimulated phosphorylation of MAP kinases in proximal tubular cells. *Kidney Int.* **69**, 2212-2218 (2006).

160 Sampaio, W. O., Henrique de Castro, C., Santos, R. A., Schiffrin, E. L. & Touyz, R. M. Angiotensin-(1-7) counterregulates angiotensin II signaling in human endothelial cells. *Hypertension* **50**, 1093-1098 (2007).

161 Heitsch, H., Brovkovych, S., Malinski, T. & Wiemer, G. Angiotensin-(1-7)-Stimulated Nitric Oxide and Superoxide Release From Endothelial Cells. *Hypertension* **37**, 72-76 (2001).

162 Hilchey, S. D. & Bell-Quilley, C. P. Association between the natriuretic action of angiotensin-(1-7) and selective stimulation of renal prostaglandin I2 release. *Hypertension* **25**, 1238-1244 (1995).

163 Li, P., Chappell, M. C., Ferrario, C. M. & Brosnihan, K. B. Angiotensin-(1-7) augments bradykinin-induced vasodilation by competing with ACE and releasing nitric oxide. *Hypertension* **29**, 394-400 (1997).

164 Paula, R. D., Lima, C. V., Khosla, M. C. & Santos, R. A. Angiotensin-(1-7) potentiates the hypotensive effect of bradykinin in conscious rats. *Hypertension* **26**, 1154-1159 (1995).

165 Kagiyama, T., Kagiyama, S. & Phillips, M. I. Expression of angiotensin type 1 and 2 receptors in brain after transient middle cerebral artery occlusion in rats. *Regul. Pept.* **110**, 241-247 (2003).

166 Bestehorn, K. & Wahle, K. Impact of losartan on stroke risk in hypertensive patients in primary care. *Clin. Drug Investig.* **27**, 347-355 (2007).

167 Dahlof, B. *et al*. Cardiovascular morbidity and mortality in the Losartan Intervention For Endpoint reduction in hypertension study (LIFE): a randomised trial against atenolol. *Lancet* **359**, 995-1003 (2002).

168 Dai, W. J., Funk, A., Herdegen, T., Unger, T. & Culman, J. Blockade of central angiotensin AT(1) receptors improves neurological outcome and reduces expression of AP-1 transcription factors after focal brain ischemia in rats. *Stroke* **30**, 2391-8; discussion 2398-9 (1999).

169 Stier, C. T.,Jr, Adler, L. A., Levine, S. & Chander, P. N. Stroke prevention by losartan in stroke-prone spontaneously hypertensive rats. *J. Hypertens. Suppl.* **11**, S37-42 (1993).

170 Inada, Y. *et al*. Protective effects of candesartan cilexetil (TCV-116) against stroke, kidney dysfunction and cardiac hypertrophy in stroke-prone spontaneously hypertensive rats. *Clin. Exp. Hypertens.* **19**, 1079-1099 (1997).

171 Nishimura, Y., Ito, T. & Saavedra, J. M. Angiotensin II AT(1) blockade normalizes cerebrovascular autoregulation and reduces cerebral ischemia in spontaneously hypertensive rats. *Stroke* **31**, 2478-2486 (2000).

172 Ito, T. *et al*. Protection against ischemia and improvement of cerebral blood flow in genetically hypertensive rats by chronic pretreatment with an angiotensin II AT1 antagonist. *Stroke* **33**, 2297-2303 (2002).

173 Groth, W., Blume, A., Gohlke, P., Unger, T. & Culman, J. Chronic pretreatment with candesartan improves recovery from focal cerebral ischaemia in rats. *J. Hypertens.* **21**, 2175-2182 (2003).

174 Lu, Q., Zhu, Y. Z. & Wong, P. T. Neuroprotective effects of candesartan against cerebral ischemia in spontaneously hypertensive rats. *Neuroreport* **16**, 1963-1967 (2005).

175 Li, J. *et al*. Angiotensin AT2 receptor protects against cerebral ischemia-induced neuronal injury. *FASEB J.* **19**, 617-619 (2005).

176 Mecca, A. P., O'Connor, T. E., Katovich, M. J. & Sumners, C. Candesartan pretreatment is cerebroprotective in a rat model of endothelin-1-induced middle cerebral artery occlusion. *Exp. Physiol.* **94**, 937-946 (2009).

177 Walther, T. *et al*. Ischemic injury in experimental stroke depends on angiotensin II. *FASEB J.* **16**, 169-176 (2002).

178 Krikov, M., Thone-Reineke, C., Muller, S., Villringer, A. & Unger, T. Candesartan but not ramipril pretreatment improves outcome after stroke and stimulates neurotrophin BNDF/TrkB system in rats. *J. Hypertens.* **26**, 544-552 (2008).

179 Li, J. M. *et al*. Temporary pretreatment with the angiotensin II type 1 receptor blocker, valsartan, prevents ischemic brain damage through an increase in capillary density. *Stroke* **39**, 2029-2036 (2008).

180 Takada, J. *et al*. Valsartan improves the lower limit of cerebral autoregulation in rats. *Hypertens. Res.* **29**, 621-626 (2006).

181 Liu, H. *et al*. Protective mechanisms of the angiotensin II type 1 receptor blocker candesartan against cerebral ischemia: in-vivo and in-vitro studies. *J. Hypertens.* **26**, 1435-1445 (2008).

182 Stenman, E. & Edvinsson, L. Cerebral ischemia enhances vascular angiotensin AT1 receptor-mediated contraction in rats. *Stroke* **35**, 970-974 (2004).

183 Faure, S. *et al*. Protective effect of candesartan in experimental ischemic stroke in the rat mediated by AT2 and AT4 receptors. *J. Hypertens.* **26**, 2008-2015 (2008).

184 Yamamoto, E. *et al*. Excess salt causes cerebral neuronal apoptosis and inflammation in stroke-prone hypertensive rats through angiotensin II-induced NADPH oxidase activation. *Stroke* **39**, 3049-3056 (2008).

185 Papademetriou, V. *et al*. Stroke prevention with the angiotensin II type 1-receptor blocker candesartan in elderly patients with isolated systolic hypertension: the Study on Cognition and Prognosis in the Elderly (SCOPE). *J. Am. Coll. Cardiol.* **44**, 1175-1180 (2004).

186 Hansson, L. *et al*. Effect of angiotensin-converting-enzyme inhibition compared with conventional therapy on cardiovascular morbidity and mortality in hypertension: the Captopril Prevention Project (CAPPP) randomised trial. *Lancet* **353**, 611-616 (1999).

187 Iwai, M. *et al*. Possible inhibition of focal cerebral ischemia by angiotensin II type 2 receptor stimulation. *Circulation* **110**, 843-848 (2004).

188 McCarthy, C. A., Vinh, A., Callaway, J. K. & Widdop, R. E. Angiotensin AT2 receptor stimulation causes neuroprotection in a conscious rat model of stroke. *Stroke* **40**, 1482-1489 (2009).

189 Carey, R. M. Cardiovascular and renal regulation by the angiotensin type 2 receptor: the AT2 receptor comes of age. *Hypertension* **45**, 840-844 (2005).

190 Viswanathan, M. & Saavedra, J. M. Expression of angiotensin II AT2 receptors in the rat skin during experimental wound healing. *Peptides* **13**, 783-786 (1992).

191 Makino, I., Shibata, K., Ohgami, Y., Fujiwara, M. & Furukawa, T. Transient upregulation of the AT2 receptor mRNA level after global ischemia in the rat brain. *Neuropeptides* **30**, 596-601 (1996).

192 Horiuchi, M., Akishita, M. & Dzau, V. J. Recent progress in angiotensin II type 2 receptor research in the cardiovascular system. *Hypertension* **33**, 613-621 (1999).

193 Lucius, R. *et al*. The angiotensin II type 2 (AT2) receptor promotes axonal regeneration in the optic nerve of adult rats. *J. Exp. Med.* **188**, 661-670 (1998).

194 Cote, F., Do, T. H., Laflamme, L., Gallo, J. M. & Gallo-Payet, N. Activation of the AT(2) receptor of angiotensin II induces neurite outgrowth and cell migration in microexplant cultures of the cerebellum. *J. Biol. Chem.* **274**, 31686-31692 (1999).

195 Reinecke, K. *et al*. Angiotensin II accelerates functional recovery in the rat sciatic nerve in vivo: role of the AT2 receptor and the transcription factor NF-kappaB. *FASEB J.* **17**, 2094-2096 (2003).

196 Raizada, M. K. & Ferreira, A. J. ACE2: a new target for cardiovascular disease therapeutics. *J. Cardiovasc. Pharmacol.* **50**, 112-119 (2007).

197 Grobe, J. L. *et al*. Prevention of angiotensin II-induced cardiac remodeling by angiotensin-(1-7). *Am. J. Physiol. Heart Circ. Physiol.* **292**, H736-42 (2007).

198 Grobe, J. L., Mecca, A. P., Mao, H. & Katovich, M. J. Chronic angiotensin-(1-7) prevents cardiac fibrosis in DOCA-salt model of hypertension. *Am. J. Physiol. Heart Circ. Physiol.* **290**, H2417-23 (2006).

199 Huentelman, M. J. *et al*. Protection from angiotensin II-induced cardiac hypertrophy and fibrosis by systemic lentiviral delivery of ACE2 in rats. *Exp. Physiol.* **90**, 783-790 (2005).

200 Ferreira, A. J. *et al*. The nonpeptide angiotensin-(1-7) receptor Mas agonist AVE-0991 attenuates heart failure induced by myocardial infarction. *Am. J. Physiol. Heart Circ. Physiol.* **292**, H1113-9 (2007).

201 Ferreira, A. J. *et al*. Evidence for angiotensin-converting enzyme 2 as a therapeutic target for the prevention of pulmonary hypertension. *Am. J. Respir. Crit. Care Med.* **179**, 1048-1054 (2009).

202 Ferreira, A. J., Santos, R. A. & Almeida, A. P. Angiotensin-(1-7): cardioprotective effect in myocardial ischemia/reperfusion. *Hypertension* **38**, 665-668 (2001).

203 Santos, R. A. *et al*. Expression of an angiotensin-(1-7)-producing fusion protein produces cardioprotective effects in rats. *Physiol. Genomics* **17**, 292-299 (2004).

204 Becker, L. K., Etelvino, G. M., Walther, T., Santos, R. A. & Campagnole-Santos, M. J. Immunofluorescence localization of the receptor Mas in cardiovascular-related areas of the rat brain. *Am. J. Physiol. Heart Circ. Physiol.* **293**, H1416-24 (2007).

205 Sampaio, W. O., Nascimento, A. A. & Santos, R. A. Systemic and regional hemodynamic effects of angiotensin-(1-7) in rats. *Am. J. Physiol. Heart Circ. Physiol.* **284**, H1985-94 (2003).

206 Botelho-Santos, G. A. *et al*. Expression of an angiotensin-(1-7)-producing fusion protein in rats induced marked changes in regional vascular resistance. *Am. J. Physiol. Heart Circ. Physiol.* **292**, H2485-90 (2007).

207 Lu, J., Zhang, Y. & Shi, J. Effects of intracerebroventricular infusion of angiotensin-(1-7) on bradykinin formation and the kinin receptor expression after focal cerebral ischemia-reperfusion in rats. *Brain Res.* **1219**, 127-135 (2008).

208 Zhang, Y. *et al*. Central administration of angiotensin-(1-7) stimulates nitric oxide release and upregulates the endothelial nitric oxide synthase expression following focal cerebral ischemia/reperfusion in rats. *Neuropeptides* **42**, 593-600 (2008).

209 Young, D., O'Neill, K., Jessell, T. & Wigler, M. Characterization of the rat mas oncogene and its high-level expression in the hippocampus and cerebral cortex of rat brain. *Proc. Natl. Acad. Sci. U. S. A.* **85**, 5339-5342 (1988).

210 Bunnemann, B. *et al*. Autoradiographic localization of mas proto-oncogene mRNA in adult rat brain using in situ hybridization. *Neurosci. Lett.* **114**, 147-153 (1990).

211 Martin, K. A., Grant, S. G. & Hockfield, S. The mas proto-oncogene is developmentally regulated in the rat central nervous system. *Brain Res. Dev. Brain Res.* **68**, 75-82 (1992).

212 Metzger, R. *et al*. Expression of the mouse and rat mas proto-oncogene in the brain and peripheral tissues. *FEBS Lett.* **357**, 27-32 (1995).

213 Kumar, M., Grammas, P., Giacomelli, F. & Wiener, J. Selective expression of c-mas proto-oncogene in rat cerebral endothelial cells. *Neuroreport* **8**, 93-96 (1996).

214 Harmer, D., Gilbert, M., Borman, R. & Clark, K. L. Quantitative mRNA expression profiling of ACE 2, a novel homologue of angiotensin converting enzyme. *FEBS Lett.* **532**, 107-110 (2002).

215 Hamming, I. *et al*. Tissue distribution of ACE2 protein, the functional receptor for SARS coronavirus. A first step in understanding SARS pathogenesis. *J. Pathol.* **203**, 631-637 (2004).

216 Gallagher, P. E., Chappell, M. C., Ferrario, C. M. & Tallant, E. A. Distinct roles for ANG II and ANG-(1-7) in the regulation of angiotensin-converting enzyme 2 in rat astrocytes. *Am. J. Physiol. Cell. Physiol.* **290**, C420-6 (2006).

217 Doobay, M. F. *et al*. Differential expression of neuronal ACE2 in transgenic mice with overexpression of the brain renin-angiotensin system. *Am. J. Physiol. Regul. Integr. Comp. Physiol.* **292**, R373-81 (2007).

218 Mecca, A. P. *et al*. Cerebroprotection by angiotensin-(1-7) in endothelin-1-induced ischaemic stroke. *Exp. Physiol.* **96**, 1084-1096 (2011).

219 Roger, V. L. *et al*. Heart disease and stroke statistics--2011 update: a report from the American Heart Association. *Circulation* **123**, e18-e209 (2011).

220 Chalmers, J. Global impact of stroke. *Heart Dis.* **2**, S13-7 (2000).

221 Anderson, V. R., Perry, C. M. & Robinson, D. M. Ramipril: a review of its use in preventing cardiovascular outcomes in high-risk patients. *Am. J. Cardiovasc. Drugs* **6**, 417-432 (2006).

222 Thone-Reineke, C., Steckelings, U. M. & Unger, T. Angiotensin receptor blockers and cerebral protection in stroke. *J. Hypertens. Suppl.* **24**, S115-21 (2006).

223 Xu, P., Sriramula, S. & Lazartigues, E. ACE2/ANG-(1-7)/Mas pathway in the brain: the axis of good. *Am. J. Physiol. Regul. Integr. Comp. Physiol.* **300**, R804-17 (2011).

224 Castro-Chaves, P., Cerqueira, R., Pintalhao, M. & Leite-Moreira, A. F. New pathways of the renin-angiotensin system: the role of ACE2 in cardiovascular pathophysiology and therapy. *Expert Opin. Ther. Targets* **14**, 485-496 (2010).

225 Li, H. *et al*. Macrophage migration inhibitory factor in hypothalamic paraventricular nucleus neurons decreases blood pressure in spontaneously hypertensive rats. *FASEB J.* **22**, 3175-3185 (2008).

226 Kopnisky, K. L. & Sumners, C. Angiotensin II-induced decrease in expression of inducible nitric oxide synthase in rat astroglial cultures: role of protein kinase C. *J. Neurochem.* **74**, 613-620 (2000).

227 Schilling, M., Strecker, J. K., Schabitz, W. R., Ringelstein, E. B. & Kiefer, R. Effects of monocyte chemoattractant protein 1 on blood-borne cell recruitment after transient focal cerebral ischemia in mice. *Neuroscience* **161**, 806-812 (2009).

228 El Khoury, J. *et al*. Ccr2 deficiency impairs microglial accumulation and accelerates progression of Alzheimer-like disease. *Nat. Med.* **13**, 432-438 (2007).

229 Panahian, N., Yoshiura, M. & Maines, M. D. Overexpression of heme oxygenase-1 is neuroprotective in a model of permanent middle cerebral artery occlusion in transgenic mice. *J. Neurochem.* **72**, 1187-1203 (1999).

230 Rothwell, N. J. & Relton, J. K. Involvement of interleukin-1 and lipocortin-1 in ischaemic brain damage. *Cerebrovasc. Brain Metab. Rev.* **5**, 178-198 (1993).

231 Jin, R., Yang, G. & Li, G. Inflammatory mechanisms in ischemic stroke: role of inflammatory cells. *J. Leukoc. Biol.* **87**, 779-789 (2010).

232 Negishi, H. *et al*. Black and green tea polyphenols attenuate blood pressure increases in stroke-prone spontaneously hypertensive rats. *J. Nutr.* **134**, 38-42 (2004).

233 Jeon, H., Lee, S., Lee, W. H. & Suk, K. Analysis of glial secretome: the long pentraxin PTX3 modulates phagocytic activity of microglia. *J. Neuroimmunol.* **229**, 63-72 (2010).

234 Peri, G. *et al*. PTX3, A prototypical long pentraxin, is an early indicator of acute myocardial infarction in humans. *Circulation* **102**, 636-641 (2000).

235 Ito, T. *et al*. Elevation of mRNA levels of tissue-type plasminogen activator and urokinase-type plasminogen activator in hippocampus and cerebral cortex following middle cerebral artery occlusion in rats. *Neurol. Res.* **22**, 413-419 (2000).

236 Magnon, C., Lucas, D. & Frenette, P. S. Trafficking of stem cells. *Methods Mol. Biol.* **750**, 3-24 (2011).

237 Lu, D. Y. *et al*. SDF-1alpha up-regulates interleukin-6 through CXCR4, PI3K/Akt, ERK, and NF-kappaB-dependent pathway in microglia. *Eur. J. Pharmacol.* **613**, 146-154 (2009).

238 Rana, I. *et al*. Microglia activation in the hypothalamic PVN following myocardial infarction. *Brain Res.* **1326**, 96-104 (2010).

239 Guo, F. *et al*. Astroglia are a possible cellular substrate of angiotensin(1-7) effects in the rostral ventrolateral medulla. *Cardiovasc. Res.* **87**, 578-584 (2010).

240 Young, D., Waitches, G., Birchmeier, C., Fasano, O. & Wigler, M. Isolation and characterization of a new cellular oncogene encoding a protein with multiple potential transmembrane domains. *Cell* **45**, 711-719 (1986).

241 Manabe, I. Chronic inflammation links cardiovascular, metabolic and renal diseases. *Circ. J.* **75**, 2739-2748 (2011).

242 Giani, J. F. *et al*. Angiotensin-(1-7) improves cardiac remodeling and inhibits growth-promoting pathways in the heart of fructose-fed rats. *Am. J. Physiol. Heart Circ. Physiol.* **298**, H1003-13 (2010).

243 Peltonen, T. *et al*. (Pro)renin receptors and angiotensin converting enzyme 2/angiotensin-(1-7)/Mas receptor axis in human aortic valve stenosis. *Atherosclerosis* **216**, 35-43 (2011).

244 da Silveira, K. D. *et al*. Anti-inflammatory effects of the activation of the angiotensin-(1-7) receptor, MAS, in experimental models of arthritis. *J. Immunol.* **185**, 5569-5576 (2010).

245 Giani, J. F. *et al*. Angiotensin-(1-7) reduces proteinuria and diminishes structural damage in renal tissue of stroke-prone spontaneously hypertensive rats. *Am. J. Physiol. Renal Physiol.* **300**, F272-82 (2011).

246 Rosamond, W. *et al*. Heart disease and stroke statistics--2007 update: a report from the American Heart Association Statistics Committee and Stroke Statistics Subcommittee. *Circulation* **115**, e69-171 (2007).

247 Saavedra, J. M. Brain angiotensin II: new developments, unanswered questions and therapeutic opportunities. *Cell. Mol. Neurobiol.* **25**, 485-512 (2005).

248 Fleegal, M. A. & Sumners, C. Drinking behavior elicited by central injection of angiotensin II: roles for protein kinase C and Ca2+/calmodulin-dependent protein kinase II. *Am. J. Physiol. Regul. Integr. Comp. Physiol.* **285**, R632-40 (2003).

249 Smeda, J. S. Hemorrhagic stroke development in spontaneously hypertensive rats fed a North American, Japanese-style diet. *Stroke* **20**, 1212-1218 (1989).

250 Smeda, J. S. Cerebral vascular changes associated with hemorrhagic stroke in hypertension. *Can. J. Physiol. Pharmacol.* **70**, 552-564 (1992).

251 Lee, S. T. *et al*. Erythropoietin reduces perihematomal inflammation and cell death with eNOS and STAT3 activations in experimental intracerebral hemorrhage. *J. Neurochem.* **96**, 1728-1739 (2006).

252 Chu, K. *et al*. Celecoxib induces functional recovery after intracerebral hemorrhage with reduction of brain edema and perihematomal cell death. *J. Cereb. Blood Flow Metab.* **24**, 926-933 (2004).

253 Jung, K. H. *et al*. HMG-CoA reductase inhibitor, atorvastatin, promotes sensorimotor recovery, suppressing acute inflammatory reaction after experimental intracerebral hemorrhage. *Stroke* **35**, 1744-1749 (2004).

254 Bruijnzeel, A. W., Rodrick, G., Singh, R. P., Derendorf, H. & Bauzo, R. M. Repeated pre-exposure to tobacco smoke potentiates subsequent locomotor responses to nicotine and tobacco smoke but not amphetamine in adult rats. *Pharmacol. Biochem. Behav.* **100**, 109-118 (2011).

255 Gonzalez, C. L. & Kolb, B. A comparison of different models of stroke on behaviour and brain morphology. *Eur. J. Neurosci.* **18**, 1950-1962 (2003).

256 Callaway, J. K., Jones, N. C. & Royse, C. F. Isoflurane induces cognitive deficits in the Morris water maze task in rats. *Eur. J. Anaesthesiol.* **29**, 239-245 (2012).

257 Gundersen, H. J. Stereology of arbitrary particles. A review of unbiased number and size estimators and the presentation of some new ones, in memory of William R. Thompson. *J. Microsc.* **143**, 3-45 (1986).

258 West, M. J., Slomianka, L. & Gundersen, H. J. Unbiased stereological estimation of the total number of neurons in thesubdivisions of the rat hippocampus using the optical fractionator. *Anat. Rec.* **231**, 482-497 (1991).

259 Sterio, D. C. The unbiased estimation of number and sizes of arbitrary particles using the disector. *J. Microsc.* **134**, 127-136 (1984).

260 Cao, W. *et al*. Halogenated aromatic amino acid 3,5-dibromo-D: -tyrosine produces beneficial effects in experimental stroke and seizures. *Amino Acids* **40**, 1151-1158 (2011).

261 Reinhard, M. K., Hottendorf, G. H. & Powell, E. D. Differences in the sensitivity of Fischer and Sprague-Dawley rats to aminoglycoside nephrotoxicity. *Toxicol. Pathol.* **19**, 66-71 (1991).

262 Jokinen, M. P. *et al*. Morphologic aspects of rodent cardiotoxicity in a retrospective evaluation of National Toxicology Program studies. *Toxicol. Pathol.* **39**, 850-860 (2011).

263 Nabika, T., Cui, Z. & Masuda, J. The stroke-prone spontaneously hypertensive rat: how good is it as a model for cerebrovascular diseases? *Cell. Mol. Neurobiol.* **24**, 639-646 (2004).

264 Saavedra, J. M. Opportunities and limitations of genetic analysis of hypertensive rat strains. *J. Hypertens.* **27**, 1129-1133 (2009).

265 Pardridge, W. M. The blood-brain barrier: bottleneck in brain drug development. *NeuroRx* **2**, 3-14 (2005).

266 Pardridge, W. M. The blood-brain barrier and neurotherapeutics. *NeuroRx* **2**, 1-2 (2005).

267 Pardridge, W. M. Molecular biology of the blood-brain barrier. *Mol. Biotechnol.* **30**, 57-70 (2005).

268 Guthrie, G. P.,Jr. Angiotensin receptors: physiology and pharmacology. *Clin. Cardiol.* **18**, III 29-34 (1995).

269 Jones, E. S., Vinh, A., McCarthy, C. A., Gaspari, T. A. & Widdop, R. E. AT2 receptors: functional relevance in cardiovascular disease. *Pharmacol. Ther.* **120**, 292-316 (2008).

270 Tsuzuki, S., Matoba, T., Eguchi, S. & Inagami, T. Angiotensin II type 2 receptor inhibits cell proliferation and activates tyrosine phosphatase. *Hypertension* **28**, 916-918 (1996).

271 Siragy, H. M., Jaffa, A. A., Margolius, H. S. & Carey, R. M. Renin-angiotensin system modulates renal bradykinin production. *Am. J. Physiol.* **271**, R1090-5 (1996).

272 Siragy, H. M. & Carey, R. M. The subtype-2 (AT2) angiotensin receptor regulates renal cyclic guanosine 3', 5'-monophosphate and AT1 receptor-mediated prostaglandin E2 production in conscious rats. *J. Clin. Invest.* **97**, 1978-1982 (1996).

273 Siragy, H. M. & Carey, R. M. The subtype 2 (AT2) angiotensin receptor mediates renal production of nitric oxide in conscious rats. *J. Clin. Invest.* **100**, 264-269 (1997).

274 Ghose, A. K., Viswanadhan, V. N. & Wendoloski, J. J. A knowledge-based approach in designing combinatorial or medicinal chemistry libraries for drug discovery. 1. A qualitative and quantitative characterization of known drug databases. *J. Comb. Chem.* **1**, 55-68 (1999).

275 Nadal, A., Fuentes, E., Pastor, J. & McNaughton, P. A. Plasma albumin is a potent trigger of calcium signals and DNA synthesis in astrocytes. *Proc. Natl. Acad. Sci. U. S. A.* **92**, 1426-1430 (1995).

276 Koch, S., Pohl, P., Cobet, U. & Rainov, N. G. Ultrasound enhancement of liposome-mediated cell transfection is caused by cavitation effects. *Ultrasound Med. Biol.* **26**, 897-903 (2000).

277 Jordao, J. F. *et al*. Antibodies targeted to the brain with image-guided focused ultrasound reduces amyloid-beta plaque load in the TgCRND8 mouse model of Alzheimer's disease. *PLoS One* **5**, e10549 (2010).

278 Jackman, K., Kunz, A. & Iadecola, C. Modeling focal cerebral ischemia in vivo. *Methods Mol. Biol.* **793**, 195-209 (2011).

279 Terpolilli, N. A. *et al*. Inhalation of nitric oxide prevents ischemic brain damage in experimental stroke by selective dilatation of collateral arterioles. *Circ. Res.* **110**, 727-738 (2012).

280 Kang, K. *et al*. Lithium pretreatment reduces brain injury after intracerebral hemorrhage in rats. *Neurol. Res.* (2012).

# BIOGRAPHICAL SKETCH

Robert W. Regenhardt was born in Saint Petersburg, Florida, USA in 1985. He graduated valedictorian in 2004 from South Sumter High School in Bushnell, Florida. In 2004, he began undergraduate studies at the University of Florida majoring in nutritional sciences and minoring in chemistry. Two years later, Robert was admitted to medical school through an early acceptance program. He later matriculated into the combined MD-PhD program after discovering a passion for research. His undergraduate honors thesis involved changes in lymphocyte subpopulations within the gut during zinc deficiency in the laboratory of Bobbi Langkamp-Henken, Ph.D. He graduated with his B.S. with highest honors after completing his first year of medical school in 2008. In 2009, Robert began his Ph.D. in the laboratory of Colin Sumners, Ph.D. His research interests include the renin angiotensin system, cardiovascular disease, and stroke. The title of his doctoral thesis is “Understanding the cerebroprotective actions of the ACE2/Ang-(1-7)/Mas axis during ischemic and hemorrhagic stroke.” This work was completed in 2012, showing for the first time anti-inflammatory properties of Ang-(1-7) in ischemic stroke and cerebroprotective effects of this peptide in hemorrhagic stroke. He is currently completing the clinical portion of his Medical Doctorate training.

In addition to his research interests, Robert has been highly involved in the Equal Access Clinic, a student run free medical clinic in downtown Gainesville. The clinic serves the under-insured populations of Gainesville and Alachua County. Robert has served in many capacities at this clinic, being Chair for Research and Chair for Behavioral Health. He has also served as president for the local chapter of the American Physician Scientist Association, an organization that he remains actively

involved in. Robert aspires to be an effective physician scientist, educator, and healthcare provider.